DOCTOR OF PHILOSOPHY

Numerical study of solute transport in deformable soil liners

Zhang, Huijie

Award date:
2012

DOCTOR OF PHILOSOPHY

Numerical study of solute transport in deformable soil liners

Huijie Zhang

2012

University of Dundee

Numerical Study of Solute Transport in Deformable Soil Liners

Huijie Zhang
BEng MSc

A thesis submitted for the degree of Doctor of Philosophy

Division of Civil Engineering

The University of Dundee

October 2012

Contents

List of Figures

List of Tables

Acknowledgements

I would first like to express my appreciation to my supervisor Professor Jeng, Dongsheng for his guidance and insight during this dissertation work and throughout my studies at University of Dundee.

I gratefully acknowledges the financial assistance provided by EPSRC. I would like to express my special thanks to Professor Jeng, Dongsheng for the supplementary support.

For providing the opportunity to undertake this research, I am particularly grateful to my supervisors Professor Jeng, Dongsheng. He did not reject me because of my non-outstanding grade of my undergraduate courses. My thanks are also extended to my second advisor Professor Dong, Ping for his encouragement and help in obtaining this scholarship.

Lots of thanks to my colleagues Wenni Deng, Jisheng Zhang, Chi Zhang, Jianhong Ye, Jovan Stojsavljevic, Ismail Ahmed for being together, sharing together and encouraging each other.

Most splendid glory is to my Lord Jesus: I am blessed so much to experience His amazing help. I am the clay, He is the potter.

"I hereby certify that the work embodied in this Thesis is the result of original research and has not been submitted for a higher degree to any other University or Institute"

Huijie Zhang

Preface

The research work presented in this thesis was conducted in the Division of Civil Engineering at the University of Dundee from September 2009 to September 2012. This work was performed under the supervision of Prof. Jeng. The purpose of the study is to examine how mechanical consolidation and heat transport can affect the migration of contaminants through quasi-saturated and unsaturated contaminant barriers. This has been largely motivated by discovery in the research literature that "consolidation induced advection" can accelerate the contaminant migration within saturated soil barriers. However, it can only partly explain some field observations of the early breakthrough of contaminants from landfill liners. Therefore, the factors which have the potentials to influence the mechanical consolidation and solute transport progresses were examined. A theoretical approach was employed to develop the mathematical models for the coupled processes. Numerical simulations were performed to solve the governing equations involved.

During the term of the candidature, several papers were published or undergoes processing as listed below:

1. Jeng D-S and Zhang H (2009). Effects of soil behavior on solute transport in groundwater. The Conference for ISCM II & EPMESC XII, 29 November - 3 December 2009, Hong Kong (CD ROM)

2. Zhang, H. J., Jeng, D.-S., Seymour, B. R., Barry, D. A., and Li, L. (2012a). Solute transport in partially-saturated deformable porous media: Application to a landfill clay liner. Advances in Water Resources, 40:1-10.

3. Zhang, H. J., Jeng, D.-S., Barry, D. A., Seymour, B. R., and Li, L. (2012b). Solute transport in unsaturated porous media under landfill clay liners: A finite deformation approach. Submitted to Journal of Hydrology.

4. Zhang, H. J., Jeng, D.-S., Barry, D. A., Seymour, B. R., and Li, L. (2012c). Organic contamination transport through non-isothermal un-saturated deforming clay liner. Submitted to Advances in Water Resources.

Abstract

For reasons of simplicity and economics, landfills are the main methods of disposing the solid waste (either household or industrial) and the highly contaminated aqueous sediments due to toxic substances. To protect the surrounding environment and groudwater from pollution, liner system is usually constructed beneath the landfill. In a modern composite basal liner system, preventing the breakthrough of volatile organic contaminants (VOCs) is a core concern to design a effective barrier.

Conventional methods of analysis assume that the soil is fully saturated. However, throughout much of the world, unsaturation exists in landfill basal liner. Although a few investigations have treated the migration of VOCs in unsaturated soil liner, no deformation of liner due to mechanical consolidation was included and VOCs only move in liquid phase. In reality, landfill compacted clay liner (CCL) is compacted on the optimum water content, where the air phase exists in the form of occluded air bubbles. However, the air phase becomes continuous when the temperature increases and then VOCs will be transported in the gaseous phase. Therefore, it is clear that the traditional approaches to assessing VOCs transport are inadequate to enable reliable assessment of VOCs break through landfill basal soil liner. This thesis attempts to make an investigation into migration of VOCs in partially saturated landfill soil liner using numerical modeling techniques.

Firstly, pore fluid storage and solute transport equations suitable for quasi-saturated porous medium were developed. In the frame of small strain, a one-dimension coupling model was non-dimensionlized, whereby relative importance of the terms related to consolidation advection were compared. Based on the non-dimensional analysis, a simplified model was proposed and applied to a hypothetical landfill CCL. Numerical results demonstrated that the longitudinal dispersivity and compressibility of the pore fluid can be significant. Furthermore, the degree of soil saturation and loading rate of the waste surcharge affect significantly the contamination advective emission, namely the cumulative contaminant mass outflow per unit area from compacted clay liner (CCL) due to advective flow.

Secondly, the coupled model was extended to include finite strain and geometric and material nonlinearity. Using the finite strain model, a parametric study was carried out to examine the influences of consolidation and several other parameters on the process of VOCs solute transport in quasi-saturated soil liner. Consolidation-induced advection was found to have a lasting effect on solute transport during and after the deformation for relatively compressible soil regardless of the sorption level, though the sorption could dramatically slow the solute transport process rate. A lower degree of saturation leads to a slower pore fluid flow and solute transport due to a narrower channel. Effective diffusion decreases during consolidation and consequently the relative importance of mechanical dispersion becomes profound. In general, reducing soil compressibility and improving sorption levels of clay are the most effective ways to retard contaminant migration.

Thirdly, a fully coupled thermal-hydraulic-mechanical-chemical (THMC) model was proposed to describe the migration of VOCs in unsaturated landfill liners with continuous air phase. In the formulation, vertical soil stress, capillary pressure, air pressure, temperature increase and dissolved solute concentration were selected as primary variables. The finite deformation was addressed by use of Lagrangian coordinate. The non-isothermal moisture transport was dependent on both temperature gradient and VOCs concentration. VOCs were assumed to reside and be transported by three phases, i.e., solid, liquid and gas phases in soil. Based on the model, an illustrative example of unsaturated landfill compacted clay liner (CCL) was presented. For the case considered, transport of gaseous phase VOCs was found to dominate the migration progress. Moreover, the temperature gradient could accelerate the breakthrough of VOC in unsaturated liner, whilst the mechanical consolidation slowed down the motion of VOCs due to soil contraction.

The theoretical models established in this study encompass several important situations in landfill basal soil liner, which can facilitate understanding of the VOCs transport process and assessment of soil liner performance. In addition, some areas where further work is required are identified.

Chapter 1

Introduction

1.1 Background

Land-based disposal in landfills is the most commonly used method for containment of municipal solid waste. In USA, over 250 million tons of municipal solid waste are annually produced and approximately 55% of this waste is disposed of in landfills (USEPA, 2007). Besides municipal solid waste which is being constantly produced, the marine sediment contaminated in history also requires proper management.

During the period 1930-1970 in Europe, industrial expansion, population concentrations, lower morality and a throw-away philosophy all contributed to the rapid intensive pollution of sediments (Figure 1.1) (Senten and Charlier, 1991). Due to the high affinity of many kinds of contaminants with solid matter, sediment can serve as a repository of pollution, and consequently long-term source of contaminants in water bodies (Massoudieh et al., 2010). Pollutants remobilization from sediments have significant effect on water quality. Beldowski et al. (2009) showed that the return soluble and particulate fluxes of mercury from the muddy sediments (in southern Baltic Sea) to the water column constitute a substantial proportion of the mercury load (20-50%) to overlying water by the transport mechanisms of diffusion and resuspension. It can significantly impair the navigational and recreational uses of rivers and harbors. Moreover, it is definitely true that the hazardous substances can be taken into human bodies through bio-concentration (Fukue et al., 1999), primarily through consumption of fish and shellfish.

In the USA, the Environmental Protection Agency (EPA) performed a series of investigations and estimated that 1.2 billion cubic meters in the upper 50 mm of sub-aqueous sediments was contaminated enough to present health risks to the aquatic food chain (USEPA, 1997) and the water bodies affected include streams, lakes, harbors, near-shore areas, and oceans (USEPA, 2004). Data is not sufficiently available in developing countries, however, it is inevitable that the rapid industrialization will cause severe pollution due to absence of regulations.

The existing state of practice to treat polluted sediments is either removal of the sediment for treatment or storage, or isolation with some combination of natural soil and/or geosynthetic layers. Some aqueous sediments are contaminated by a wide variety of contaminants. In these cases, the sediments are usually dredged instead of using in situ remediation methods. Apart from remediation, dredging is necessary to prevent flooding, to facilitate navigation and to allow for the uses of a given water system. According to a estimation from SedNet (European Sediment Network), around 100 and 200 million cubic meters of contaminated sediment might be produced yearly in Europe (Bert et al., 2009). Confined disposal to a CDF (confined disposal facility) or licensed landfill is the most widely used option for managing contaminated sediments.

1.2 Problem definition

Although land disposal of waste has been practiced since ancient times, numerous serious pollution problems and other hazards to human and environmental health caused by landfilled wastes have been identified in many industrialized countries. This has stimulated extensive researches into the causes of landfill pollution as well as the development of many improvements in waste disposal design technology and practice.

Advances made in controlling landfill pollution are based on understanding and minimizing the transport of contaminants from the waste into the surrounding environment. The containment strategy is to encapsulate the waste in some forms of seepage barrier that assists in isolating the waste from the groundwater systems and adjacent natural surface. Generally,

Figure 1.1: Historical pollution at Odda (Norway) before clean-up operations (www.miljostatus.no/PageFiles/283)

the barrier systems include cover and liner components. The cover placed over the waste after emplacement is designed to limit water infiltration from the surface and also contain the landfill gas in some instances. Liner systems primarily function to prevent contaminated liquid (leachate) from exiting a landfill through its bottom.

Earthen contaminant barriers are widely used in landfills and other waste containment facilities, e.g., for disposal of dredged sediments. Modern composite barrier systems include a geomembrane underlain by a low permeability soil layer. Providing that geomembrane defects are few and good adhesive contact with soil barrier layer is achieved, the system will be particularly effective to prevent breakthrough of contaminants. Alternatively, a thin extremely low permeability geosynthetic clay liner (GCL) may also be used. By the virtue of its low cost, it can be used in addition to an (engineered or natural) earthen layer to improve overall barrier integrity. However, it is not wise to use GCL to replace engineered soil liner. Due to the small thickness, GCL has a small attenuation volume and investigations have found that the mass flux of organic substances, such as toluene through the GCL composite liner is two to three orders of magnitude greater than the CCL (Nguyen et al., 2011).

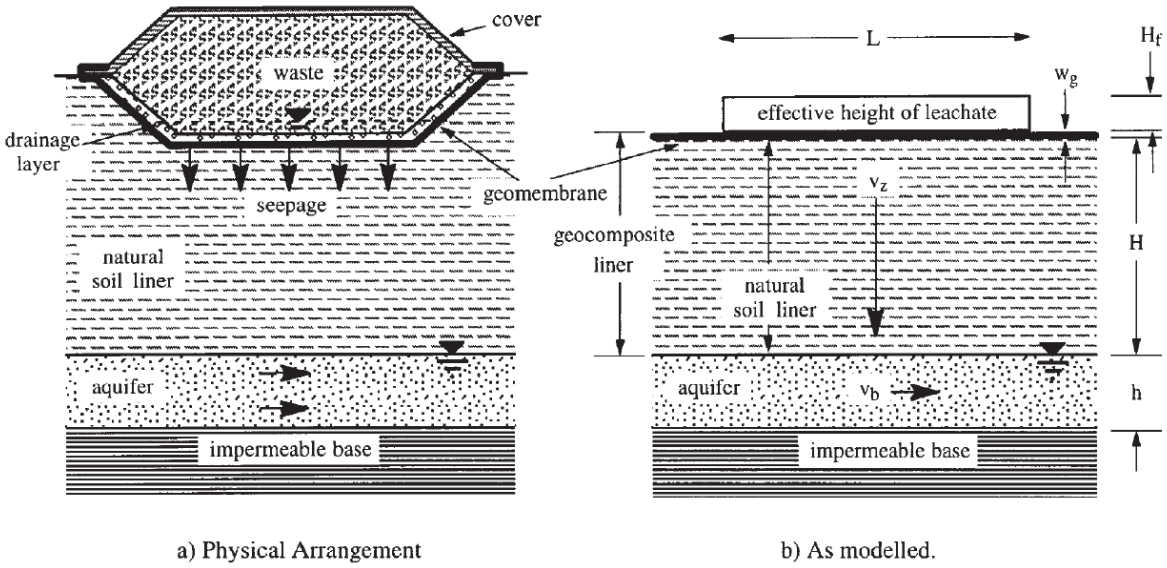

Figure 1.2: Schematic of typical landfill arrangement (Fityus et al., 1999)

A typical illustration of composite liner system is shown in Figure 1.2. Well-constructed geomembrane is impervious to water and soluble inorganic contaminants. However, the organic compounds can diffuse through the geomembrane and invade the soil liner underneath.

Typically, the low permeability soil can be natural low permeability geological deposit or an engineered soil layer such as a CCL. In some circumstances, the mineral processing wastes (e.g., red mud from alumina refining) and soils produced from crushed mudrocks are utilized in areas where the natural low-permeability soils are scarce. When economic constraint is predominant, the costly highly engineered barrier systems are impractical. In such cases, the abundant natural soft clay deposits are used as substitute for CCL. Since the soft clayey soil generally provides a relatively good contact adhesion with a geomembrane, the effectiveness may be expected.

The liner systems are generally simultaneously subjected to mechanical loading arising from the overburden load. Conventionally, the effects of mechanical loading are ignored in contaminant barrier design. However, the validity of this has been challenged by some recent field observations of accelerated contaminant migration at landfills. Conceptually, this is obvious in liners where the one-way, outward drainage of pore water from the barrier due

to consolidation leads to unanticipated advection of contaminants. This is likely to be increasingly important as the size and depth of landfill becomes much larger than in the past as a result of the difficulties in permitting new landfill sites. For example, the recently opened Woodlawn landfill near Sydney, Australia is 170 meters deep. Moreover, the consolidation will be more pronounced when relatively soft natural sclay deposits are utilized instead of CCL. Strictly speaking, the liner systems are also affected by chemical effects. But when there are few defects in geomembrane, the chemical effects can be neglected because the impervious geomembrane prevents leachate including inorganic compounds and the concentration of organic chemical encountered is low. In fact, the mass flux through defects because of the small area of defects considered is negligible compared with that through the intact part of composite liner system (Nguyen et al., 2011).

Most current researches assume that the liner is fully-saturated. However, the soil beneath a landfill is partially saturated when the landfill is constructed in arid or semiarid environments. At presence of the low-permeability capping layers and liners, the partially saturated conditions will prevail beneath landfills. On the other hand, some of the municipal solid waste constituents will biodegrade over time which generate heat. The rising temperature can significantly impact the geotechnical properties of cover and liner system by increasing the hydraulic conductivity and chemical diffusivity of the barriers. Zhou and Rowe (2005) suggests that heat generated in a landfill waste body could cause significant loss of water content in clay liners and therefore more cautions should be put on heat in landfill design. When the soil de-saturates due to loss of water content in response to heat, the initially occluded air bubbles becomes continuous and moisture movement by diffusive water vapor transfer and partial pressure gradients becomes possible. In that case, VOCs may break through liner system in a manner of multi-phase transport.

1.3 Motivation and aim

To acquire a safe barrier design, an adequate transport modeling is essential. The conventional simplified models assume a non-deformable medium, or a full-saturated deformable

liner and neglect the heat generated from waste degradation. These assumptions may not be valid and lead to important errors when these models are used to predict contaminants migration in some circumstances.

The primary aim of this study is to propose and verify more elaborate mathematical models able to describe the behavior of soil liner with respect to contaminant migration under conditions of overburden and heat generation. Furthermore, the models also can aid understanding of chemical transport in polluted sediments either dredged and placed in CDF or capped in situ. Due to the inaccessibility, there is a lack of available field data on both the consolidation of barriers and chemical mobility behavior. Therefore, theoretical approach based on mathematical modeling is employed in the current work.

Chapter 2

Literature Review

This study is based on the existing knowledge on mass (e.g., contaminant and heat) transport in soil medium and soil consolidation theory. A detailed review of previous work is presented in this section. Then, comments are made with respect to the specific aim of this thesis. And, the organization of the thesis will be presented. Following it, the symbols used within this chapter will be listed.

2.1 Constituents of soil liner

As a naturally-made deposit, the soil has a complex structure. In the scope of this thesis, the scale of macro-scope is of interest. In general, soil is commonly recognized as a mixture of several phases: soil solid, pore water and pore air. The contaminant can reside in three phases or only solid and aqueous phase depending on the characteristics of specific substance.

The fluid phase and solid phase are continuum concepts, obtained from the molecular level by volume averaging over appropriate representative elementary volume (REV) (Bear and Cheng, 2010), which is used to represent the characteristics of porous medium at all points in the domain. The size of REV is selected so that (1) the average value of any geometrical characteristic of the microstructure of the void space, at any point in a porous medium, can be approximated by a unique function within an acceptable error and (2) the average value should remain more or less constant within REV.

By virtue of the concept of REV, the relative proportions of constituent volumes are expressed by the porosity n and the degree of saturation, S_r:

$$n = \frac{V_v}{V_t}, S_r = \frac{V_f}{V_v} \tag{2.1}$$

where V_t is the total volume, V_v is the pore volume, and V_f is the fluid volume.

The degree of saturation, S_r can be used to divide the soil into three groups (Fredlund and Rahardjo, 1993):

1. $S_r = 100\%$, fully saturated soil: There is no air appearing ideally and all voids are filled with pore water.

2. $S_r = 0\%$, completely dry soil: No free water is present except the water absorbed onto the diffusion layer of solid grain particle.

3. $0\% < S_r < 100\%$, unsaturated soil: The voids are partially filler with pore water and the pore air can be continuous or discontinuous.

The subdivision of "unsaturated soil" is primarily a function of the degree of saturation, S_r. There exists a critical value for S_r, around which the transition of air phase takes place. When the degree of saturation is above the critical value, the air is in the form of occluded air bubbles. This state is referred to as "nearly saturated" or "quasi saturated".

The critical degree of saturation depends on the soil type (Corey, 1957). Its typical value is from 85% to 90% (Fredlund and Rahardjo, 1993; Corey, 1957) while Bear (1979) indicated a degree of saturation of greater than 75%. For compacted clays, Barden (1965) suggested the air voids are continuous up to a degree of saturation of 90%. In terms of moisture content, he quoted Gilbert (1959) who claimed that air voids are fully continuous when moisture contents is lower than optimum moisture content up to 4%, and are fully disconnected at a moisture content of 3% above optimum in a similar material.

Since there will be certain amount of air dissolved in soil pore water, the full saturation, however, is hardly ever attainable in field conditions. Actually, the fully-saturated and completely dry soil condition are satisfied only in laboratory controlled environment. Therefore,

most of the soil liner falls into the partially saturated state particularly when the requirement of optimum water content (the water content at which a specified compactive force can compact a soil mass to its maximum dry unit weight) for CCL dictates that the soil is of an unsaturated condition.

Individual soil phase and its volume and mass in a unit volume of soil are shown in Figure 2.1. The mass (pore water, heat and contaminant) conservation equations are based on this information of the mass and volume proportions of each phase in soil.

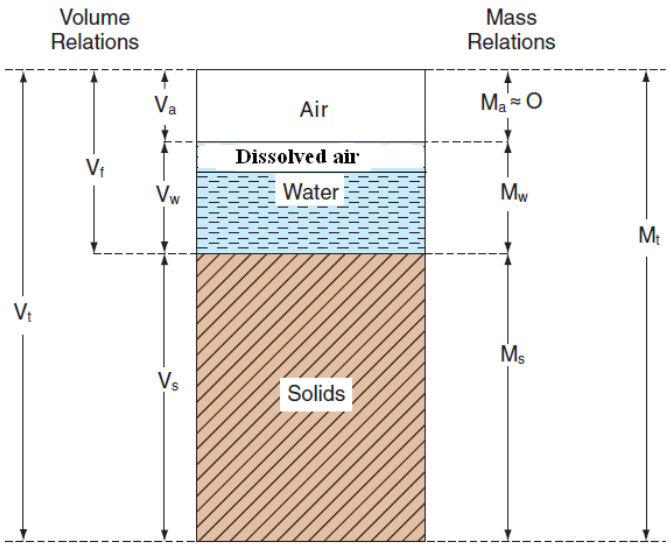

Figure 2.1: Schematic of soilwater characteristic

2.2 Contaminant transport in soil liner

Cartwright et al. (1977) collected leachate from a sanitary landfill and passed them through clay columns in laboratory. It was found that heavy metals, such as Pb, Cd, and Zn, were attenuated by even small amounts of clay. Therefore, natural clay deposits and compacted clay liners are widely used as landfill barriers to attenuate and prevent the pollution of water resources by landfill leachate. Numerous investigation have been done to model the landfill leachate migration through clay liner system. Generally, the models employed fall into two groups: saturated and unsaturated models.

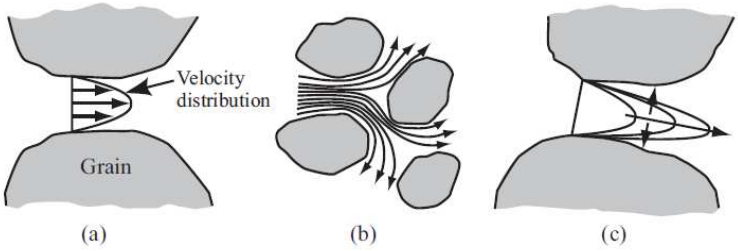

Figure 2.2: Mechanical dispersion (a, b) and molecular diffusion (c) (Bear, 1979)

2.2.1 Solute transport in saturated soil

When the clayey barriers are located below the water table and compacted with the water content on the wet side of the optimum moisture content, they can be assumed to be saturated (or nearly saturated) (Rowe, 1989). In this subsection, a brief review of the investigation of solute transport in saturated clay liner will be presented.

Rowe and Booker (1985) developed a technique to analyze one-dimensional single solute transport in a layer of finite thickness. The movement of contaminants through clayey liner was described by the combination of advection, diffusion-dispersion and chemical retardation. Advection represents the carrying of dissolved chemical species by the pore fluid flow in porous medium. Diffusion is a physical process where the chemical species move from the location of high concentration to points of low concentration, which can be modeled using Ficks law. The contaminant plume spreading phenomenon in a porous medium domain is called mechanical dispersion. The schematic of diffusion-dispersion of solute in porous medium is illustrated in Fig. 2.2.

Although the mechanism of mechanical dispersion is totally different from the diffusion process, it is adequate for most practical purpose for them to be mathematically modeled in the same way. Hence, a composite parameter D called the "coefficient of hydrodynamic dispersion" is used to lump the two processes together (Rowe and Booker, 1985). Considering the mass balance, Rowe and Booker (1985) gave the solute transport equation for saturated soil as

$$(n + \rho K_d)\frac{\partial c}{\partial t} = nD\frac{\partial^2 c}{\partial z^2} - nv\frac{\partial c}{\partial z} \tag{2.2}$$

where n is soil porosity, ρ represents the bulk density of soil, c denotes the contaminant concentration at a depth z at time t, K_d is the distribution coefficient, v is the average linearized ground water velocity and also referred to as "advection velocity". The advection velocity depends on the hydraulic conductivity of the clay and the hydraulic head gradient at a disposal site. In the parametric analysis for the advection effect on contaminant transport, Rowe and Booker (1985) assumed a range of spatially and temporally constant advection velocity values.

Equ. (2.2) simply states that rate of contaminant concentration change within represent element volume (REV) equals the increase in mass due to advective-diffusive transport minus the mass of contaminant removed from solution by sorption process. When the mass concentration is relatively low as encountered in practical applications, the sorption process can be approximated by a linear relationship. Based on the governing equation, Rowe and Booker (1985) modeled a finite quantity of pollutant in the landfill break through a saturated clay liner underlain by coarse sand base and Rowe (1989) discussed the relative importance of transport mechanisms such as diffusion, dispersion and advection as well as the significance of attenuation mechanisms. Rowe and Booker (1986) extended the model to pollutant migration through a three dimensional layered soil medium.

Rowe and Badv (1996b) performed diffusion and advection-diffusion tests for chloride through single fine sand, silt, and clayey silt and a two-layer soil system consisting of a compacted clayey silt underlain by either a fine sand or silt. For near-saturated soil, the soil porosity, n in the model was replaced with volumetric water content, θ to simulate chloride migration in soil column. The model predictions compared well with the experimental results. Rowe and Badv (1996b) claimed that the solute transport theory used can adequately predict chloride migration through a compacted clay layer and underlying sand or silt layer at near-saturated conditions for Darcy velocities at least up to the maximum value examined (0.0183 m/yr). However, it should be noted that the seepage flow in the tests is generated by a water reservoir placed on top of the soil column and there was no external loading and no significant deformation involved in the tests procedure.

Considerable amounts of VOCs, such as Benzene, toluene, and m-xylene were detected in leachate of solid waste landfills (Gibbon et al., 1992; Krug and Ham, 1995; Kim et al., 1995). To prevent the seepage flow due to the leachate, the modern solid waste landfill liner systems add a geomembrane layer at the top of clay liner. The geomembrane is typically a 1.5-mm sheet made from high density polyethylene (HDPE) and is essentially impervious to diffusion of inorganic solutes compared to many organic solutes (Haxo and Lahey, 1988; Giroud and Bonaparte, 1989). However, long-term (of the order of decades) migration of VOCs remains as a primary concern because the low attenuation capacity of soil liners (Cartwright et al., 1977), high diffusion rates through geomembranes (Park and Nibras, 1993) and the health hazards at low concentration levels of VOCs (Kim, 1997).

In order to compare the migration of VOCs from a composite liner system and a compacted clay liner, Kim (1997) utilized a one-dimensional mass transport of a contaminant through a saturated soil liner with the first order degradation expressed as follows

$$\frac{\partial c}{\partial t} = \frac{D}{R_f}\frac{\partial^2 c}{\partial z^2} - \frac{v}{R_f}\frac{\partial c}{\partial z} - \frac{K_r}{R_f}c \tag{2.3}$$

where K_r represent the first order degradation rate in the soil liner and R_f is dimensionless retardation factor. The equation was solved numerically by the implicit finite difference scheme. In the composite liner, the seepage velocity is the greater one between the leakage rate through the physical defects on geomembrane and the seepage capacity of soil liner. With the assumption of linear sorption, R_f can be estimated using

$$R_f = 1 + \frac{(1-n)\,\rho_s K_d}{n} \tag{2.4}$$

in which ρ_s denotes dry density of the soil solid.

Foose et al. (2002) compared the performances of three types of composite liners which consist of a geomembrane and underlying geosynthetic clay liner (GCL, thin factory manufactured clay liners 10-mm thick that are filled with bentonite clay), thiner or thicker compacted clay liner, respectively. Both inorganic and organic contaminants can move through

the geomembrane defects by advection and diffusion. When analyzing the contaminants transport through intact composite liners, one dimensional solute transport equsation similar to Equ. (2.3) was used except that the chemical reaction was not concluded, i.e., $K_r = 0$ and $v = 0$ because the bulk porous flow is avoided due to the impervious geomembrane. Hence, the solute transport through clay liner solely via the pure diffusion mechanism. Peters and Smith (2002) also used the pure diffusion equation as baseline model when investigating the effect of consolidation on solute transport in CCL.

Mathur and Jayawardena (2008) made a attempt to estimiate numerically the optimum thickness of clay barriers by using a one-dimensional model based on the leachate travel time for dissolved organic carbon and chlorides. The assumption of saturated clay liner was claimed to be validated by a more conservative results.

Nguyen et al. (2011) developed a finite difference model of diffusive transport through intact liners on the basis of the "pure diffusion" transport mechanism. The model was used to estimate the VOCs mass flux through four different municipal solid waste landfill liner systems, i.e., Subtitle D composite liner system (the liner prescribed in Subtitle D of the Resource Conservation and Recovery Act, US EPA), composite liner system with a geosynthetic clay liner (GCL) instead of low permeability compacted soil, Wisconsin NR500 liner system (the liner prescribed in the Wisconsin Administrative Code Section NR500), and a proposed four-component composite liner system that is a combination of the GCL composite liner system and the Subtitle D liner (with a 61 cm or 91.5 cm thick compacted clay liner). In the simulations, all the composite liner were assumed to be without significant defects.

Mueller et al. (1998) developed an analytical solution for the steady-state flux of VOCs diffusing in a composite liner. However, the equations solved did not include boundary condition in terms of solute flux or concentration at the base of the liner (Foose et al., 2002).

Using the "pure diffusion" equation, Foose (2002) reported an analytical solution for transient solute diffusion of volatile organic compounds in a composite liner, which included a geomembrane and a compacted soil liner or geosynthetic clay liner. A condition of continuity of solute flux is imposed on the internal boundary, i.e., the interface between geomembrane and soil liner. In addition, there is a constant non-zero concentration of solute at top of

geomembrane and the concentration of solute beneath the composite liner is zero. Based on two criteria (leachate constitute concentration and flux at the bottom of liner, respectively), a transit-time design method was proposed. The assumption of saturated conditions for compacted soil liners was made to approximate the high saturation ($S_r \geq 85\%$) in construction after Benson et al. (1999).

Edil (2003) presented a review of recent researches on developing the approaches to determine mass transport parameters for transport of VOCs in liquid phase through saturated compacted clay liners, geosynthetic clay liners (GCLs), and geomembranes.

In summary, the advection-dispersion equation has been intensively used to simulate migration of both organic and inorganic contaminant within saturated clay liner. At presence of impervious geomembrane with respect to inorganic substances, the transport of VOCs in intact saturated clay liner is mostly modeled using the "pure diffusion" equation.

2.2.2 Solute transport in unsaturated soil

There are many situations where the clay liner at bottom of a landfill is partially saturated. The unsaturation arises from two respects: first, the surrounding environment in which the liner is constructed. If the landfills are constructed in arid or semiarid environments, where groundwater table is located at some distance below the geomembrane, the liner could not be fully-saturated. Bonaparte and Gross (1990) investigated 55 landfills and reported that 53 had water tables below the base of the landfill. Particularly, when the air-entry value of the soil is not too high, certain depth of soil beneath the landfill will be in a state of partial saturation (Fityus et al., 1999). Next, the well-built geomembrane avoid seepage of leachate into the compacted clay liner, which is partially saturated due to the requirement of compaction. Therefore, the partially saturated conditions prevailing beneath landfills is a commonplace occurrence (Fityus et al., 1999). Unfortunately, there are much fewer literature on solute through unsaturated clay liner compared with in saturated case.

The contaminant transport in unsaturated soil is mostly represented by the advection-dispersion equation and the accompanying porous flow is modeled by Richards equation (van Genuchten, 1991). However, the porosity, n appearing in the corresponding equation

for saturated liner should be replaced with the volumetric water content, θ. Assuming the moisture content is spatially and temporally invariant, van Genuchten (1981) presented an analytic solution to the dispersion-advection equation in a partially saturated soil.

Rowe and Badv (1996a) presented a method for estimating the advective-diffusive transport of sodium chloride through a layered system consisting of a compacted clayey layer over unsaturated fine gravel where the degree of saturation varies substantially between the bottom of the clay and water table. Over the range of conditions examined, Rowe and Badv (1996a) concluded that solute transport equation is adequate in simulations.

Fityus et al. (1999) predicted the transient nonvolatile contaminant distributions beneath a landfill using the advection-dispersion equation upon the assumption of steady-state unsaturated moisture distributions. A finite layer formulation was used to simplify the linear, second-order, partial differential one-dimensional contaminant mass transport equation, and the heterogeneity was accounted for as well. In order to highlight differences between contaminant transport through saturated and unsaturated soils, Fityus et al. (1999) postulate a function to relate volumetric water content and effective hydrodynamic dispersion coefficient, which was deomonstrated to have a significant effect on diffusive mass transfer through soil liner. In modeling of Fityus et al. (1999), the invariant advective pore water velocity was determined from hydraulic gradient across the soil liner and hydrological conductivity. The diffusive contaminant mass transport through geomembrane was predicated upon the assumption that the mass transfer is proportional to the contaminant concentration difference across the membrane. The boundary conditions took into account the finite contaminant mass, namely, the mass concentration at top of liner will gradually decrease as contaminant moves into the liner-aquifer system. Fityus et al. (1999) employed Laplace transform and obtained the mass flux expressed in terms of concentration as boundary condition.

Regarding the assumption of steady-state unsaturated moisture distributions, Fityus et al. (1999) justified it from two respects. Firstly, due to the impervious geomembrane overlying, the water content in the partially saturated soils is expected to attain an ultimate steady state. Secondly, the time period over which transient moisture change occurs is relatively shorter with respect to the time scale for contaminant mass transfer from the landfill barrier.

Therefore, the error introduced by assuming that contaminant transport takes place through soil with steady-state moisture conditions is acceptable from the viewpoint of an engineering contaminant transport design analysis. Fityus et al. (1999) also performed a analysis using Richards equation based on sand and clay soil to verify the this assumption. As expected, equilibrium moisture conditions were achieved more quickly for the coarser soil (in a matter of days for sand soil). For the clay soil, the time required to reach moisture equilibrium could be around 8 years. However, it was sufficiently small relative to the time taken for say 10% of the contaminant mass to break through the unsaturated soil liner, which was of the order of one hundred year. Hence, Fityus et al. (1999) concluded that the temporally constant moisture profile beneath the landfill is a reasonable approximation.

Fityus et al. (1999) found that unsaturated condition does not ensure a reduction in mass flux. Although it has the obvious effect of reducing the conductive cross-sectional area through which a contaminant may flow, the increase in moisture content with depth serves to dilute the contaminant concentration as it is transported through the soil liner, which can increase the spatial concentration gradient and eventually speed up the diffusion. Therefore, the degree of sensitivity of mass transfer characteristic of liner to S_r depends on the net effect of the two opposing effects.

In the very few existing investigations concerning solute transport in unsaturated clay liner, Richards equation is conventionally used to describe unsaturated porous flow. It is based on the assumption that the water vapor flow is small and can be neglected under isothermal conditions (Fredlund and Rahardjo, 1993; Fityus et al., 1999). On the other hand, the solute transport occurs solely in aqueous phase. However, volatile organic compounds resides not only in the dissolved phase and solid phase, but also in gaseous phase. When the degree of saturation is sufficiently low, the air phase in clay liner becomes continuous. Due to the largely greater (around three to four orders) diffusion of VOCs in air phase than in liquid phase, the advection-dispersion equation established solely for aqueous phase will significantly underestimate the migration of VOCs in unsaturated clay liner. Therefore, the approach based on the advection-dispersion equation (ADE) for liquid phase is only acceptable for transport of the dissolved nonvolatile organic or inorganic solute; Or, for the cases

where the degree of saturation of clay liner is high so that the soil air phase exists in the form of occluded bubbles.

Additionally, solute transport characteristics for VOCs in unsaturated clay liner depend on degree of saturation. According to the available experimental data, the diffusion coefficient is significantly reduced as the soil becomes unsaturated (Barraclough and Tinker, 1981; Conca and Wright, 1990; Fityus et al., 1999), which can be attributed to the decreasing continuity and increasing tortuosity as the volumetric moisture content of the soil decreases.

2.3 Consolidation theory

In real environment, the landfill clay liner inevitably experiences volume change during its serving life. For instance, the pore water and air will be expelled due to the placement of waste (namely, mechanical consolidation progress). Moreover, changes in the chemistry of the pore fluid as a result of leachate in clay liner can lead to "osmotical consolidation" (Kaczmarek and Hueckel, 1998). In some soil (for example, kaolinitic clay) at low water content, osmotically induced fluid flow occurs in response to contaminant concentration gradients (Fityus et al., 1999). The mechanism behind it is that the soil can act as a imperfect semipermeable membrane. In the scope of this thesis, focus is put on the effect of mechanical consolidation on porous flow, which can be estimated via the consolidation theory.

Mechanical consolidation is the progress whereby the pore fluid flows out and excess pore fluid pressure dissipates. Meanwhile, soil volume decreases as there is a gradual transfer of stress due to external loading from the pore fluid to the soil skeleton. The rate of consolidation is determined by the rate at which pore fluid can flow out of the soil. Hence, it is a deformation and pore fluid flow coupling problem. The consolidation equation follows from the integration of mass conservation equations (fluid phase and solid phase) and force equilibrium. As for the soil, it is limited to poroelastic material in this thesis.

2.3.1 Deformation and flow coupling for saturated soil

2.3.1.1 Infinitesimal small strain model

Terzaghi (1925) proposed the widely used one-dimensional consolidation theory based on the fowllowing assumptions:

- the homogeneous soil is fully saturated by pore water,
- water flow and soil deformation only occur in the vertical direction,
- pore water flow is governed by Darcy's law with constant coefficient of permeability,
- the soil particles and water are incompressible,
- change in the thickness of soil column is negligiblly small,
- the total stress remains constant everywhere throughout the consolidation process and the strains are caused only by the change of pore fluid pressure.

Terzaghi one-dimensional consolidation theory with the basic variable of excess pore water pressure is also referred to as "linear consolidation". Though it enjoyed a vast application due to simplicity, some of the assumptions severely restrict its use in practice. Thereafter, many researchers attempted to relax some of the assumptions that Terzaghi (1925) made.

Biot (1941) developed a three-dimensional consolidation theory based on the primary variables of soil displacement components and pore water pressure. The interaction between skeleton and pore fluid is explicitly included in the formulations. The soil stresses are related to displacement components using the linear stress-strain relations.

Davis and Raymond (1965) evolved Terzaghi's model by taking into account decreasing of permeability and compressibility within the soil as pressure is increasing. Regarding the time varying load and total stress, Olson (1977) derived a analytical expression for one-dimensional consolidation of homogeneous soil layers subject to ramp loading and Conte and Troncone (2006) presented an analytical solution for the analysis of one-dimensional consolidation of saturated soil layers subjected to general time-dependent loading. The modified

Terzaghi consolidation equation is capable of accounting for the compressibility of pore water and air mixture for the nearly saturated soil where the pore air exist in the form of occluded bubbles and can flow under the pore water pressure gradient.

Bear and Cheng (2010) presented a pore fluid storage equation in a deformable saturated porous medium. In the derivation process, the deformable porous media were featured as: 1) time-dependent porosity, i.e., $\partial n/\partial t \neq 0$, 2) moving solid matrix, i.e., $\overrightarrow{\mathbf{v}_s} \neq 0$, the fluid flux was expressed relative to the moving solid. In the derivation of fluid equation, the density of pore fluid was assumed to depend on fluid pressure, i.e., $\rho_f = \rho_f(p)$. With the definition of the coefficient of fluid compressibility, β by $\partial\rho_f/\partial t = \rho_f\beta\partial p/\partial t$, temporal and spatial variation of fluid density were included.

Generally speaking, the above consolidation equations can fall into two categories of Terzaghi and Biot types. Explicitly coupling deformation and fluid storage equation provides the latter one with greater versatility. For example, by the virtue of separate stress equivalence equation, the total stress in soil can vary both temporally and spatially. In the case of consolidation due to or affected by soil self-weight, this feature will be essential. Moreover, more advanced soil elastoplastic characteristics can be included in the deformation (stress equilibrium) equation as well.

2.3.1.2 Finite strain model

In some circumstances, large deformation occurs due to the heavy loading acted on relatively soft soil. Thus, the assumption of constant thickness is not rational any more. Meanwhile, the void changes significantly during deformation and consequently the coefficient of permeability and compressibility of soil skeleton (characterized by coefficient of compressiblity, m_v or shear modulus, G) will vary during the consolidation. Therefore, a nonlinear consolidation theory is desirable.

The first work in deriving an equation without the limitation of the infinitesimal strain in the normal consolidation theory was Gibson et al. (1967), which removed the approximations of constant permeability parameter and compressibility coefficient. Instead, they

were taken as functions of the effective stress. Moreover, the density of pore fluid is dependent on local fluid pressure. The nonlinear consolidation equation was featured by 1) being casted in Lagrange co-ordinate system, in which the conservation of solid mass is conveniently expressed, 2) by virtue of concept of effective stress, the gradient of fluid pressure which used to govern Darcy's flow is expressed in term of gradient of effective stress and total stress, where the former one is in turn related to void ratio gradient and the latter one is provided by the vertical force equilibrium. Eventually, the equation is based on the primary variable of void ratio. For sake of reducing the degree of complexity, Gibson et al. (1967) introduced extra approximation to make it a linear finite-strain equation. The nonlinear consolidation proposed by Gibson et al. (1967) has been extensively employed since its commencement. For example, Morris (2005) presented analytical solutions for linear finite-strain one-dimensional consolidation of initially unconsolidated soil layers with surcharge loading for both one and two-way drainage.

However, some boundary or initial conditions are not easily expressed in terms of void ratio in practical applications. As an alternative approach for large strain consolidation solution, Fox and Berles (1997) developed a piecewise-linear finite difference scheme for one dimensional large strain consolidation. In the piecewise-linear, or "piecewise-iterative" method, all variables pertaining to problem geometry, material properties, fluid flow, and effective stress are updated at each time step with respect to a fixed coordinate system (Fox and Berles, 1997). The Lagrangian approach was retained to ensure the solid mass conservation. The shortcomings of this method arise from the computing effort and complex solving procedure involved.

Apart from these approaches, other investigations also have been performed to solve the nonlinear consolidation. For instance, Papanicolaou and Diplas (1999) solved the non-linear consolidation induced by self-weight numerically in the Eulerian coordinate system.

The aforementioned consolidation models either for infinitesimal small strain or finite strain all treat pore fluid flow in soil as a single phase. This is only applicable to the completely-saturated or quasi-saturated soil.

2.3.2 Deformation and flow coupling for unsaturated soil

In this section, attempts made in solving consolidation in nearly-saturated and unsaturated soil with continuous air phase are reviewed. The difference between models for unsaturated soil and saturated soil is the treatment of air phase. First, the attention is paid to the nearly-saturated soil, which differs from saturated soil in the compressibility of pore fluid due to presence of air bubble and dissolved air. At present, the mostly used method is to take the air-water mixture as a compressible homogeneous fluid. Following it, the models for general unsaturated soil with continuous air phase will be presented.

2.3.2.1 Nearly-saturated soil: occluded bubble and its influences

Vaughan (2003) reviewed the behavior of clay fill containing occluded air bubbles and gave three situations where air bubbles can be generated:

- The occluded air state may be caused during the procedure of compaction;
- For a fine-grained soil initially compacted with continuous air, the sufficient loading may expel enough air volume and then create a discontinuous state. Accompanying it, the negative pore water pressure would change to positive.
- A occluded air state can be caused by when a filling material initially with continuous air is flooded with water due to either gravity or pressure.

Moreover, the pore air pressure in occluded bubbles is thought to be unlikely to affect effective stress (Vaughan, 2003), which is defined by the difference between pore water pressure and total stress proposed for fully-saturated soil.

Additional evidences have been reported in the literature that persistence of occluded air bubbles can remarkedly influence the soil behavior (Fourie et al., 2001). Sherard et al. (1963) took undisturbed soil samples near the upstream slope of a compacted earth dam which had been in operation for 25 years and found that 8% of total soil volume was filled was air. St-Arnaud (1995) discovered that the occurrence of occluded air bubbles contribute to reduction of the permeability characteristics of downstream filters in earth dams. Fourie et al. (2001)

experimentally investigated the effect of occluded air bubbles on liquefaction potential of the tailings sand. The response to undrained loading of the pore pressure within the tailings specimens was found to be greatly affected due to even a very small percentages of occluded air by volume.

By capillarity, pore water pressure in unsaturated soils must be lower than pore air pressure. For a quasi-saturated soil, the pore water pressure in the field is above atmospheric. Therefore, the air pressure must be higher still (Vaughan, 2003) and hence exists in the form of occluded bubbles. Since air pressure is unknown within air bubbles (Fredlund and Rahardjo, 1993), it is difficult to mathematically determine the variation of air bubbles volume, though it is clear that the volume will decrease if the pore pressure increases.

For saturated soil, the pore water is commonly assumed to be incompressible. However, the presence of occluded air bubbles increases the compressibility of pore fluid (air and water mixture) significantly. The compressibility of the air-water mixture has been investigated using Boyle's and Henry's Laws. Boyle's Law dictates that "at a constant temperature, the volume of a given quantity of any gas varies inversely as the pressure to which the gas is subjected" (Weast, 1980) while Henry's Law states that "the weight of gas dissolved in a fixed quantity of liquid at constant temperature, is directly proportional to the pressure of the gas above the solution" (Fredlund, 1976).

Bishop and Eldin (1950) developed expressions for the compressibility without accounting for surface tension effects, which implied that the air bubbles within the water were at the same pressure as the water. Schuurman (1966) claimed that it was essential to include surface tension effects in an air-water compressibility formulation. Neglecting the compressibility of pore water, he wrote his expressions in terms of the current volume of air as opposed to the original volume (Akers, 2001). However, there is an inconvenience in applying the formula proposed because it requires the radius of the air bubbles, yet little if any experimental data was available to provide this necessary information.

Following it, Fredlund (1976) also developed an expression which assumed that the water had a finite compressibility and was able to consider the surface tension in a manner that did not require a knowledge of air bubble sizes. In the expression, Fredlund (1976) used a

pore pressure parameter which could be evaluated experimentally to describe the difference between the air and water pressures. The difference was assumed to vanish when the air becomes occluded. Later, Chang and Duncan (1977) proposed their expressions for the compressibility of an air-water mixture similar to the equations of Schuurman (1966) where the water was assumed to be incompressible.

Alonso and Lloret (1982) reexamined the previous compressibility curves developed by different investigators and formulated their own expressions for the compressibility of an air-water mixture. They assumed a finite compressibility for water and accounted for surface tension in the same manner as Fredlund (1976). In this study, the compressibility of pore fluid, i.e., the mixture of air-water, is based on expression of Fredlund (1976).

Concerning the effect of occluded air bubbles on consolidation of quasi-saturated soil, researchers usually based it on the Terzaghi consolidation. For example, Barden (1974) stated that if the soil skeleton compressibility, m_v was defined with respect to overall settlement (initial plus consolidation), the predicted amount of water leaving the clay was the same as if the air bubbles were not present, which was in agreement with Terzaghi (1943). In this sense, the compressibility of the pore-fluid should not be a particularly important factor and Terzaghi theory should prove adequate.

Avoiding to unravel the complexities involved in analyzing flow and deformation in unsaturated soils, Vaziri and Christian (1994) developed a general form of Terzaghi's one-dimensional consolidation theory which was demonstrated to qualitatively capture the consolidation behavior of nearly saturated soils with S_r above 92%. Employing Terzaghi's assumptions, Vaziri and Christian (1994) transformed the unsaturated soil into a material whose pores were fully saturated with an equivalent compressible fluid and derived a consolidation equation which was same as Terzaghi in the form but with the exception that the consolidation coefficient, c_v was replaced with c_v^*. c_v^* was obtained by dividing c_v with a reducing factor which accounts for the effect of pore fluid compressibility. The proposed equation was restricted to all the other assumptions and limitations embodied in Terzaghi's consolidation theory which include the assumption of a constant hydraulic conductivity, K throughout the consolidation period.

It is conceivable for small spherical bubbles to exist temporarily (Hilf, 1956) and travel with the free pore-water as a homogeneous compressible fluid. However, in clays which is compacted with the water content on the wet side of the optimum value (especially when the degree of saturation is relatively low, say 75% to 80%), the dispersed fabric implies a low value of permeability, and it is unlikely that a sufficiently high number of free bubbles will be of such a microscopic radius to flow freely through a clay soil and exert an important influence on the flow process (Barden, 1974). In this case, the reduction in the volume of pore water and hence the permeability of the soil decreasing from the fully saturated case should not be neglected.

2.3.2.2 General unsaturated soil

There are two groups of coupling unsaturated flow theories: single phase flow and multi-phase flow. The former theory couples force equilibrium equation with a variant of Richard's equation, while the latter models the mass conservation of pore water and pore air separately.

Coupling four partial differential equations of force equilibrium in three directions and the water continuity equations, Biot (1941) proposed the general equations to describe the phenomena of transient flow and displacements occurring in three-dimensional deforming porous media. Based on the ideas of Biot's work, Bear and Corapcioglu (Bear and Corapcioglu, 1981a,b; Corapcioglu and Bear, 1983) presented a mathematical formulation to predict the land subsidence due to pumping from confined or unconfined aquifers. Pore water pressure was governed by the flow equation which was on the basis of continuity (or conservation) for compressible flow considering the volume change due to varying soil stress. The degree of saturation was a function of fluid pressure obtained by the retention curve in unsaturated media, which implied that it was applicable in either saturated or unsaturated conditions. When treating the pore fluid compressibility, Bear and Corapcioglu adopted directly the compressibility coefficient, while Biot (1941) introduced a multitude of physical constants. In the single-phase unsaturated porous flow model, the air pressure was assumed to equal atmospheric pressure. Consequently, air flow could be neglected. This approach

was extensively used to solve the coupled porous flow and unsaturated aquifer settlement during water pumping (Yeh et al., 1999; Kim and Parizek, 1999; Kim, 2000).

However, for general unsaturated soil, air and water phases within the unsaturated soil will flow due to excess pore-air and pore-water pressures in response to external load applied. This process continues until equilibrium conditions are achieved. To compute the transient change of the excess fluid pressure, two partial differential equations for pore air and pore water need be solved simultaneously. The equations can be established through considering the continuity of the water and air phases separately.

Based on the multi-phase flow, Fredlund and Hasan (1979) presented a general one-dimensional consolidation (or swelling) theory for unsaturated soils. Similar to Terzaghi theory, the flow of the liquid phase was described by Darcy's law. As for the air phase, its flow was assumed to be governed by Fick's law which states that the velocity of air flow is proportional to the vapor pressure gradient. The vapor pressure gradient depends on the concentration gradient of vapor. Different from the concept of effective stress applied to saturated or nearly-saturated soil, unsaturated soil requires set of stress indexes including the pore air pressure. In Fredlund's derivation, the net stress, $\sigma - p_a$ (where σ is total stress, and p_a is pore air pressure) and suction pressure, $p_a - p_l$ (p_l is pore liquid pressure) were selected to derive the constitutive equations for fluid flow.

In development of the isothermal multi-phase flow unsaturated soil consolidation theory, Fredlund and Hasan (1979) ignored the effects of air diffusing through water and the movement of water vapor. Following it, Fredlund continued to extended it to include temperature transfer (Dakshanamurthy and Fredlund, 1980, 1981) and three-dimensional consolidation model (Fredlund, 1982; Dakshanamurthy et al., 1984).

In parallel to Fredlund and Hasan (1979), Lloret and Alonso (1980) developed a general model of unsaturated consolidation which incorporated the joint swelling-collapse behavior and large variations in permeability coefficients with the saturation and deformation of unsaturated soils. Since it is not possible to formulate the consolidation behavior of unsaturated soil in terms of basic parameters which are conventionally employed in saturated consolidation (Lloret and Alonso, 1980), the same set of stress variables as Fredlund and Hasan

(1979) were selected in derivation and the effective stress concept was replaced by state surfaces. According to Matyas and Radhakrishna (1968), the state parameters such as state of stress, void ratio e, degree of saturation S_r and soil structure can precisely define the state of a soil element without reference to its previous history. Through experiments, relationship between those state parameters can be obtained and termed as "state surfaces". For case of monotonic changes in degree of saturation, S_r, these relationship functions provide unique state surfaces (Lloret and Alonso, 1980).

In the model of Lloret and Alonso (1980), the general equations expressing air and water continuity in an unsaturated soil were proposed in a manner that the volume change behavior of unsaturated soil is described using the experimentally attained state surfaces. When expressing the continuity of air phase, the dissolved air in pore water is also included with Henry's law. As a result, the mass conservation for air phase is directly coupled with water phase via the water velocity occurring in the air phase continuity equation. Moreover, an additional coupling is provided by the dependence of state parameters S_r and n on both water and air pressure.

Water permeability has been recognized to depend on soil gradation and composition, void ratio, fabric and degree of saturation (Lambe and Whitman, 1969). For a given soil with no significant change of fabric during consolidation process, void ratio and degree of saturation dominate permeability. Since variation of permeability with void ratio has been well documented and empirical relationships are also available (Gardner, 1960) based on suction (highly dependent on saturation), Lloret and Alonso (1980) combined them together to consider the effects of void ratio and saturation simultaneously.

Once occlusion of air bubbles prevails, the transfer of air mass within the soil matrix occurs mainly through three mechanisms (Lloret and Alonso, 1980): carrying by the free pore water flow in form of small air bubbles; transfer through the small percentage of interconnected air voids still existing within the soil; and movement with pore water in form of dissolved air. Lloret and Alonso (1980) claimed that the macroscopic coefficient of permeability can consider the first two mechanisms in a global way , and the motion of dissolved air had been successfully included in air phase continuity equation. In this sense, Lloret's

model is applicable to partially saturated soil in general, provided the state surface functions can accommodate large range of degree of saturation.

In the construction of the isothermal model, Lloret and Alonso (1980) ignored the continuity of the solid phase and the hysteresis effects due to the saturation history. What is more, vapor phase transfer was excluded in the isothermal formulations. However, Gardner (1960) asserts that even under isothermal condition, a noticeable changes in the vapour pressure can be caused by the high suctions in relatively dry soils.

Works of Fredlund and Lloret formed a theoretical framework for the study of the behavior of unsaturated soils. Despite the restrictions and assumptions embedded in, the models envisage the transitions in theory from a saturated soil to an unsaturated soil.

2.4 Non-isothermal porous flow in unsaturated soil

2.4.1 Thermo-mechanical-hydraulic model for unsaturated soil

Non-isothermal moisture movement in porous media has been of considerable interest. Compared with the isothermal cases, the driving forces associated with the liquid and vapor phases are not only the hydraulic potential gradient, but also the thermal gradients.

Philip and de Vries (1957) developed equations describing moisture and heat transfer in porous materials under combined moisture and temperature gradients. The moisture fluxes consisted of vapor and liquid and took into account of the effect of relative humidity (or soil water pressure) on the transfer. Additionally, the difference between average temperature gradient in the air-filled pores and in the soil as a whole was considered and the transfer of latent heat by distillation was included in the heat transfer equation. In the model derivation, Philip and de Vries (1957) neglected the dry air flow and the influence of soluble salts on the water humidity and pressure.

Model developed by Philip and de Vries (1957) for predicting the movement of water in rigid unsaturated soils in response to an imposed temperature gradient showed acceptable agreement with the observed water movement (Cassel and Nielsen, 1969) and consequently

has been widely accepted. However, the assumption of incompressible soil restricts its application when the pore fluid pressure is a function of changing total stress due to the applied load and the compressibility of the soil matrix.

For the moisture and heat transfer in rigid porous medium, Bear et al. (1991) also made a remarkable attempt. In order to supply information for the planned storage of thermal energy in unsaturated soils and for hot waste storage, Bear et al. (1991) presented a heat and mass transfer model. The model consisted of the macroscopic mass and energy conservation equations which were obtained by averaging the microscopic ones over a Representative Elementary Volume (REV) of the porous medium domain. The heat fluxes were considered in all the phases that comprised the porous medium. The energy transfer processes included conduction, advection through liquid and vapor water fluxes and phase change between vapor and water. In the the balance equation for the total mass of water, Bear et al. (1991) added the advective flux of the gas driven by nonuniform distribution of the gas-water surface tension (pressure gradients in the gaseous phase was neglected) in addition to the liquid and water vapor fluxes. The other idealizations included 1) the hysteresis associated with capillary pressure curves, effective permeability and transport coefficients depend on moisture content were disregarded, 2) a thermal equilibrium was assumed among all the phases present in the porous medium domain. In other words, the temperature is identical for all soil phases (Milly, 1982a).

Based on the two-phase flow consolidation theory of Fredlund and Hasan (1979), Dakshanamurthy and Fredlund (1980) developed the model further to predict the moisture flow in an unsaturated soil under isothermal and nonisothermal conditions. In adddition to the two partial differential equations written for mass conservation of water and air phase, a partial differential heat flow equation was solved and the solution of heat was used to adjust the corresponding pore-water and pore-air pressures by the method of superposition.

Later, Dakshanamurthy and Fredlund (1981) converted temperature changes in the soil to a change in pore-air and pore-water pressure and modified the pore-air and pore-water partial differential equations in Dakshanamurthy and Fredlund (1980). Three partial differential equations governing heat flow and mass of water and air flow were solved simultaneously

for changes in the combined thermal and hydraulic boundary conditions. The heat flow was assumed to be driven only by conduction mechanism. In derivation of the partial differential equations, Dakshanamurthy and Fredlund (1981) took the coefficients of permeability and volume change moduli to be constant during consolidation. However, in the solving process using the finite difference technique, it was possible to update their values in accordance with any desired functional relationship. This treatment of varying coefficients would miss some terms associated with their spatial gradients. In addition, the vapor pressure gradients and the dissolution of air in the water are not considered in the analysis.

On the basis of the work proposed by Philip and de Vries (1957), Thomas et al. (1996) included the effect of air transfer and the deformation characteristics of the soil. The air pressure was included and solved by introducing a new governing equation for dry air flow and the air dissolved in pore water. As to the vapour velocity equation, Ewen and Thomas (1989) made two changes to Philip & de Vries' expression. Firstly, Ewen and Thomas (1989) claimed that the data presented by Philip and de Vries (1957) to support their development of the vapour velocity equation should be interpreted in a different way. The data did not appear to show the choking of the vapour flow at high moisture content as expressed by Philip and de Vries (1957). Instead, Ewen and Thomas (1989) used a straightforward approach to assume that the vapour flow area was equal to the porosity and there was no choking. The predicted vapour velocity in this way also gave a good agreement with the experiment data. Secondly, Ewen and Thomas (1989) included the area factor in both the temperature and moisture gradient terms. Thomas et al. (1996) describe the vapor transfer with the approach proposed by Philip and de Vries (1957) but the vapour flow velocity equation was modified according to Ewen and Thomas (1989). The deformation was predicted using a force equilibrium equation, in which an incremental form of stress-strain relationship was incorporated. Thereby, either elastic, thermoelastic, elasto-plastic or thermoplastic models for soil may be employed. Especially in the non-linear elastic model, the stress-strain behaviour of the soil was included by using elasticity theory combined with the so called state surface approach. The state surface was a tool to link the volumetric strain to the stress, suction and temperature changes in the soil.

So far, the basic framework for a thermal-mechanical-hydraulic model to describe the non-isothermal porous flow in an unsaturated soil has been established. The multi-phase flow comprises liquid flow, vapor flow and dry air (with dissolved air in liquid) flow and influenced by the presence of temperature gradient. Deformation is determined by force equilibrium with the soil displacement components as basic variables. The soil volumetric change in response to soil stress and flow of pore fluid is reflected in the transient solution.

2.4.2 Thermo-mechanical-hydraulic model for landfill soil liner

Although the temperature generated by breakdown of solid waste in a landfill could not be extremely high (under 30 °C or 60 °C (Rowe, 2005)), transport of the volatile organic matter can be significantly influenced by the following reasons: 1) Temperature gradient can act as a driving force in moisture transport. Especially for the unsaturated soil with connected pore air phase, moisture flow caused by water vapor density variation can play a important role. In this case, multi-phase flow modeling is necessary. 2) The rising temperature influences soil, hydrological and solute transport characteristics involved in both water and contaminant transport modeling. Therefore, non-isothermal multi-phase moisture flow should be included in modeling organic solute transport within an unsaturated landfill clay liner with inter-connected pore air.

Composite bottom liner for a waste disposal site is anticipated to work well because geomembrane is impermeable to liquid water and the mineral liner forms the diffusion and sorption barrier for compounds that can diffuse through geomembrane. Even when the geomembrane has become leaky, the mineral liner with low permeability is intended to prevent the water flux. However, the composite liner system will not function well when there are cracks occurring in the mineral liner. The crack can substantially increase the hydraulic conductivity of the liner (Zhou and Rowe, 2003). The risk does exist when a downward temperature gradient enhances downward movement of liquid water and water vapour for a warm landfill (Döll, 1996). Biodegradation of organic matter in the waste body pose a threat for a temperature increases above the bottom liner. In fact, the measured temperatures in the liner system have been reported to range from 10 °C to 65 °C (Collins, 1993; Rowe,

1998; Zhou and Rowe, 2003). To assess this risk of liner cracking due to desiccation, a nonisothermal porous flow model has been applied to the landfill bottom liner.

Döll (1996) sampled the mineral bottom liner of a 7 years old municipal landfill (without geomembrane) to assess the risk of desiccation and cracking of liners below warm waste disposal sites. A numerical model of one-dimensional coupled moisture and heat transport in unsaturated soils was employed to simulate the water content distribution. In the model, moisture and heat transport in the same mechanisms as proposed by Philip and de Vries (1957) and Milly (1982b).

Zhou and Rowe (2003) developed a fully coupled heat-moisture-air flow model to study heat and moisture transfer in landfill liner systems. The effect of mechanical deformation on all governing equations were included and solved simultaneously. With the resulting stress field, the potential of desiccation cracking was evaluated. The model accounted for the non-linear constitutive relationship concerning the dependence of void ratio and volumetric water content on stress, capillary pressure and temperature. By expressing the governing equations in terms of temperature and capillary pressure, the model was claimed to be suitable for both unsaturated and saturated soil (Zhou and Rowe, 2003). Furthermore, mass conservative numerical schemes were proposed to improve the accuracy of the finite element solution to the governing equations.

Although the thermo-mechanical-hydraulic models were originally intended to assess the risk of landfill soil liner cracking under condition of non-isothermal porous flow, they can be applied to provide the information of flow for volatile organic chemicals migration within the liner as well.

2.5 Coupling model of solute transport in soil liner

2.5.1 Isothermal solute transport in saturated deformable soil

The dispersion-advection equation (Bear, 1972) is conventionally used in the analysis of contaminant migration through soil liner beneath a landfill (Smith, 2000). The assumption behind it is that the porous media through which the contaminant migrates is stationary.

However, the landfills bottom soil liner will experience time-dependent deformation as the soil consolidates in respense to the waste implacement. Therefore, the contaminant can migrate through a deforming porous medium in both the fluid phase and solid phase as well (Smith, 2000).

In order to clarify the influence of soil deformation on the rate of contaminant transfer beneath the landfill, Smith (2000) developed a one-dimensional theory of contaminant migration through a saturated deforming porous media. To aid the extension of dispersion-advection equation to include the effect of solid motion, the well-known one-dimensional consolidation theory was derived. Thereby, various quantities required in a contaminant transport analysis were identified. Henceforth, a transport equation is constructed on the basis of the conservation of mass in both solid and fluid phase. The sorption was assumed to be linear, reversible.

By selection of suitable parameters, the model reverted to the conventional advection-dispersion equation for a rigid saturated soil. Based on the consolidation and solute transport coupling model, small strain and large strain analysis were performed. Smith (2000) analyzed migration of VOCs through a a composite landfill bottom liner, which consists of geomembrane overlying a natural clay soil liner. At quasi-steady state (which means the VOC concentration profile has reached a steady-state condition while the soil porosity continues to change), the deformation can significantly increase the mass flux through the consolidating soil liner. Nevertheless, the difference due to consolidation in the quasi-steady contaminant distribution is relatively small.

Through the establishment of one-dimensional transport theory, Smith (2000) pointed a logical way to derive a solute transport equation for an compressible porous medium. Further, the model pioneered the investigations of solute transport in porous medium with presence of mechanical consolidation.

Peters and Smith (2002) extended the theory of Smith (2000) to simulate the transient solute transport through a deforming porous medium in both spatial and material coordinate systems. For the same landfill liner problem as used in Smith (2000), a comparison between

the theory for a rigid porous medium, and small and large deformation analysis of a deforming porous medium was conducted. It was found that the large deformation model produces shorter solute breakthrough times, followed by the small deformation model, and then the rigid porous medium model. Moreover, the spatial and temporal void ratio variations significantly influence the results in the large deformation analysis.

Alshawabkeh et al. (2004, 2005) presented a one-dimensional nonlinear advection-dispersion equation with the advective transport component determined by the rate of Terzaghi small deformation consolidation and excess pore pressure dissipation. Alshawabkeh et al. (2004) conducted a laboratory experiment to measure the mass expelled from consolidating kaolinite samples which were placed under water. The upper half the soil sample was mixed with bromide, a non-reactive tracer. Flux of bromide as a result of consolidation was measured by monitoring the concentration of bromide in the water surrounding the kaolinite sample. Comparison of the amount of flow out pore fluid and amount of the bromide flux showed a good agreement. Therefore, Alshawabkeh et al. (2004) claimed that the bromide concentration changes were directly related to the advective pore fluid flux during the consolidation process. However, the approach adopted in the experiment did not measure the distribution of bromide and assess the influence of consolidation on the its evolution. Alshawabkeh et al. (2004) also solved a hypothetical case to demonstrate the effect of consolidation on contaminant transport and breakthrough under single and double drainage. Alshawabkeh et al. (2004) concluded that the impact of consolidation depends on the drainage condition, i.e., single or double drainage of soil column. Under single drainage conditions, consolidation significantly impacts the diffusional flux and decrease the solute breakthrough time to less than 5% of that predicted without considering of consolidation. Nevertheless, consolidation in doubly drained clay influences only the concentration profiles but not the breakthrough of the diffusive flux.

Alshawabkeh et al. (2005) employed the model in Alshawabkeh et al. (2004) to predict a hypothetical case of the contaminant transport through a consolidating sub-aqueous sediment and the overlying cap. The consolidation of partially contaminated sediment was induced by

the buoyant weight of the cap. The results showed that advection due to consolidation can speed up the breakthrough of contaminant through the cap by orders of magnitude.

In the derivation of solute transport equation, Alshawabkeh et al. (2004, 2005) made a non-consistent manipulation: the advective solute transport occurs due to total hydraulic head (sum of excess head and hydrostatic head) gradient, while the advective pore fluid flow was driven by the dissipation of excess head gradient alone in the consolidation formula. The excess pore head is generated due to the partially or undrained loading experienced by soils. In fact, the total hydraulic head should be combination of excess, hydrostatic and gravity head. Since the latter two balance each other in the initial state, the pore fluid flow occurring in both consolidation and solute transport equation should be driven by only the excess head gradient. Moreover, in the hypothetical cases used by Alshawabkeh et al. (2004, 2005) for purpose of illustration, the compressibility and other parametric data employed in the analysis have not been fully specified and reported (Lewis et al., 2009).

Based on the one-dimensional, large-deformation model of coupled mechanical consolidation and solute transport developed by Smith (2000) and Peters and Smith (2002), Lewis et al. (2009) investigated the VOCs transport through a clay landfill liner. The large-deformation was generalized to take into account both non-linearities in geometry as well as constitutive relations. Unlike the model used by Peters and Smith, Lewis et al. (2009) employed constitutive material properties relating the compressibility, hydraulic conductivity and the effective diffusion coefficient to the void ratio. It was found that the extent to which the consolidation made a difference strongly depended on the compressibility of soil. For barriers of low compressibility, little difference was observed between the consolidation-transport coupling model and pure diffusion model. However, for contaminant barriers made of more compressible soils, consolidation was found to significantly accelerate transport. Moreover, the geometric non-linearity played a important role which indicated that large-deformation formulations should be utilized when the settlement during consolidation process is large.

Fox (2007a) developed a piece-wise approach for the simulation of coupled nonlinear large strain consolidation and solute transport in saturated porous media. The consolidation

algorithm was one-dimensional, while the solute transport algorithm was two-dimensional thereby both longitudinal and transverse dispersion could be included. In the solute transport algorithm, two Lagrangian fields of elements were defined to follow the motions of fluid and solid phases separately, which proved helpful in reducing the numerical dispersion.

Utilizing the model from Fox (2007a), Fox (2007b) analyzed consolidation-induced solute transport for a single composite liner system and a confined disposal facility for dredged contaminated sediments. In both cases, consolidation advection was found to have a significant influence on solute migration. Since the transient advective flows change the distribution of solute mass which becomes the initial condition for the subsequent solving, consolidation can have a lasting effect on solute migration.

2.5.2 Non-isothermal solute transport in unsaturated soil

Temperature gradients can cause pore liquid to move and this in turn influences the solute advection. Lindstrom and Piver (1985) presented a one-dimensional mathematical model to predict the simultaneous transfer of heat, moisture, and chemicals in non-isothermal unsaturated salty soil. Based on the assumption that the soil solute concentration was sufficiently low, the solution osmotic pressure head effects on water movement were not included in the model. Therefore, the water and temperature gradients can affect solute flow, but solute gradient had no effect on water and heat flows. Bear and Gilman (1995) included the effect of solute concentration on water vapor pressure, but not on heat transfer and liquid flow.

Nassar and Horton (1992) constructed three governing equations to theoretically describe the simultaneous transient transfer of heat, water, and solute in a one-dimensional soil column. The diffusivity coefficients involved in the partial differential equations are dependent on soil water content, temperature, and solute concentrations. The primary assumptions were: no deformation happens in the porous media, presence of solute will not change the properties of materials, i.e., the porous media are inert, hysteresis of retention curves (matric pressure head vs. water content) or the water transport coefficients is neglected, the total gas phase pressure is uniformly distributed and constant, and there is no dry air flow existing.

To make the theory of Nassar and Horton (1992) suitable for nonhomogeneous porous media, Nassar and Horton (1997) modified the equations and described simultaneous heat, water, and solute transfer in terms of total pressure head, temperature, and solute concentration gradients.

Thomas and Ferguson (1999) presented a two-dimensional coupled non-isothermal mass transfer numerical model for basal, perimeter and capping liners in a sanitary landfill site. The model consists of four non-linear partial differential equations with the basic variables of capillary potential, temperature, pore air pressure and the molar concentration of contaminant gas. The pore gas was mixture of dry air, water vapor and a contaminant gas and the ideal gas law was assumed to be valid. Further, the gas mixture was assumed to be inert. In other words, no reaction occurs between either gas-gas and gas-soil. However, Thomas and Ferguson (1999) did not consider deformation of the liner.

Based on the non-isothermal moisture and solute transport model developed by Nassar and Horton (1997), Nassar and Horton (1999) extended it to include the transfer and fate of volatile organic chemicals in a rigid porous system. The organic chemical was assumed to exist in all three phases of the porous media (liquid, vapor, and solid phases) and move by mechanisms of diffusion and advection in both liquid and vapor phases. The sorption-equilibrium at three phase interfaces was employed to describe the internal-phase transfer of VOC. The molecular diffusivity of water vapor and organic compound in a multicomponent gas mixture (water vapor, air and vapor of the VOC) were determined in a way allowing the interaction between gas mixture constituments (Welty et al., 1984) . The effect of temperature and VOC concentration on the matric water pressure head were considered through the surface tension model. The theory is capable of predicting transient distribution of moisture content, temperature, inorganic concentration and the total concentration of VOC (and its concentration in each phase as well) within a porous medium. The underlying assumptions included: the sorbed phase for both inorganic and organic chemicals were immobile, and there was no dry air flow.

Nassar et al. (1999) performed a laboratory experiment to observe the water content, chloride concentration and benzene concentration distributions in soil under isothermal and

non-isothermal conditions. The model developed by Nassar and Horton (1999) was used to simulate the observed data. There was an agreement between the predicted and observed soil temperature and water content distributions. The trend of observed benzene distributions was also adequately predicted but the measured gas phase concentration was greater than predicted at some positions.

In the nuclear waste disposal research community, the fully coupled thermo/hydro/chemical/mechanical (THCM) models emerged. For example, Olivella et al. (1994) made a early attempt to propose a general formulation for nonisothermal multiphase flow of brine and gas through saline media. The balance equations included mass balance of three phase (salt, water and air), equilibrium of stresses and energy balance. Cleall et al. (2007) continued to address the multi-component reactive chemical transport behavior in the THCM model. The governing equation for deformation was presented in terms of displacements and a elasto-plastic constitutive model was employed.

For sake of clarity, the typical coupling models for solute (or VOCs) transport in landfill basal soil liner and relevant works in the existing literature are summarized in Table 2.1-2.2.

2.5.3 Summary on the VOCs migration in landfill soil liner modeling

Landfill is widely utilized for disposing the solid waste and the dredged aqueous sediments highly contaminated due to toxic substances. To protect the surrounding environment and groudwater from pollution, liner system is usually constructed beneath the landfill. In a modern composite basal liner system, there is an impervious geomembrane overlying the soil liner which helps to prevent inorganic contaminants. The mass flux through possible defects in geomembrane is not significant relative to that through intact parts. Since VOCs can diffuse through the geomembrane, minimizing the breakthrough of volatile organic contaminants (VOCs) is a core concern to design an effective barrier. Most of the landfill basal soil liners are partially saturated and undergo deformation due to the filling process. Also, a temperature gradient loading is possible when the heat is generated by decomposition of organic landfill waste. Numerous attempts have been made to construct coupling model for

Table 2.1: Typical hydro/chemical/mechanical models for solute transport in saturated soil

Authors	Contents	Note
Smith (2000)	dissolved VOCs transport in deformable saturated clay liner	pointed a logical way to derive the solute transport in deformable media
Peters and Smith (2002)	the effect of consolidation on dissolved VOCs in saturated clay liner	extended the theory of Smith (2000) to simulate the transient solute transport
Alshawabkeh et al. (2004)	nonlinear advection-dispersion equation coupled with Terzaghi small deformation consolidation, measure the mass expelled from consolidating kaolinite samples	experiment data is limited
Alshawabkeh et al. (2005)	contaminant transport through a hypothetical sub-aqueous sediment and overlying cap	model identical to Alshawabkeh et al. (2004), no fully specified parameters
Lewis et al. (2009)	VOCs transport through a saturated clay landfill liner	nonlinear with respect to geometry as well as constitutive relations
Fox (2007a)	coupled nonlinear large strain consolidation and solute transport in saturated porous media	piece-wise approach
Fox (2007b)	consolidation-induced solute transport for a single composite liner system and a confined disposal facility for dredged contaminated sediments	effect of consolidation advection on solute transport is found to be lasting

Table 2.2: Typical non-isothermal coupling models for solute (or VOCs) transport in unsaturated soil

Authors	Contents	Note
Lindstrom and Piver (1985)	one-dimensional model for transfer of heat, moisture, and chemicals in unsaturated salty soil	solute concentration does not affect moisture and heat transport
Bear and Gilman (1995)	THC model	included the effect of solute concentration on water vapor pressure
Nassar and Horton (1992)	THC model	diffusivity coefficients involved in the partial differential equations are dependent on soil water content, temperature, and solute concentrations
Nassar and Horton (1997)	THC model, rewrite the equations of Nassar and Horton (1992) in terms of total pressure head, temperature, and solute concentration gradients	suitable for nonhomogeneous porous media
Thomas and Ferguson (1999)	a two-dimensional coupled non-isothermal mass transfer numerical model for basal, perimeter and capping liners in a sanitary landfill site	no sorption between contaminant gas and solid
Nassar and Horton (1999)	the moisture, heat and VOCs transfer in a rigid porous system	VOCs resides in three phases of soil, VOCs concentration affects moisture transfer properties
Nassar et al. (1999)	laboratory experiment to assess performance of model in Nassar and Horton (1999)	
Olivella et al. (1994)	non-isothermal multiphase flow of brine and gas through saline media	THMC model, deformation is in small-deformation frame
Cleall et al. (2007)	THCM model with multicomponent reactive chemical transport behavior	no chemical in gaseous phase

VOCs or contaminant solute transport in landfill basal soil liner. By review of the existing literature, the following limitations can be pointed out:

- Most consolidation and solute transport coupling models treat the soil liner as fully-saturated.
- For porous flow in nearly-saturated and unsaturated soil liner, Richards equation is used to model the porous flow, which does not include deformation due to mechanical consolidation.
- For the nearly-saturated soil liner, the effect of occluded bubbles on solute transport is not considered.
- Regarding the general unsaturated soil liner with continuous air phase, VOCs transport via gaseous phase is neglected.
- Although the effect of temperature gradient is widely recognized in prediction of desiccation of soil liner, it is always ignored in the VOCs transport modeling.
- Deformation of soil is ignored in the current heat-hydro-chemical coupling models, or is determined in a small strain frame for the poro-elastic material.

2.6 Objectives and organization of thesis

The overall aim of this thesis is to investigate the solute transport in deformable unsaturated soil and apply the theory to the migration of volatile organic contaminant through partially saturated landfill basal clay liner. The study presented in this thesis intends to increase engineering knowledge in the areas where these previous researches have had limitations and shortcomings. In view of the above summary on current state of knowledge concerning VOCs migration in landfill soil liner, this thesis aims to achieve the following specific objectives:

- To develop a model of solute transport in a deformable nearly-saturated soil liner. Due to the complexity, a mathematical model for the volume change of occluded bubbles is not available. As a first approximation, degree of saturation is taken as temporally and spatially constant in this study. The small or finite deformation is assumed to be caused solely by the mechanical consolidation. In addition to increasing compressibility of the homogeneous pore fluid, occluded air bubbles lead to a considerable reduction in the cross-section through which pore liquid and solute flow. In the thesis, this task is divided into two parts of small deformation and finite deformation modeling.

- To develop a non-isothermal multi-phase moisture and solute transport model for an unsaturated soil. Heat generated in the landfill creates a temperature gradient for the unsaturated composite liner system. Movement of moisture de-saturates the soil liner and consequently the air phase becomes continuous. VOCs resides and moves in three phases of soil (solid, liquid and gas). The multi-phase moisture and VOCs flow are affected by the interaction between the simultaneous presence of pore liquid water, water vapor, dry air and contaminant gas and solute.

The thesis is organized as:

1. In Chapter 3, a new pore fluid storage equation for quasi-saturated soil will be developed. The mixture of pore water and pore air is assumed to be a homogeneous fluid. In addition to the compressibility of pore fluid due to presence of occluded air bubbles, reduction in section of flow is considered as well. The volumetric change of soil skeleton due to consolidation is incorporated. In the derivation of advection-dispersion equation, advective solute transport is caused by motion of both solid and pore fluid. The transient velocities are provided by the solution of consolidation equations. Therefore, a coupling hydro-mechanical-chemical model is constructed. For a one-dimensional problem, the formulations are non-dimensionalized to examine the relative importance of each term in the coupling partial differential equations. Based on the dimensionless analysis, a simplified model is proposed and applied to a landfill bottom CCL.

2. Chapter 4 extends a one-dimensional coupled consolidation and solute transport model for a partially saturated porous medium to include finite strain and the geometric and material nonlinearity. All the equations are written in Lagrangian coordinate system. The consolidation equation is expressed in term of void ratio. The model is employed to reexamine the effect of mechanical consolidation, nonlinearity of geometry and materials and unsaturation on the VOCs solute transport in landfill soil liner.

3. Following it, Chapter 5 establishes a fully coupled thermal-hydraulic-mechanical-chemical (THMC) model to describe the migration of volatile organic contaminants (VOCs) in unsaturated landfill liners. In the formulations, vertical soil stress, capillary pressure, air pressure, temperature increase and dissolved solute concentration are selected as primary variables. The finite deformation is addressed by use of Lagrangian coordinates. The non-isothermal moisture transport is dependent on both temperature gradient and VOCs concentration. VOCs is assumed to reside and be transported by three phases, i.e., solid, liquid and gas phases in soil. Based on the model, an illustrative example of VOCs migration in an unsaturated landfill compacted clay liner (CCL) is presented.

4. Finally, conclusions for the work in the thesis and recommendations for future researches are presented in Chapter 6.

2.7 Notation

The following notation is used in Chapter 2:

Roman Letters:

c, the contaminant mass concentration, ML^{-3}

c_v, the consolidation coefficient, $\mathrm{L}^2\mathrm{T}^{-1}$

c_v^*, the equivalent consolidation coefficient, $\mathrm{L}^2\mathrm{T}^{-1}$

G, soil shear modulus, $\mathrm{ML}^{-1}\mathrm{T}^{-2}$

K, hydraulic conductivity, LT^{-1}

K_d, the distribution (portioning) coefficient, L^3M^{-1}

K_r, the first order degradation rate in the soil liner, T^{-1}

n, soil porosity

M_a, the pore air mass, M

M_w, the pore water mass, M

M_s, the solid mass, M

M_t, the total mass, M

m_v, coefficient of soil compressiblity, LT^2M^{-1}

p, fluid pressure, $ML^{-1}T^{-2}$

p_l, liquid pressure, $ML^{-1}T^{-2}$

p_a is pore air pressure, $ML^{-1}T^{-2}$

R_f, dimensionless retardation factor

S_r, the degree of saturation

t, time, T

z, vertical coordinate, L

v, the average linearized ground water velocity, LT^{-1}

$\overrightarrow{\mathbf{v}_s}$, solid velocity vector, LT^{-1}

V_a, the pore air volume, L^3

V_w, the pore water volume, L^3

V_s, the solid volume, L^3

V_f, the fluid volume, L^3

V_t, the total volume, L^3

V_v, the pore volume, L^3

Greek Letters:

ρ, the bulk density of soil, ML^{-3}

ρ_s, dry density of the soil solid, ML^{-3}

ρ_f, density of pore fluid, ML^{-3}

θ, volumetric water content

β, the coefficient of fluid compressibility, LT^2M^{-1}

σ, total soil stress, $ML^{-1}T^{-2}$

Abbreviation:

ADE, advection-dispersion equation

CCL, compacted clay liner

GCL, geosynthetic clay liner

HDPE, high density polyethylene

HPF, homogeneous pore fluid

REV, represent element volume

SWCC, Soil-Water Characteristic Curve

VOCs, volatile organic chemicals

Chapter 3

Solute Transport in Isothermal Deformable Soil: Small Strain Model

3.1 Introduction

Various environmental situations are typically investigated using solutions of the solute transport equations considering the porous medium to be rigid, e.g., (Bear, 1972; Barry and Sposito, 1989; Barry, 1990, 1992; Li et al., 2001). In such cases, no volume change occurs during the transport process and therefore the advection is determined solely by the hydraulic gradient. However, porous medium deformations can lead to unsteady advective flow. Some examples include solute transport through a clay liner during waste-filling operations, dredged contaminated sediment after placement in a confined disposal facility, consolidation of contaminated sediments due to overburden of capping material, and solute transport in cartilage under mechanical load, e.g., (Smith, 2000; Arega and Hayter, 2008; Zhang and Szeri, 2005). In these cases, the deformation and solute transport processes occur simultaneously and coupled effects should be considered.

As reviewed in the previous chapter, considerable efforts have been put in modeling solute transport in a consolidating saturated porous medium (Potter et al., 1994; Smith, 2000; Peters and Smith, 2002; Alshawabkeh et al., 2005; Arega and Hayter, 2008; Lewis, 2009; Fox, 2007a,b; Fox and Lee, 2008). However, the assumption of fully saturation is not always reasonable. In real environments, unsaturated porous media are common (Fityus et al., 1999; Hsu et al., 1995; Jeng and Lin, 1997). For example, marine sediments are often unsaturated

due to gas produced in biochemical processes. Another case is where the groundwater table is located some distance below a landfill geomembrane, in which case the soil beneath the landfill will be partially saturated (Fityus et al., 1999).

In this chapter, a one-dimensional single-phase isothermal unsaturated porous flow and solute transport model is constructed. Biot consolidation equation is used to describe flow in an unsaturated porous medium incorporating the self-weight of the liner. In order to account for the effect of occluded air bubbles on both pore fluid compressibility and reduction of the cross-section through which flow pass, a new fluid storage equation is derived. The situation considered is that of compressible pore water at a fixed saturation. Solute exists in both solid and aqueous phase. The ADE that is typically used to describe solute transport through a rigid porous medium (Bear, 1972) is modified to include partial saturation, CPW (compressible pore water), SVP (spatial variation of porosity) and longitudinal dispersivity. The equations are non-dimensionalized, identifying nine important parameters. The importance of these parameters is discussed for a range of physical conditions. A hypothetical engineered landfill liner is used as an illustrative example, demonstrating the influence of partial saturation and the loading process on contaminant migration. Finally, the symbols used within this chapter are summarized. This chapter forms the paper of Zhang et al. (2012).

3.2 Theoretical formulation

3.2.1 Consolidation equation

Here we state the basic equations linking flow velocity with excess pore pressure. The one-dimensional unsaturated fluid storage (Appendix 3A) and force balance equations are, respectively,

$$S_r n\beta\frac{\partial p^e}{\partial t} + S_r\frac{\partial^2 u}{\partial t\partial z} = \frac{1}{\rho_w g}\frac{\partial}{\partial z}\left(K\frac{\partial p^e}{\partial z}\right), \tag{3.1}$$

$$G\frac{2(1-\nu)}{(1-2\nu)}\frac{\partial^2 u}{\partial z^2} + \left(1-n^0\right)(\rho_s - S_r\rho_w)\, g\frac{\partial u}{\partial z} = \frac{\partial p^e}{\partial z}. \tag{3.2}$$

where p^e is excess pore pressure, u is soil displacement. S_r, n, n^0, K, G and ν represent degree of saturation, current porosity, initial porosity, hydraulic conductivity, shear modulus and Poisson's ratio, respectively; ρ_w, ρ_s are the density of pore water and solid materials, respectively. The form of Equ. (3.2) is similar to the vertical force equivalence equation used in Tsai et al. (2006). However, the second term which is used to represent the self-weight of soil is modified to include the degree of saturation. Furthermore, the first term on LHS is the gradient of vertical effective soil stress, for which tension is taken as positive.

In this study, density of both components of soil are independent of the dilute solute concentration (Klett et al., 2005). When the sorption occurs, the mass of a unit volume of solid grains (i.e., density) ρ_s becomes $\rho_s(1 + K_d c_f)$. Using the clay liner as an example, the measured VOC concentration in the landfill leachate ranges from 10 to 10^4 μg/l (Klett et al., 2005). Lewis et al. (2009) adopted the distribution coefficient $K_d = 1$ l/mg, leading to the change of the density of solid due to sorption is less than 0.001%, which is negligible. Consequently, it is reasonable to assume that ρ_s is independent of the solute mass concentration. Therefore, the assumption of volume-preserving deformation of the solid phase embedded in derivation (Appendix 3A) can be ensured, i.e., $\nabla \bullet \vec{v}_s = 0$ (Bear and Cheng, 2010).

The compressibility of pore fluid in clay, β, depends on the degree of saturation S_r, the amount of dissolved air in pore water and absolute air pressure. It can be estimated by (Fredlund and Rahardjo, 1993)

$$\beta = \frac{S_r}{K_{w0}} + \frac{1 - S_r + r_h S_r}{P_a + P_0}, \tag{3.3}$$

where K_{w0} is the pore water bulk modulus, r_h denotes volumetric fraction of dissolved air within pore water, P_a denotes gauge air pressure and P_0 represents the atmosphere pressure. In the high saturation limit, when $r_h = 0.02$, $S_r = 0.8 \sim 1.0$ and β falls into the range of $2 \times 10^{-6} \sim 2 \times 10^{-7}$ Pa^{-1}.

3.2.2 Solute transport equation

Following Peters and Smith (2002), the solute transport equation in a one-dimensional deforming porous medium is

$$\frac{\partial\left(nS_r c_f\right)}{\partial t} + \frac{\partial[(1-n)\,c_s]}{\partial t} = -\frac{\partial}{\partial z}\left[nS_r\left(-D\frac{\partial c_f}{\partial z} + v_f c_f\right) + (1-n)\,v_s c_s\right], \tag{3.4}$$

where c_f and c_s are the concentration of the solute in the fluid and solid phase, respectively; D, which represents the hydrodynamic dispersion coefficient, is the sum of the effective molecular diffusion, D_m, and mechanical dispersion, $\alpha_L(v_f - v_s)$, where v_f denotes the average fluid velocity and v_s is the velocity of the solid. Here, the effective molecular diffusion tensor, mechanical dispersion tensor and consequently the hydrodynamic dispersion tensor reduce to scalar for the one-dimensional isotropic soil.

By definition the concentration of the contaminant in the solid phase is

$$c_s = \rho_s S = \rho_s F(c_f, t), \tag{3.5}$$

where S is the mass of contaminant sorbed onto the solid phase per unit mass of solid phase, and F is a function describing the relationship. If sorption is an equilibrium linear reversible process, then (Smith, 2000)

$$S = K_d c_f, \tag{3.6}$$

where K_d describes the partitioning of the contaminant.

Based on the mass balance equations for the fluid, Eq. (3.34), and solid phases, Eq. (3.41) (introduced in the Appendix 3A), and considering the solid particles as incompressible (i.e., ρ_s is constant), Eq. (3.4) becomes

$$\begin{aligned} S_r n\frac{\partial c_f}{\partial t} + (1-n)\frac{\partial c_s}{\partial t} =& \frac{\partial}{\partial z}\left(S_r n D\frac{\partial c_f}{\partial z}\right) - S_r n v_f\frac{\partial c_f}{\partial z} - (1-n)\,v_s\frac{\partial c_s}{\partial z} \\ &+ S_r n\beta\left(\frac{\partial p^e}{\partial t} + v_f\frac{\partial p^e}{\partial z}\right)c_f. \end{aligned} \tag{3.7}$$

Assuming the linear sorption relationship described by Eqs. (3.5) and (3.6), and using Eq. (3.56) in the Appendix 3B, Eq. (3.7) becomes

$$\begin{aligned}\left[S_r n + (1-n)\rho_s K_d\right]\frac{\partial c_f}{\partial t} &= S_r n D_m \frac{\partial^2 c_f}{\partial z^2} - \alpha_L \frac{K}{\rho_w g}\frac{\partial p^e}{\partial z}\frac{\partial^2 c_f}{\partial z^2} \\ &+ \frac{\partial c_f}{\partial z}\left\{-\alpha_L S_r n\beta \frac{\partial p^e}{\partial t} - \alpha_L S_r \frac{\partial^2 u}{\partial z \partial t}\right. \\ &+ \frac{\alpha_L \beta K}{\rho_w g}\left(\frac{\partial p}{\partial z}\right)^2 + S_r D_m \frac{(1-n)^2}{1-n^0}\frac{\partial^2 u}{\partial z^2} \\ &\left.+ \frac{K}{\rho_w g}\frac{\partial p^e}{\partial z} - \left[S_r n + (1-n)\rho_s K_d\right]\frac{\partial u}{\partial t}\right\} \\ &+ S_r n\beta \frac{\partial p^e}{\partial t} c_f - \beta \frac{K}{\rho_w g}\left(\frac{\partial p^e}{\partial z}\right)^2 c_f + S_r n\beta \frac{\partial u}{\partial t}\frac{\partial p^e}{\partial z} c_f.\end{aligned} \tag{3.8}$$

Details of the derivation are given in the Appendix.

It is worthwhile to compare the transport equation proposed by Peters and Smith (2002) (Eq. (30) in their paper) with that given here. In the present notation, their result is

$$n\frac{\partial c_f}{\partial t} + (1-n)\frac{\partial c_s}{\partial t} = \frac{\partial}{\partial z}\left(nD\frac{\partial c_f}{\partial z}\right) - nv_f\frac{\partial c_f}{\partial z} - (1-n)v_s\frac{\partial c_s}{\partial z}. \tag{3.9}$$

Comparing Eqs. (3.7) and (3.9), it is clear that Eq. (3.9) is a special case of Eq. (3.7) with $S_r = 1, \beta = 0$, while new terms due to the compressibility of the pore water are contained in our equation.

Using the relationship between n and n^0 (Tsai et al., 2006), i.e.,

$$n = n^0 + \left(1 - n^0\right)\frac{\partial u}{\partial z}, \tag{3.10}$$

the equations become considerably more complex. However, our main focus is on the effect of unsaturated condition and compressibility of pore water. If the deformation is relatively small, the volume strain, i.e., $\partial u/\partial z$ herein is consequently small, therefore n in Eq. (3.1) and Eq. (3.8) will not differ appreciably from n^0 (Peters and Smith, 2002). On the other hand, although the reducing porosity can narrow the aqueous solute transport path, it tends

to result in a bigger intrinsic pore water velocity and in turn the advective flux. Therefore, it is reasonable to assume constant n in the following non-dimensional analysis. This approach has been used in the previous investigations (Peters and Smith, 2002; Alshawabkeh et al., 2005). Keeping temporal and spatial variations of porosity, the governing equations Eqs. (3.1), (3.2) and (3.8) become, respectively

$$S_r n^0 \beta \frac{\partial p^e}{\partial t} + S_r \frac{\partial^2 u}{\partial t \partial z} = \frac{1}{\rho_w g} \frac{\partial}{\partial z} \left(K \frac{\partial p^e}{\partial z} \right), \tag{3.11}$$

$$G \frac{2(1-\nu)}{(1-2\nu)} \frac{\partial^2 u}{\partial z^2} + \left(1 - n^0\right) \left(\rho_s - S_r \rho_w\right) g \frac{\partial u}{\partial z} = \frac{\partial p^e}{\partial z}, \tag{3.12}$$

and

$$\begin{aligned} \left[S_r n^0 + \left(1 - n^0\right) \rho_s K_d \right] \frac{\partial c_f}{\partial t} &= S_r n^0 D_m \frac{\partial^2 c_f}{\partial z^2} - \alpha_L \frac{K}{\rho_w g} \frac{\partial p^e}{\partial z} \frac{\partial^2 c_f}{\partial z^2} \\ &+ \frac{\partial c_f}{\partial z} \left\{ -\alpha_L S_r n^0 \beta \frac{\partial p^e}{\partial t} - \alpha_L S_r \frac{\partial^2 u}{\partial z \partial t} \right. \\ &+ \frac{\alpha_L \beta K}{\rho_w g} \left(\frac{\partial p}{\partial z} \right)^2 + S_r D_m \left(1 - n^0\right) \frac{\partial^2 u}{\partial z^2} \\ &\left. + \frac{K}{\rho_w g} \frac{\partial p^e}{\partial z} - \left[S_r n^0 + \left(1 - n^0\right) \rho_s K_d \right] \frac{\partial u}{\partial t} \right\} \\ &+ S_r n^0 \beta \frac{\partial p^e}{\partial t} c_f - \beta \frac{K}{\rho_w g} \left(\frac{\partial p^e}{\partial z} \right)^2 c_f + S_r n^0 \beta \frac{\partial u}{\partial t} \frac{\partial p^e}{\partial z} c_f. \end{aligned} \tag{3.13}$$

3.2.3 Non-dimensional analysis of coupled equations

To understand the influence of each term in the governing equations, here the variables are non-dimensionalized and the order of each term is considered with a scaled quantity relative to a characteristic unit,

$$p^* = \frac{p^e}{p_c},\ t^* = \frac{t}{t_c},\ z^* = \frac{z}{l_c},\ u^* = \frac{u}{u_c},\ c^* = \frac{c_f}{c_0}, \tag{3.14}$$

$$t_c = \frac{(1-2\nu)L^2 S_r \rho_w g}{2(1-\nu)GK}, \tag{3.15}$$

$$p_c = \frac{2(1-\nu)G\left[S_r n^0 + \left(1-n^0\right)\rho_s K_d\right]}{(1-2\nu)S_r}, \tag{3.16}$$

$$u_c = \frac{L\left[S_r n^0 + \left(1-n^0\right)\rho_s K_d\right]}{S_r}, \tag{3.17}$$

where the characteristic unit for length, l_c, is the thickness of the soil layer and c_0 is the reference solute mass concentration.

Here, t_c is similar to the consolidation time factor T_v in Terzaghi consolidation theory (Terzaghi, 1925). However, t_c incorporates the degree of saturation rather than L^2/c_v ($c_v = [2(1-\nu)GK]/[\rho_w g(1-2\nu)]$, is the coefficient of consolidation). Both p_c (related to the soil shear modulus) and u_c reflect the influence of unsaturated condition and solute retardation due to sorption.

With the coefficients A_i given in Table 3.1, the non-dimensional governing equations are

$$A_1 \frac{\partial p^*}{\partial t^*} + \frac{\partial^2 u^*}{\partial t^* \partial z^*} = \frac{\partial^2 p^*}{\partial z^{*2}}, \tag{3.18}$$

$$\frac{\partial^2 u^*}{\partial z^{*2}} + A_2 \frac{\partial u^*}{\partial z^*} = \frac{\partial p^*}{\partial z^*}, \tag{3.19}$$

$$\begin{aligned}\frac{\partial c^*}{\partial t^*} = {} & A_3 \frac{\partial^2 c^*}{\partial z^{*2}} - A_4 \frac{\partial p^*}{\partial z^*}\frac{\partial^2 c^*}{\partial z^{*2}} + \frac{\partial c^*}{\partial z^*}\left(-A_1 A_4 \frac{\partial p^*}{\partial t^*} - A_4 \frac{\partial^2 u^*}{\partial z^* \partial t^*} + A_5 \frac{\partial p^*}{\partial z^*}\frac{\partial p^*}{\partial z^*}\right. \\ & \left. + A_6 \frac{\partial^2 u^*}{\partial z^{*2}} + \frac{\partial p^*}{\partial z^*} - A_7 \frac{\partial u^*}{\partial t^*}\right) + A_1 \frac{\partial p^*}{\partial t^*} c^* - A_8 \left(\frac{\partial p^*}{\partial z^*}\right)^2 c^* + A_1 A_7 \frac{\partial u^*}{\partial t^*}\frac{\partial p^*}{\partial z^*} c^*.\end{aligned} \tag{3.20}$$

We interpret the coefficients in Eqs. (3.18)-(3.20) as follows. A_1 represents the ratio of skeleton modulus to that of pore fluid, which becomes notable for an unsaturated stiff porous

Table 3.1: Coefficients $A_1 - A_8$ used in the governing equations (Eqs. (3.18-3.20))

Coefficient	Expression	Physical meaning
A_1	$\frac{2G(1-\nu)n^0\beta}{1-2\nu}$	Ratio of skeleton modulus to that of pore fluid
A_2	$\frac{\left(1-n^0\right)(\rho_s-S_r\rho_w)gL(1-2\nu)}{2G(1-\nu)}$	Body force effect on consolidation
A_3	$\frac{S_r^2 n^0 D_m \rho_w g(1-2\nu)}{2\left[S_r n^0+\left(1-n^0\right)\rho_s K_d\right]G(1-\nu)K}$	Reciprocal of Péclet number with modification for retardation and unsaturation
A_4	$\frac{\alpha_L}{L}$	Longitudinal dispersivity per unit length
A_5	$\frac{A_1 A_4 A_7}{n^0}$	-
A_6	$\frac{A_3 A_7\left(1-n^0\right)}{n^0}$	-
A_7	$\frac{S_r n^0+\left(1-n^0\right)\rho_s K_d}{S_r}$	Modified retardation factor
A_8	$\frac{A_1 A_7}{n^0}$	-

medium. A_2 represents the body force effect on consolidation, and is analogous to the "body force number" in Tsai et al. (2006). When it is negligible, the effect of self-weight can be ignored. $A_3 = \left(t_c S_r \left(n^0\right)^2 D_m\right) / \left([S_r n^0 + (1-n^0)\rho_s K_d]L^2\right)$ can be seen as the reciprocal of Péclet number with the modifications of retardation and unsaturation. A_4 is longitudinal dispersivity per unit length. A_7 is the modified retardation factor including unsaturation.

3.3 Application to a landfill profile

The landfill liner system is similar to the operational liner investigated previously (Peters and Smith, 2002), as depicted in Fig. 3.1. It includes a primary leachate collection system (PLCS), a geomembrane overlying a compacted clay liner (CCL), and a secondary leachate collection system (SLCS). The water table is at the same level of top of SLCS, where the pore water existing in the CCL during the process of compaction can be drained. The origin of the vertical axis is located on the top of the CCL.

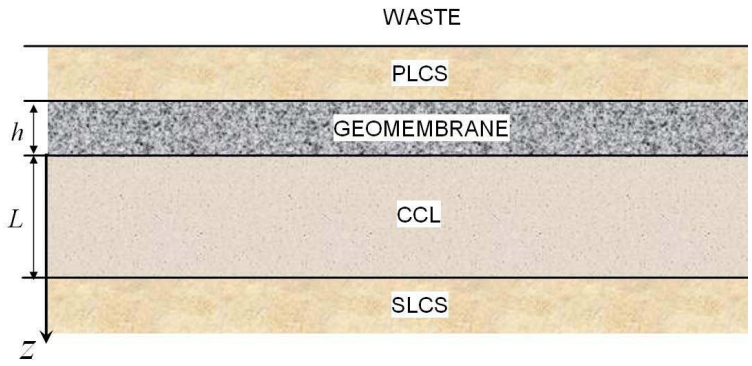

Figure 3.1: A schematic of an engineered landfill liner

The landfill is assumed to fill with waste at a fixed loading rate until it reaches its capacity. At the top boundary, the impermeable geomembrane prevents Darcy flow, and the total vertical stress equals the surcharge loading, i.e.,

$$q(0,t) = -\frac{K}{\rho_w g}\frac{\partial p^e(0,t)}{\partial z} = 0, \quad G\frac{2(1-\nu)}{(1-2\nu)}\frac{\partial u(0,t)}{\partial z} = -Q(t) + p^e. \tag{3.21}$$

The volatile organic compounds diffuse through the thin (relative to CCL) geomembrane at the top boundary, and the solute flux can be approximated as

$$f(0^-,t) = -D_G\frac{c_f(0^+,t) - c_0}{h}, \tag{3.22}$$

while the flux in the CCL at the interface is

$$f(0^+,t) = -nD\frac{\partial c_f}{\partial z}(0^+,t). \tag{3.23}$$

Equating Eq. (3.22) and Eq. (3.23) (Peters and Smith, 2002)

$$\frac{\partial c_f}{\partial z}(0,t) - \frac{D_G}{n(0^+,t)hD}c_f(0,t) = -\frac{D_G}{n(0^+,t)hD}c_0. \tag{3.24}$$

Here, the zero Darcy flow but non-zero contaminant solute flux makes it impossible to utilize analytical solutions. Some analytical solutions for solute transport in porous media without

a geomembrane are available (Rowe and Booker, 1985; Guerrero and Skaggs, 2010; Li and Cleall, 2011).

At the lower fixed boundary of the clay liner, the pore fluid is assumed to drain freely, and the gradient of solute concentration is assumed to be zero (Danckwert's boundary condition, (Danckwerts, 1953)), although different interpretations of this condition are possible, e.g., (Barry and Sposito, 1988):

$$p^e(L,t) = 0, \quad u(L,t) = 0, \quad \frac{\partial c_f}{\partial z}(L,t) = 0. \tag{3.25}$$

The initial excess pore water pressure, soil displacement and solute concentration in the clay liner are zero. That is,

$$p^e(z,0) = 0, \;\; u(z,0) = 0, \;\; c_f(z,0) = 0. \tag{3.26}$$

3.3.1 Comparison with previous work of Peters and Smith (2002)

FEM codes for various models were constructed using the multiphysics modeling software package COMSOL 3.5a (COMSOL, 2010). These involve solution of consolidation under ramp surcharge and the solute transport equation. Since there are no models or experimental data considering the present case, it is only possible to reduce the present model to previously reported special cases (i.e., full saturation, $S_r = 1, \beta = 0$). When $A_1, A_2, A_4 \sim A_6$ and A_8 are zero, the present model reduces to the small deformation model of Peters and Smith (2002). In the FEM analysis, the system was discretized into unstructured Lagrange-linear elements with a maximum global element size of 10^{-2} m, and maximum local element size at the end boundaries (where the most rapid changes occur) of 10^{-4} m. The time step was 10^{-2} year. The sizes of mesh and time step were tested so that they would not affect the simulation results. As shown in Fig. 3.2, the present model agrees well with earlier results (Peters and Smith, 2002).

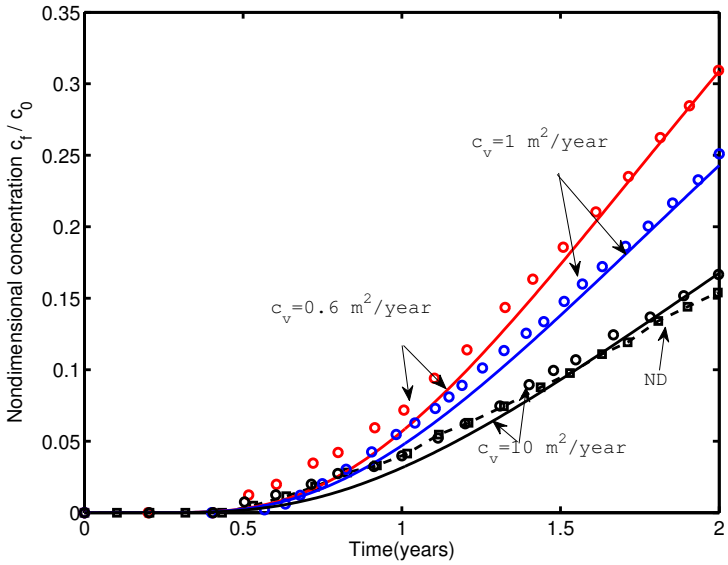

Figure 3.2: Comparison with previous work (Peters and Smith, 2002). Present model: lines; results from Peters and Smith (2002): circles; result of the no-deformation model (ND) from Peters and Smith (2002): dashed line with square symbol. $L = 0.914$ m, $n^0 = 0.25$, $D_m = 0.1$ m^2/y ($S_r = 1$ and $\beta = 0$).

3.3.2 Dimensionless analysis

In this section, we discuss the significance of each term in the governing equations. Based on the numerical examples used in Peters and Smith (2002) and Lewis et al. (2009), the input data or parameters adopted in the landfill clay barrier system are listed in Table 3.2. It should be noted that inter-relationships exist among the various A_is. Further, $(2G(1-\nu)K)/(1-2\nu)$ in A_3 should be restricted to a reasonable range of c_v. Additionally, given the assumption on porosity, the choice of parameters should ensure that the non-dimensional soil deformation is relatively small, e.g., less than 20%. Assuming $S_r = 0.8 \sim 1.0$, $\alpha_L = 0.1$ m, $\nu = 0.33$, we focus on variations of $S_r(\beta)$, D_m, K, G and present the magnitude of each coefficient as in Table 3.3. The characteristic parameters are, $t_c = 4.97 \times 10^7$ s (1.576 y), $p_c = 6.50 \times 10^5$ Pa, $u_c = 0.33$ m for case 1 and $t_c = 3.98 \times 10^6$ s (0.126 y), $p_c = 6.50 \times 10^6$ Pa, $u_c = 0.33$m for case 2.

The corresponding non-dimensional form for the boundary conditions (BCs) and initial conditions (ICs) are

Table 3.2: Typical parameter values for a landfill clay barrier system

Parameter	Value
Waste loading, $Q(t)$	ramp loading, 2×10^5 Pa/y $\times$ 2 y
Thickness of geomembrane, h	0.0015 m
Thickness of CCL, L	0.914 ~ 1.22 m
Mass transfer coefficient of geomembrane, D_G	10^{-4} m^2/y
Partitioning coefficient, K_d	0
Effective coefficient of molecular diffusion in the clay, D_m	$5 \times 10^{-10} \sim 5 \times 10^{-9}$ m^2/s
Coefficient of consolidation in clay, c_v	0.6 ~ 10 m^2/y
Shear modulus, G	$5 \times 10^5 \sim 5 \times 10^6$ Pa
Hydraulic conductivity of clay, K	$10^{-10} \sim 1.5 \times 10^{-10}$ m/s
Initial porosity of clay, n^0	0.33
Acceleration due to gravity, g	9.8 m/s^2
Initial density of the pore fluid, ρ_w	10^3 kg/m^3
Density of the solid phase, ρ_s	2.6×10^3 kg/m^3

Table 3.3: Magnitude of coefficients $A_1 - A_8$ used in the landfill case and simulation cases

Coefficient	Order	Case 1	Case 2
A_1	$0.13 \sim 14.05$	0.13	14.05
A_2	$5.33 \times 10^{-4} \sim 10^{-3}$	5.33×10^{-3}	5.33×10^{-4}
A_3	$1.65 \times 10^{-3} \sim 0.248$	0.248	1.99×10^{-3}
A_4	0.1	0.1	0.1
A_5	$1.30 \times 10^{-2} \sim 1.4$	1.3×10^{-2}	1.4
A_6	$1.11 \times 10^{-3} \sim 0.166$	0.166	1.33×10^{-3}
A_7	0.33	0.33	0.33
A_8	$0.13 \sim 14.05$	0.13	14.05

$$\frac{\partial p^*(0,t^*)}{\partial z^*} = 0, \quad p^*(1,t^*) = 0, \quad p^*(z^*,0) = 0; \tag{3.27}$$

$$\frac{\partial u^*(0,t^*)}{\partial z^*} = \frac{(1-2\nu)Lp_c}{2G(1-\nu)u_c}\left[\frac{-Q(t^*t_c)}{p_c} + p^*\right] = \frac{-Q(t^*t_c)}{p_c} + p^*, \tag{3.28}$$
$$u^*(1,t^*) = 0, \quad u^*(z^*,0) = 0;$$

$$\frac{\partial c^*(0,t^*)}{\partial z^*} = \frac{D_G L}{n^0 h D_m}(c^* - 1) = A_9(c^* - 1), \quad \frac{\partial c^*(1,t^*)}{\partial z^*} = 0, \quad c^*(z^*,0) = 0. \tag{3.29}$$

where the ratio of the mass transfer coefficients of geomembrane and clay is specified as $D_G/D_m = 10^{-3}$, then $A_9 = 2.02$.

3.3.3 Simplification analysis

Peters and Smith (2002) and Lewis et al. (2009) performed a small deformation analysis using a spatial coordinate system. In their models (Peters and Smith, 2002; Lewis et al., 2009),

Table 3.4: Governing equations, boundary and initial conditions used in the models

Governing equations	Boundary & Initial conditions	Note
Eqs. (3.18-3.20)	Eqs. (3.27-3.29)	Eqs. (3.18-3.19) are coupled and Eq. (3.20) is solved separatedly

the spatial variation of porosity, self-weight of the clay liner (SW) and longitudinal dispersivity were not considered (Peters and Smith, 2002; Lewis et al., 2009). That is because they emphasized mechanical consolidation-induced advective solute transport and the differences made by geometric and material non-linearity compared with linear models. A useful metric is the "breakthrough time", which is defined as the time for the contaminant concentration in the SLCS to reach a predetermined concentration, say 0.1 times that of concentration in landfill, i.e., $c^* = 0.1$ in the present non-dimensional analysis.

At the bottom boundary, there is only an advective contaminant flux component because of the zero gradient in c_f. Besides the breakthrough time, the advective emission, i.e., the cumulative contaminant mass outflow per unit area from the barrier system due to advective flow, is also assessed to evaluate the influence of deformation on the solute transport. Provided the fixed bottom boundary, the non-dimensional advective emission can be taken as

$$E^*_{adv} = \int_0^{t^*} -\frac{\partial p^*(\tau)}{\partial z^*} c^*(\tau) d\tau. \tag{3.30}$$

Based on the present model, the effect of SW, SVP, CPW and longitudinal dispersion on solute transport in terms of advective solute emission at the exit boundary is examined. The governing equations, boundary and initial conditions employed are listed in the Table 3.4. Since the transient porous flows influence the solute transport process but the solute transport is assumed to have no effect on the porous flows, the associated equation for solute transport can be solved separately while the equations to govern the force balance and storage of pore fluid should be solved simultaneously.

Table 3.5: Details of each model

Model	Details
Mode A	$A_1 \frac{\partial p^*}{\partial t^*} c^*$ is omitted
Mode B	$A_1 A_7 \frac{\partial u^*}{\partial t^*} \frac{\partial p^*}{\partial z^*} c^*$ is omitted
Mode C	$A_8 = 0$, $A_1 \frac{\partial p^*}{\partial t^*} c^*$ and $A_1 A_7 \frac{\partial u^*}{\partial t^*} \frac{\partial p^*}{\partial z^*} c^*$ are omitted
Mode D	$A_4 \frac{\partial p^*}{\partial z^*} \frac{\partial^2 c^*}{\partial z^{*2}}$ is omitted
Mode E	$A_1 A_4 \frac{\partial p^*}{\partial t^*} \frac{\partial c^*}{\partial z^*}$ is omitted
Mode F	$A_4 \frac{\partial^2 u^*}{\partial z^* \partial t^*} \frac{\partial c^*}{\partial z^*}$ is omitted
Mode G	$A_5 = 0$ and $A_1 A_4 \frac{\partial p^*}{\partial t^*} \frac{\partial c^*}{\partial z^*}$ are omitted

For cases 1 and 2, results are given in Figs. 3.3 - 3.5, and the details for model A-G are tabulated in Table 3.5. As shown in Table 3.3, A_2, A_3 and A_6 are relatively small. However, A_3 represents molecular diffusion mechanism, which is the main contaminant transport mechanism in the post-consolidation period. Therefore, A_3 is kept in the present model. Fig. 3.3 shows that the effect of SW and SVP are negligible for case 1; both can be omitted without inducing a discernible difference. Regarding case 2, the differences due to SW and SVP are even smaller because of the smaller values of A_3 and A_6 than in case 1.

When $A_1 = 0$, the compressibility of pore water is ignored in the consolidation and transport equations. In the latter, the CPW gives rise to three terms similar to sources/sinks, and also terms that couple with dispersivity. Fig. 3.4 shows that the influence of CPW is increasingly important in case 2 (the advective emission (or flux) increases approximately four times for the case including CPW). Furthermore, results of mode C are close to that of the full model, which indicates that the terms arising due to CPW in the transport equations matter little, while the terms due to CPW in the consolidation equation alter the flows and dominate the emission flux.

Fig. 3.5 shows that the effect of longitudinal dispersivity increases when D_m decreases. In case 2, the advective emission predicted by the model with longitudinal dispersivity is

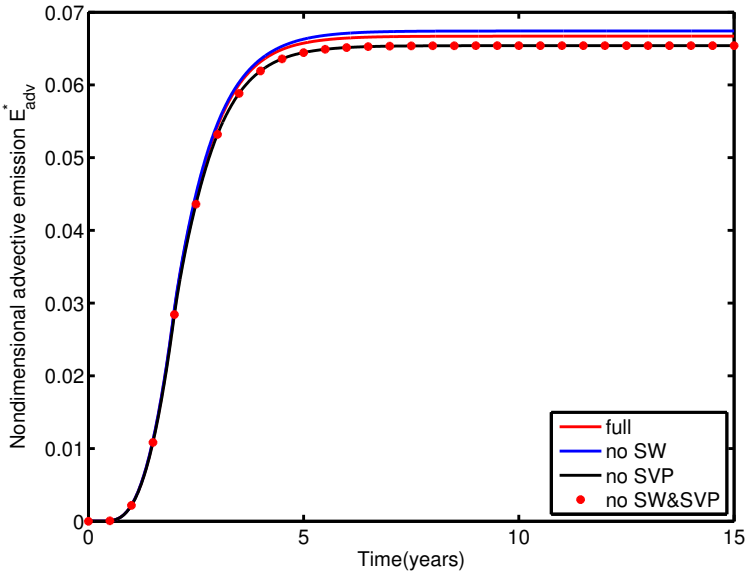

(a) Case 1

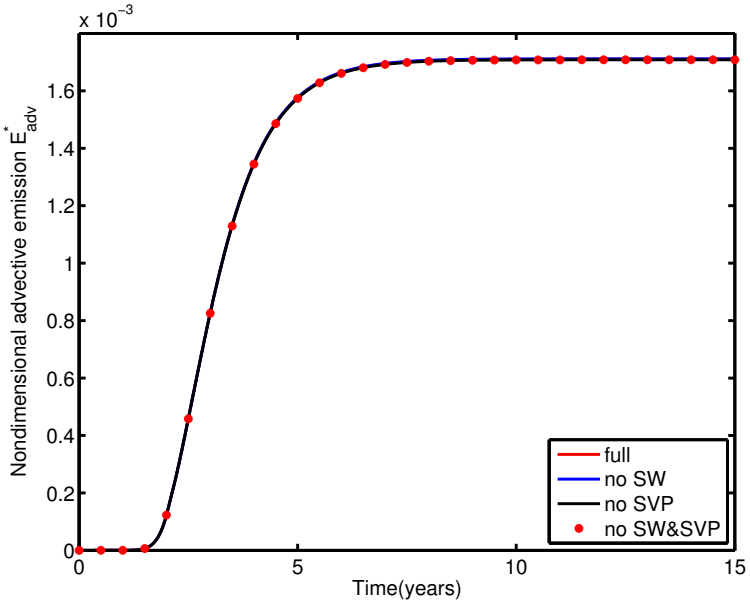

(b) Case 2

Figure 3.3: Influence of self-weight (SW) and spatial variation of porosity (SVP) on advective emission

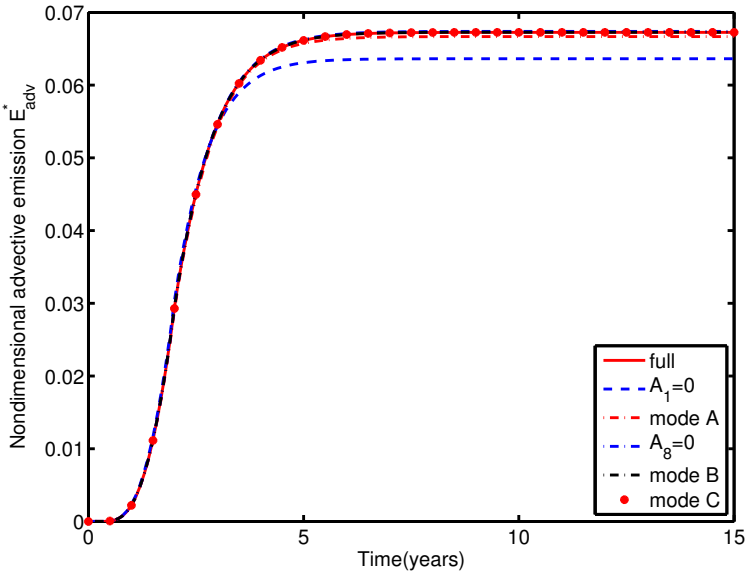

(a) Case 1

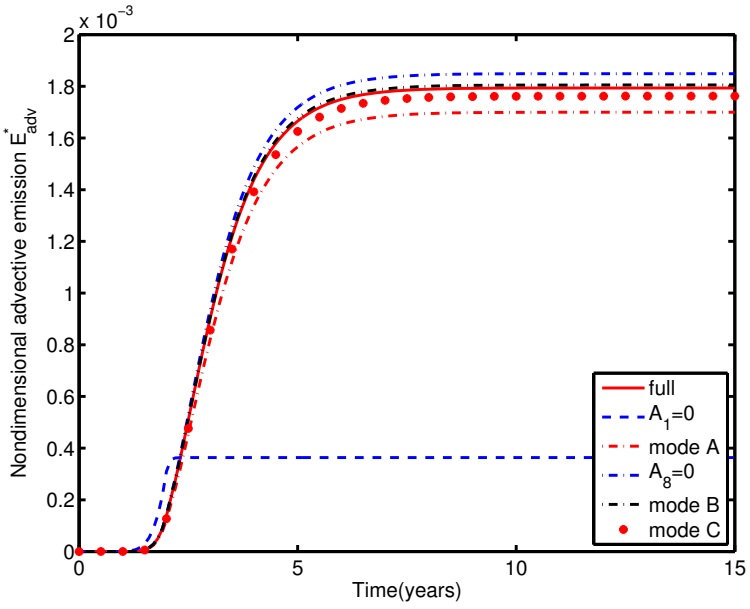

(b) Case 2

Figure 3.4: Influence of compressibility of pore water (CPW) on advective emission

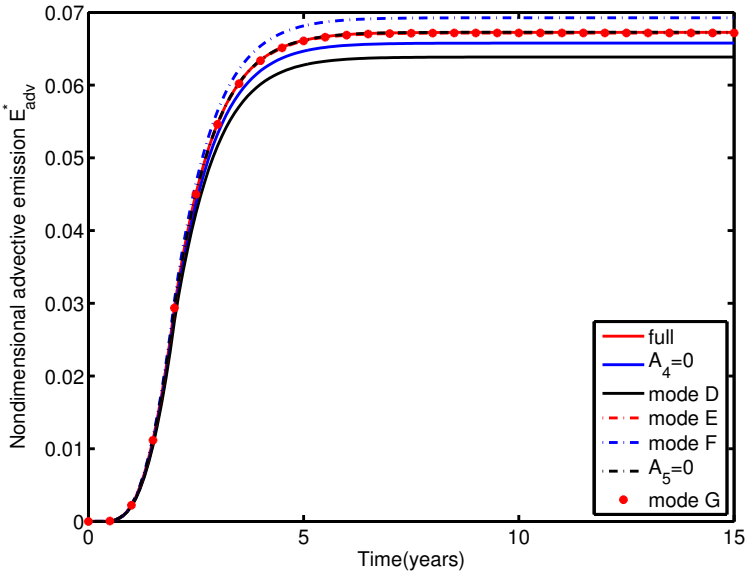

(a) Case 1

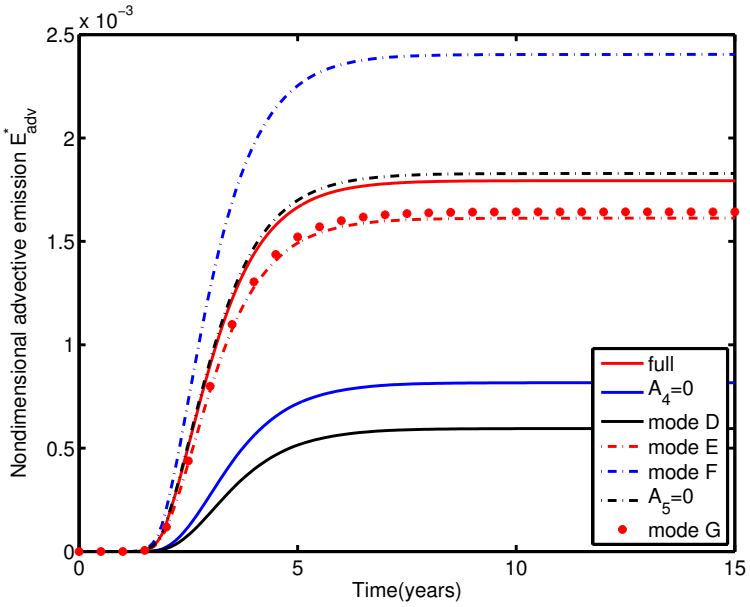

(b) Case 2

Figure 3.5: Influence of longitudinal dispersivity on advective emission

twice that of the model without longitudinal dispersivity. Among these four longitudinal dispersivity terms, the influence of $(\partial p^*/\partial z^*)\partial^2 c^*/\partial z^{*2}$ and $(\partial^2 u^*/\partial z^*\partial t^*)\partial c^*/\partial z^*$ are much greater than that of $(\partial p^*/\partial t^*)\partial c^*/\partial z^*$ and $(\partial p^*/\partial z^*)\partial c^*/\partial z^*$. Therefore, it is reasonable to retain only the former two terms as in mode G.

Based on the above analysis, the complete model can be simplified as

$$\frac{2G(1-\nu)n^0\beta}{1-2\nu}\frac{\partial p^*}{\partial t^*}+\frac{\partial^2 u^*}{\partial t^*\partial z^*}=\frac{\partial^2 p^*}{\partial z^{*2}}, \tag{3.31}$$

$$\frac{\partial^2 u^*}{\partial z^{*2}}=\frac{\partial p^*}{\partial z^*}, \tag{3.32}$$

$$\begin{aligned}\frac{\partial c^*}{\partial t^*}=&\frac{S_r^2 n^0 D_m \rho_w g(1-2\nu)}{2\left[S_r n^0+(1-n^0)\rho_s K_d\right]G(1-\nu)K}\frac{\partial^2 c^*}{\partial z^{*2}}-\frac{\alpha_L}{L}\frac{\partial p^*}{\partial z^*}\frac{\partial^2 c^*}{\partial z^{*2}}\\&+\frac{\partial c^*}{\partial z^*}\left\{-\frac{\alpha_L}{L}\frac{\partial^2 u^*}{\partial z^*\partial t^*}+\frac{\partial p^*}{\partial z^*}-\frac{\left[S_r n^0+\left(1-n^0\right)\rho_s K_d\right]}{S_r}\frac{\partial u^*}{\partial t^*}\right\}.\end{aligned} \tag{3.33}$$

As shown in Fig. 3.6, the proposed model gives a reasonable approximation to the full model.

3.3.4 Effects of degree of saturation and loading

Based on the simplified model, the effect of degree of saturation S_r and loading progress on the contaminant breakthrough and advective emission are examined. Fig. 3.7 shows that S_r has no discernible effect on the transit time for contaminant to pass through the landfill liner. Furthermore, there is little change in the advective emission during the loading period (Fig. 3.8). However, a lower degree of saturation leads to greater average fluid velocity (Fig. 3.9), which further increases the emission flux, yielding significantly different advective emission in the post-loading period (Fig. 3.8). It should be noted that the smaller average fluid velocity for higher degree of saturation is artificially produced by the assumption of constant hydraulic conductivity. Physically, the hydraulic conductivity decreases for lower degree of

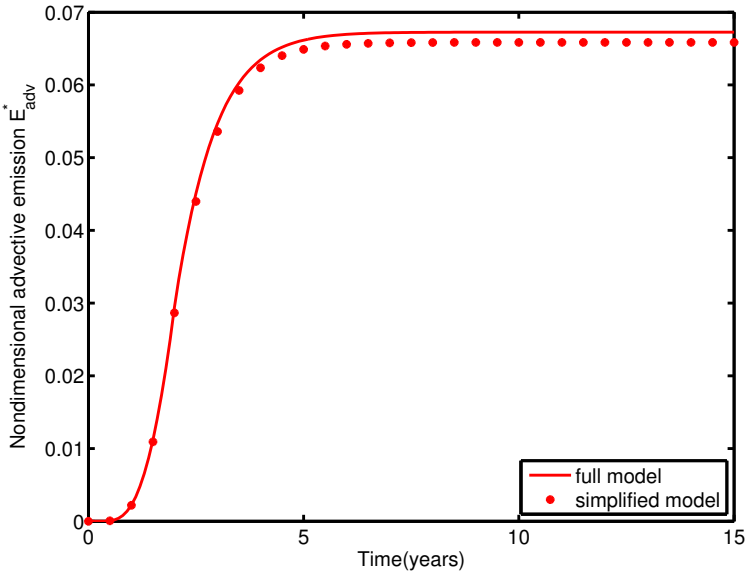

(a) Case 1

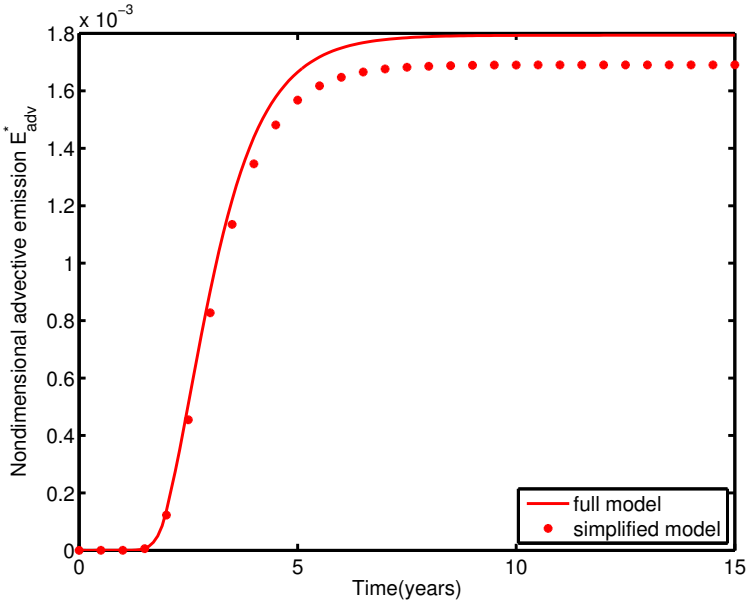

(b) Case 2

Figure 3.6: Comparison of advective emission between the simplified and complete full models

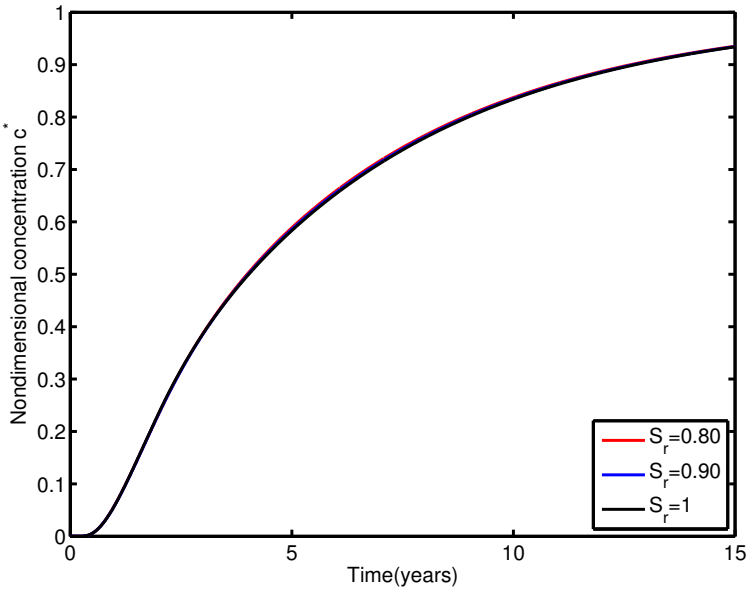

Figure 3.7: Influence of degree of saturation S_r on relative solute concentration at liner bottom, c^*. $D_m = 5 \times 10^{-9}$ m^2/s, $K = 1 \times 10^{-10}$ m/s, $G = 5 \times 10^5$ Pa.

saturation and consequently the average fluid velocity is expected to be smaller. However, the effect of CPW for soil with lower degree of saturation is more obvious. In other words, the consolidation process is slowed down more notably for smaller degree of saturation and a relatively larger level of average fluid tends to occur when the concentration of solute becomes higher at the drainage boundary. Therefore, the advective emission for lower degree of saturation may still be larger than that of a higher degree of saturation.

In this study, the degree of saturation is assumed to be spatially and temporally constant. However, the pore fluid pressure (except near the drainage boundary) experiences a increase in response to the external ramp loading and then gradually decreases after the completion of waste filling. Therefore, it is conceivable that the volume of occluded air bubbles at a location of high pore fluid pressure may decrease to a extent at which they can possibly flow with the pore water. In that case, the degree of saturation will increase slightly and the solute transport will be faster.

Figs. 3.10-3.12 show that a larger loading rate results in smaller advective emission with the same total surcharge. Faster loading leads to faster solute transit initially, but the concentration at the exit boundary will reach the same level (Fig. 3.10). Although the final

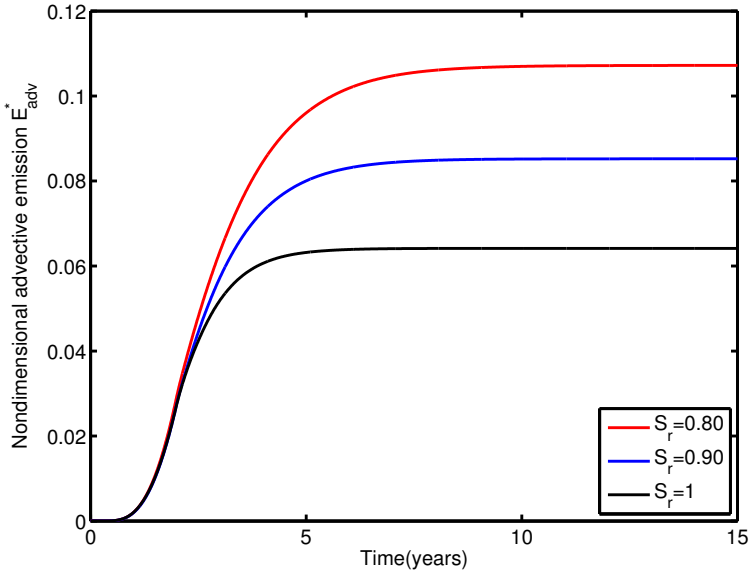

Figure 3.8: Influence of degree of saturation S_r on the accumulative solute emission at liner bottom, E^*_{adv}. $D_m = 5 \times 10^{-9}$ m^2/s, $K = 1 \times 10^{-10}$ m/s, $G = 5 \times 10^5$ Pa.

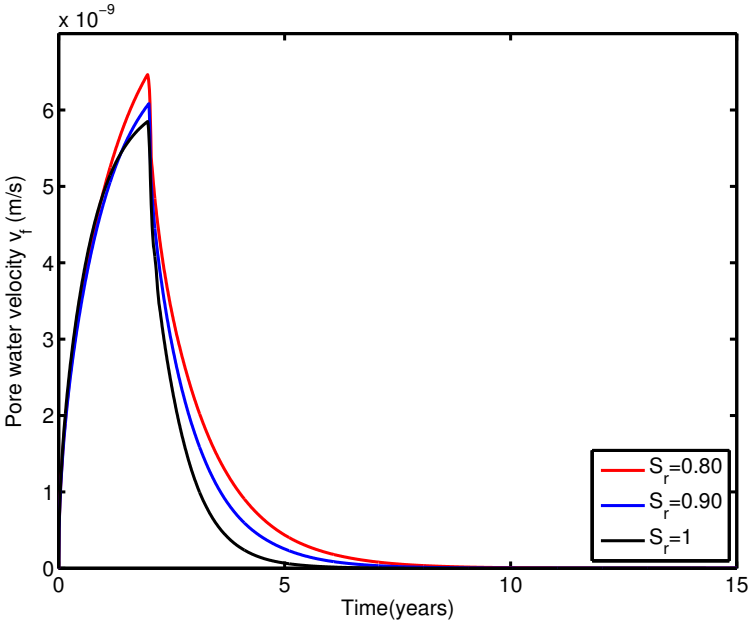

Figure 3.9: Influence of degree of saturation S_r on the average liner pore water velocity at liner bottom, v_f. $D_m = 5 \times 10^{-9}$ m^2/s, $K = 1 \times 10^{-10}$ m/s, $G = 5 \times 10^5$ Pa.

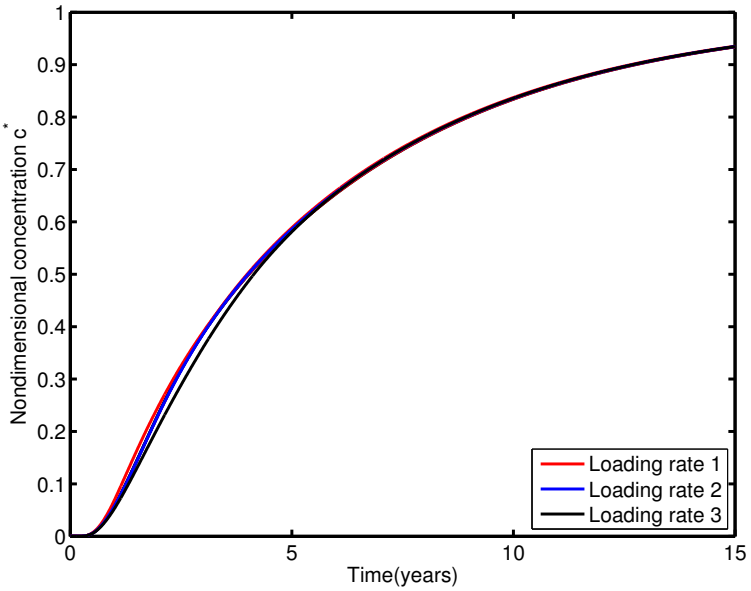

Figure 3.10: Influence of loading process on relative solute concentration at liner bottom, c^*: loading rate 1 ~ 3 represent 4×10^5 Pa/y continuing for 1 year, 2×10^5 Pa/y continuing for 2 year and 1×10^5 Pa/y continuing for 4 year, respectively. $S_r = 0.9$, $D_m = 5 \times 10^{-9}$ m^2/s, $K = 1 \times 10^{-10}$m/s, $G = 5 \times 10^5$ Pa.

water emission is the same (in Fig. 3.12), the gap in advective emission of solute is huge (Fig. 3.11), more than two orders of magnitude in the considered case. This is attributed to fluid velocities, as the fluid acts as the carrier of solute. During the early stage, greater fluid velocity of fast loading occurs earlier that of slow loading. However, the concentration of solute takes time to rise and consequently the advection flux of solute is relatively smaller at this stage. Therefore, the final advective emission of fast loading is less than that of slow loading. This finding can serve as a guide for planning of loading in landfill facilities.

3.4 Summary

In this chapter, the fluid storage equation and advective-diffusive equation for nearly saturated deformable porous media was proposed. Non-dimensional analysis of the comprehensive equations in the landfill liner application demonstrated that the influences of self-weight and spatial variation of porosity are negligible. However, the effects of longitudinal dispersivity and compressibility of pore water are significant in some circumstances. The

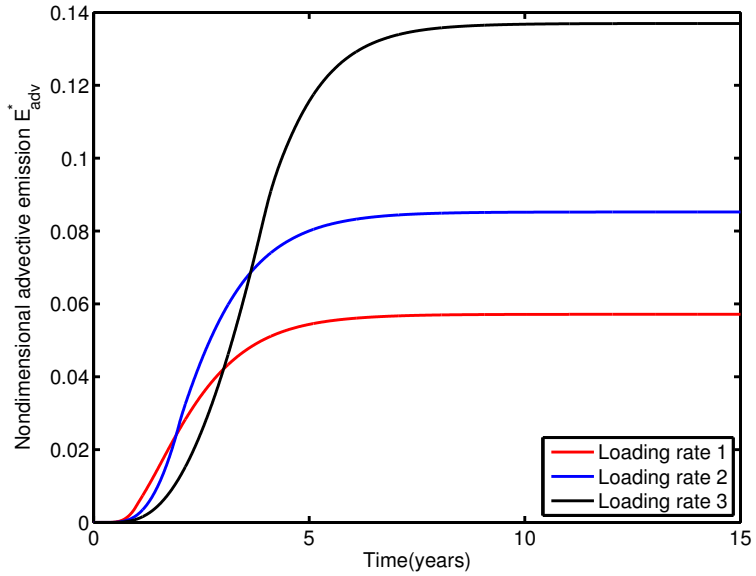

Figure 3.11: Influence of loading process on the accumulative solute emission at liner bottom, E^*_{adv}: loading rate 1 ~ 3 represent 4×10^5 Pa/y continuing for 1 year, 2×10^5 Pa/y continuing for 2 year and 1×10^5 Pa/y continuing for 4 year, respectively. $S_r = 0.9$, $D_m = 5 \times 10^{-9}$ m^2/s, $K = 1 \times 10^{-10}$m/s, $G = 5 \times 10^5$ Pa.

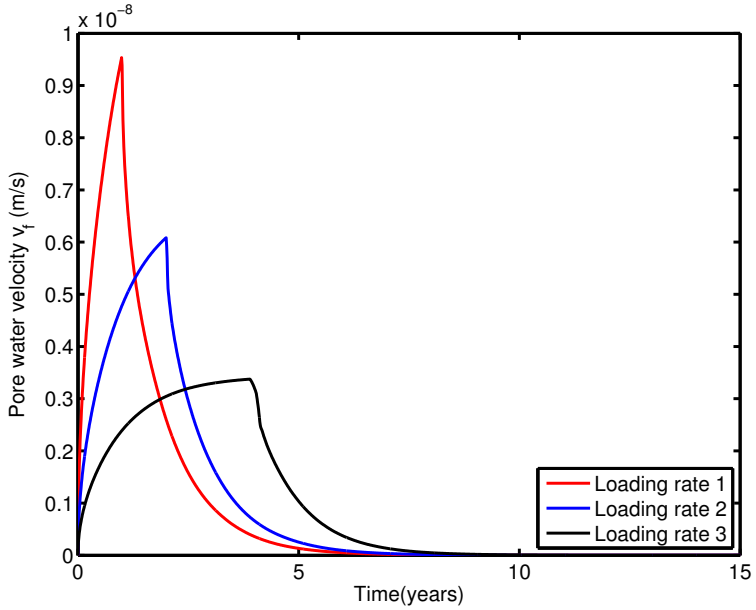

Figure 3.12: Influence of loading process on the average liner pore water velocity at liner bottom, v_f: loading rate 1 ~ 3 represent 4×10^5 Pa/y continuing for 1 year, 2×10^5 Pa/y continuing for 2 year and 1×10^5 Pa/y continuing for 4 year, respectively. $S_r = 0.9$, $D_m = 5 \times 10^{-9}$ m^2/s, $K = 1 \times 10^{-10}$m/s, $G = 5 \times 10^5$ Pa.

parametric analysis investigated both breakthrough and advective emission of contamination, and the results indicated that the lower saturation leads to more advective emission due to greater fluid velocity, and that the slow loading rate of surcharge increases the total advective emission significantly. Nevertheless, the variation of degree of saturation and different waste implacement rates have little influence on the solute relative concentration evolution at landfill liner bottom, namely, the time for VOCs break through CCL.

3.5 Appendices

3.5.1 Appendix 3A: Derivation of fluid storage equation

Representative elementary volume (REV) is used to represent the characteristics of porous medium at all points in the domain. The macroscopic mass conservative equation for pore water can be obtained from the molecular level by volume averaging over REV. Its general form is (Bear and Cheng, 2010)

$$\frac{\partial}{\partial t}\left(\theta\rho_w\right) = -\nabla\cdot\left(\rho_w\theta\overrightarrow{\mathbf{v}_f}\right), \tag{3.34}$$

where the volume fraction θ is related to porosity n and degree of saturation S_r by $\theta = S_r n$, ρ_w is density of pore water, $\overrightarrow{\mathbf{v}_f}$ denotes the average fluid velocity vector, which can be related to specific discharge relative to solid, $\overrightarrow{\mathbf{q}_r}$ based on Darcy's law by

$$\overrightarrow{\mathbf{q}_r} = \theta\left(\overrightarrow{\mathbf{v}_f} - \overrightarrow{\mathbf{v}_s}\right) = -\frac{K}{\rho_w g}\nabla p^e, \tag{3.35}$$

where $\overrightarrow{\mathbf{v}_s}$ is velocity of the solid and the hydraulic conductivity, K is taken as constant in this chapter.

Assuming ρ_w depends only on p, and with the definition of coefficient of compressibility β $(= (1/\rho_w)d\rho_w/dp)$, Eq. (3.34) yields

$$\frac{\partial S_r n}{\partial t} + \nabla\cdot\left(S_r n\overrightarrow{\mathbf{v}_f}\right) = -S_r n\beta\left(\frac{\partial p^e}{\partial t} + \overrightarrow{\mathbf{v}_f}\cdot\nabla p^e\right). \tag{3.36}$$

Based on the assumption that the degree of saturation, S_r is constant, and Darcy's law, Eq. (3.36) becomes

$$\frac{\partial S_r n}{\partial t} + S_r \nabla \cdot \left(n\overrightarrow{\mathbf{v}_s}\right) - \nabla \cdot \left(\frac{K}{\rho_w g}\nabla p^e\right) = -S_r n\beta\left(\frac{\partial p^e}{\partial t} + \overrightarrow{\mathbf{v}_f} \cdot \nabla p^e\right). \tag{3.37}$$

Using the chain rule, we have

$$\nabla \cdot \left(\frac{K}{\rho_w g}\nabla p^e\right) = \frac{1}{\rho_w g}\nabla \cdot (K\nabla p^e) - \frac{K}{\rho_w g}\beta\nabla p^e \cdot \nabla p^e. \tag{3.38}$$

Substituting this expression and Eq. (3.35) into Eq. (3.37) gives

$$\begin{aligned}\frac{\partial S_r n}{\partial t} + S_r \nabla \cdot (n\overrightarrow{\mathbf{v}_s}) - \frac{1}{\rho_w g}\nabla \cdot (K\nabla p^e) - S_r n\beta(\overrightarrow{\mathbf{v}_f} - \overrightarrow{\mathbf{v}_s}) \cdot \nabla p^e \\ = - S_r n\beta(\frac{\partial p^e}{\partial t} + \overrightarrow{\mathbf{v}_f} \cdot \nabla p^e).\end{aligned} \tag{3.39}$$

Rearranging,

$$\frac{\partial S_r n}{\partial t} + S_r \nabla \cdot \left(n\overrightarrow{\mathbf{v}_s}\right) - \frac{1}{\rho_w g}\nabla \cdot (K\nabla p^e) = -S_r n\beta\left(\frac{\partial p^e}{\partial t} + \overrightarrow{\mathbf{v}_s} \cdot \nabla p^e\right). \tag{3.40}$$

Regarding the solid phase, its mass conservation equation is given by

$$\frac{\partial}{\partial t}\left[(1-n)\rho_s\right] = -\nabla \cdot \left((1-n)\rho_s\overrightarrow{\mathbf{v}_s}\right). \tag{3.41}$$

Since the deformation modulus of soil particles is relatively large under usual loading, deformation of the solid phase is assumed to be volume preserving, i.e., $D_s\rho_s/Dt = 0$ (where D_s/Dt is the material derivation), hence,

$$\frac{\partial n}{\partial t} = (1-n)\nabla \cdot \overrightarrow{\mathbf{v}_s} - \overrightarrow{\mathbf{v}_s} \cdot \nabla n = \nabla \cdot \overrightarrow{\mathbf{v}_s} - \nabla \cdot (n\overrightarrow{\mathbf{v}_s}). \tag{3.42}$$

Assuming the degree of saturation, S_r is constant in time and space, Eq. (3.40) becomes

$$S_r \nabla \cdot \overrightarrow{\mathbf{v}}_s - \frac{1}{\rho_w g} \nabla \cdot (K \nabla p^e) = -S_r n \beta \left(\frac{\partial p^e}{\partial t} + \overrightarrow{\mathbf{v}}_s \cdot \nabla p^e \right). \tag{3.43}$$

In case of relatively small deformations, it is reasonable to make the assumption that the advective component variation of p^e can be ignored (Bear and Cheng, 2010), i.e.,

$$|\frac{\partial p^e}{\partial t}| \gg |\overrightarrow{\mathbf{v}}_s \cdot \nabla p^e|, \tag{3.44}$$

thus,

$$S_r n \beta \frac{\partial p^e}{\partial t} + S_r \nabla \cdot \overrightarrow{\mathbf{v}}_s = \frac{1}{\rho_w g} \nabla \cdot (K \nabla p^e). \tag{3.45}$$

When $S_r = 1$, it leads to

$$n \beta \frac{\partial p^e}{\partial t} + \nabla \cdot \overrightarrow{\mathbf{v}}_s = \frac{1}{\rho_w g} \nabla \cdot (K \nabla p^e), \tag{3.46}$$

which is equivalent to the well-known storage equation of Verruijt (1969).

3.5.2 Appendix 3B: Derivation of solute transport equation

Within a fixed representative element volume (REV), the concentration of solute is constant. Conservation of solute mass in the fluid phase can be achieved by averaging the microscopic continuity equation over REV and is written as

$$\frac{\partial \left(n S_r c_f \right)}{\partial t} + s = -\frac{\partial}{\partial z} \left[n S_r \left(-D \frac{\partial c_f}{\partial z} + v_f c_f \right) \right], \tag{3.47}$$

where, s is the rate of solute mass source per unit volume. The rate of solute loss by sorption onto the solid phase is equal to the rate of the solute gain by the solid phase from the fluid phase. It is noted that the amount and identity of matter in the REV may change with time, while the shape and position of this volume remain fixed. However, for the deformable

porous medium considered in this study, the porosity n is time-dependent, and the macroscopic velocity of the solid matrix is not zero.

Conservation of solute mass for the solid phase is given by

$$\frac{\partial[(1-n)c_s]}{\partial t} - s = -\frac{\partial}{\partial z}\left[(1-n)v_s c_s\right]. \tag{3.48}$$

Finally, the transport equation for a solute in a deforming porous medium is expressed by combination of Eqs. (3.47) and (3.48),

$$\frac{\partial\left(nS_r c_f\right)}{\partial t} + \frac{\partial[(1-n)c_s]}{\partial t} = -\frac{\partial}{\partial z}\left[nS_r\left(-D\frac{\partial c_f}{\partial z} + v_f c_f\right) + (1-n)v_s c_s\right]. \tag{3.49}$$

By the use of the mass balance equations for the fluid phase (Eq. (3.36)), and solid phases (Eq. (3.41)), and keeping in mind that ρ_s is constant, Eq. (3.49) can be simplified to

$$\begin{aligned} S_r n\frac{\partial c_f}{\partial t} + (1-n)\frac{\partial c_s}{\partial t} =& \frac{\partial}{\partial z}\left(S_r nD\frac{\partial c_f}{\partial z}\right) - S_r n v_f\frac{\partial c_f}{\partial z} \\ & - (1-n)v_s\frac{\partial c_s}{\partial z} + S_r n\beta\left(\frac{\partial p^e}{\partial t} + v_f\frac{\partial p^e}{\partial z}\right)c_f. \end{aligned} \tag{3.50}$$

Assuming the linear sorption relationship as described by Eq. (3.5) and (3.6), expanding Eq. (3.50) leads to

$$\begin{aligned} \left[S_r n + (1-n)\rho_s K_d\right]\frac{\partial c_f}{\partial t} =& S_r nD\frac{\partial^2 c_f}{\partial z^2} + \frac{\partial c_f}{\partial z}\left(S_r n\frac{\partial D}{\partial z} + S_r D\frac{\partial n}{\partial z} + \frac{K}{\rho_w g}\frac{\partial p^e}{\partial z}\right. \\ & \left. - \left[S_r n + (1-n)\rho_s K_d\right]\frac{\partial u}{\partial t}\right) + S_r n\beta\frac{\partial p^e}{\partial t}c_f \\ & - \beta\frac{K}{\rho_w g}\left(\frac{\partial p^e}{\partial z}\right)^2 c_f + S_r n\beta\frac{\partial u}{\partial t}\frac{\partial p^e}{\partial z}c_f. \end{aligned} \tag{3.51}$$

It is noted that the spatial derivative of porosity exists in Eq. (3.51). Volume conservation of the solid phase in soil can be utilized to develop its expression. For an incompressible solid:

$$U_s = U_m(1-n) = constant, \tag{3.52}$$

where U_s, U_m denote solid particle volume and the porous medium volume in the representive volume element, respectively. We separate U_m into the initial volume U_{m0} and incremental volume U_m^e, Eq. (3.52) becomes

$$U_s = (U_{m0} + U_m^e)(1-n). \tag{3.53}$$

By definition, volumetric strain $\varepsilon_v = U_m^e/U_{m0}$. Dividing both sides of Eq. (3.53) by U_{m0} obtains

$$1 - n^0 = (1+\varepsilon_v)(1-n). \tag{3.54}$$

Therefore,

$$\nabla\left((1+\varepsilon_v)(1-n)\right) = 0. \tag{3.55}$$

Correspondingly,

$$\nabla n = \frac{(1-n)}{1+\varepsilon_v}\nabla\varepsilon_v = \frac{(1-n)^2}{1-n^0}\nabla\varepsilon_v. \tag{3.56}$$

In the analysis of Peters and Smith (2002), the spatial variation of n was neglected. Here, this can be accommodated by use of Eq. (3.56). Therefore, Eq. (3.51) becomes

$$\begin{aligned}\left[S_r n + (1-n)\rho_s K_d\right]\frac{\partial c_f}{\partial t} = {} & S_r n D\frac{\partial^2 c_f}{\partial z^2} + \frac{\partial c_f}{\partial z}\left(S_r n\frac{\partial D}{\partial z} + S_r D\frac{(1-n)^2}{1-n^0}\frac{\partial^2 u}{\partial z^2}\right.\\ & \left. + \frac{K}{\rho_w g}\frac{\partial p^e}{\partial z} - [S_r n + (1-n)\rho_s K_d]\frac{\partial u}{\partial t}\right)\\ & + S_r n\beta\frac{\partial p^e}{\partial t}c_f - \beta\frac{K}{\rho_w g}\left(\frac{\partial p^e}{\partial z}\right)^2 c_f + S_r n\beta\frac{\partial u}{\partial t}\frac{\partial p^e}{\partial z}c_f.\end{aligned} \tag{3.57}$$

Taking into account the constant longitudinal dispersivity, Eq. (3.57) changes to

$$
\begin{aligned}
[S_r n + (1-n)\rho_s K_d]\frac{\partial c_f}{\partial t} &= S_r n D_m \frac{\partial^2 c_f}{\partial z^2} + S_r n \alpha_L (v_f - v_s)\frac{\partial^2 c_f}{\partial z^2} \\
&+ \frac{\partial c_f}{\partial z}\left\{ S_r \alpha_L n \frac{\partial (v_f - v_s)}{\partial z} + S_r D_m \frac{(1-n)^2}{1-n^0}\frac{\partial^2 u}{\partial z^2} \right. \\
&+ S_r \alpha_L (v_f - v_s)\frac{\partial n}{\partial z} + \frac{K}{\rho_w g}\frac{\partial p^e}{\partial z} \\
&\left. - [S_r n + (1-n)\rho_s K_d]\frac{\partial u}{\partial t} \right\} \\
&+ S_r n \beta \frac{\partial p^e}{\partial t} c_f - \beta \frac{K}{\rho_w g}\left(\frac{\partial p^e}{\partial z}\right)^2 c_f + S_r n \beta \frac{\partial u}{\partial t}\frac{\partial p^e}{\partial z} c_f .
\end{aligned} \tag{3.58}
$$

Recall the chain rule,

$$
\begin{aligned}
S_r \alpha_L n \frac{\partial \left(v_f - v_s\right)}{\partial z} + S_r \alpha_L \left(v_f - v_s\right)\frac{\partial n}{\partial z} &= \alpha_L \frac{\partial \left[S_r n \left(v_f - v_s\right)\right]}{\partial z} \\
&= -\alpha_L \frac{\partial \left(\frac{K}{\rho_w g}\frac{\partial p^e}{\partial z}\right)}{\partial z},
\end{aligned} \tag{3.59}
$$

and employing Eq. (3.38) and Eq. (3.45), Eq. (3.58) becomes

$$
\begin{aligned}
[S_r n + (1-n)\rho_s K_d]\frac{\partial c_f}{\partial t} &= S_r n D_m \frac{\partial^2 c_f}{\partial z^2} - \alpha_L \frac{K}{\rho_w g}\frac{\partial p^e}{\partial z}\frac{\partial^2 c_f}{\partial z^2} \\
&+ \frac{\partial c_f}{\partial z}\left\{ -\alpha_L S_r n \beta \frac{\partial p^e}{\partial t} - \alpha_L S_r \frac{\partial^2 u}{\partial z \partial t} \right. \\
&+ \frac{\alpha_L \beta K}{\rho_w g}\left(\frac{\partial p^e}{\partial z}\right)^2 + S_r D_m \frac{(1-n)^2}{1-n^0}\frac{\partial^2 u}{\partial z^2} \\
&\left. + \frac{K}{\rho_w g}\frac{\partial p^e}{\partial z} - [S_r n + (1-n)\rho_s K_d]\frac{\partial u}{\partial t} \right\} \\
&+ S_r n \beta \frac{\partial p^e}{\partial t} c_f - \beta \frac{K}{\rho_w g}\left(\frac{\partial p^e}{\partial z}\right)^2 c_f + S_r n \beta \frac{\partial u}{\partial t}\frac{\partial p^e}{\partial z} c_f .
\end{aligned} \tag{3.60}
$$

3.5.3 Appendix 3C: Determination of the characteristic units in nondimensionalization

Assuming K is constant, instituting (3.14) into (3.11) - (3.13) obtains

$$\frac{S_r n^0 \beta p_c}{t_c}\frac{\partial p^*}{\partial t^*} + \frac{S_r u_c}{l_c t_c}\frac{\partial^2 u^*}{\partial t^* \partial z^*} = \frac{K p_c}{\rho_w g l_c^2}\frac{\partial^2 p^*}{\partial z^{*2}} \tag{3.61}$$

$$G\frac{2(1-\nu)u_c}{(1-2\nu)l_c^2}\frac{\partial^2 u^*}{\partial z^{*2}} + \frac{(1-n^0)(\rho_s - S_r\rho_w)g u_c}{l_c}\frac{\partial u^*}{\partial z^*} = \frac{p_c}{l_c}\frac{\partial p^*}{\partial z^*} \tag{3.62}$$

$$\begin{aligned}
&\frac{[S_r n^0 + (1-n^0)\rho_s K_d]c_0}{t_c}\frac{\partial c^*}{\partial t^*} = \frac{S_r n^0 D_m c_0}{l_c^2}\frac{\partial^2 c^*}{\partial z^{*2}} - \alpha_L \frac{K}{\rho_w g}\frac{p_c c_0}{l_c^3}\frac{\partial p^*}{\partial z^*}\frac{\partial^2 c^*}{\partial z^{*2}} \\
&+ \frac{\partial c^*}{\partial z^*}\{-\alpha_L S_r n\beta\frac{p_c c_0}{t_c l_c}\frac{\partial p^*}{\partial t^*} - \alpha_L S_r \frac{u_c c_0}{l_c^2 t_c}\frac{\partial^2 u^*}{\partial z^* \partial t^*} + \alpha_L \frac{\beta K p_c^2 c_0}{\rho_w g l_c^3}\frac{\partial p^*}{\partial z^*}\frac{\partial p^*}{\partial z^*} \\
&+ \frac{S_r(1-n^0)D_m u_c c_0}{l_c^3}\frac{\partial^2 u^*}{\partial z^{*2}} + \frac{K p_c c_0}{\rho_w g l_c^2}\frac{\partial p^*}{\partial z^*} - \frac{[S_r n^0 + (1-n^0)\rho_s K_d]u_c c_0}{t_c l_c}\frac{\partial u^*}{\partial t^*}\} \\
&+ \frac{S_r n^0 \beta p_c c_0}{t_c}\frac{\partial p^*}{\partial t^*}c^* - \beta\frac{K}{\rho_w g}\frac{p_c^2}{l_c^2}c_0(\frac{\partial p^*}{\partial z^*})^2 c^* + S_r n^0 \beta\frac{u_c p_c c_0}{t_c l_c}\frac{\partial u^*}{\partial t^*}\frac{\partial p^*}{\partial z^*}c^*
\end{aligned} \tag{3.63}$$

Further, they can be written as

$$\frac{S_r n^0 \beta \rho_w g l_c^2}{t_c K}\frac{\partial p^*}{\partial t^*} + \frac{S_r u_c \rho_w g l_c}{t_c K p_c}\frac{\partial^2 u^*}{\partial t^* \partial z^*} = \frac{\partial^2 p^*}{\partial z^{*2}} \tag{3.64}$$

$$\frac{\partial^2 u^*}{\partial z^{*2}} + \frac{(1-n^0)(\rho_s - S_r\rho_w)g(1-2\nu)l_c}{2G(1-\nu)}\frac{\partial u^*}{\partial z^*} = \frac{p_c(1-2\nu)l_c}{2G(1-\nu)u_c}\frac{\partial p^*}{\partial z^*} \tag{3.65}$$

$$\begin{aligned}
&\frac{\partial c^*}{\partial t^*} = \frac{S_r n^0 D_m t_c}{[S_r n^0 + (1-n^0)\rho_s K_d]l_c^2}\frac{\partial^2 c^*}{\partial z^{*2}} - \alpha_L \frac{K}{\rho_w g}\frac{p_c t_c}{[S_r n^0 + (1-n^0)\rho_s K_d]l_c^3}\frac{\partial p^*}{\partial z^*}\frac{\partial^2 c^*}{\partial z^{*2}} \\
&+ \frac{\partial c^*}{\partial z^*}\{-\alpha_L \frac{S_r n\beta}{[S_r n^0 + (1-n^0)\rho_s K_d]}\frac{p_c}{l_c}\frac{\partial p^*}{\partial t^*} - \alpha_L \frac{S_r u_c}{[S_r n^0 + (1-n^0)\rho_s K_d]l_c^2}\frac{\partial^2 u^*}{\partial z^* \partial t^*} \\
&+ \alpha_L \frac{\beta K p_c^2 t_c}{[S_r n^0 + (1-n^0)\rho_s K_d]\rho_w g l_c^3}\frac{\partial p^*}{\partial z^*}\frac{\partial p^*}{\partial z^*} + \frac{S_r(1-n^0)D_m u_c t_c}{[S_r n^0 + (1-n^0)\rho_s K_d]l_c^3}\frac{\partial^2 u^*}{\partial z^{*2}} \\
&+ \frac{K p_c t_c}{[S_r n^0 + (1-n^0)\rho_s K_d]\rho_w g l_c^2}\frac{\partial p^*}{\partial z^*} - \frac{u_c}{l_c}\frac{\partial u^*}{\partial t^*}\} + \frac{S_r n^0 \beta p_c}{[S_r n^0 + (1-n^0)\rho_s K_d]}\frac{\partial p^*}{\partial t^*}c^* \\
&- \beta\frac{K}{\rho_w g}\frac{p_c^2 t_c}{[S_r n^0 + (1-n^0)\rho_s K_d]l_c^2}(\frac{\partial p^*}{\partial z^*})^2 c^* + S_r n^0 \beta\frac{u_c p_c}{[S_r n^0 + (1-n^0)\rho_s K_d]l_c}\frac{\partial u^*}{\partial t^*}\frac{\partial p^*}{\partial z^*}c^*
\end{aligned} \tag{3.66}$$

Let

$$\frac{S_r u_c \rho_w g l_c}{t_c K p_c} = 1, \quad \frac{p_c(1-2\nu) l_c}{2G(1-\nu)u_c} = 1, \quad \frac{K p_c t_c}{\rho_w g l_c^2 [S_r n^0 + (1-n^0)\rho_s K_d]} = 1 \tag{3.67}$$

providing that excess pore pressure (p^*) and soil displacement (u^*) are fully coupled, and coefficient for advective solute flux is bigger than diffusion flux. Let l_c equals thickness of soil layer, L, (3.15) - (3.17) can be obtained.

3.6 Notation

The following notation is used in Chapter 3:

Roman Letters:

A_i, coefficients in dimensionless equations

c^*, non-dimensional mass concentration of the solute in the fluid phase

c_0, the reference solute mass concentration, ML^{-3}

c_f, concentration of the solute in the fluid phase, ML^{-3}

c_s, concentration of the solute in the solid phase, ML^{-3}

c_v, coefficient of consolidation, $\mathrm{L}^2\mathrm{T}^{-1}$

D, hydrodynamic dispersion coefficient, $\mathrm{L}^2\mathrm{T}^{-1}$

D_G, mass transfer coefficient of geomembrane, $\mathrm{L}^2\mathrm{T}^{-1}$

D_m, effective molecular diffusion coefficient, $\mathrm{L}^2\mathrm{T}^{-1}$

F, function to relate S and c_f

G, shear modulus of soil, $\mathrm{ML}^{-1}\mathrm{T}^{-2}$

g, gravity acceleration, LT^{-2}

h, thickness of geomembrane, L

K, hydraulic conductivity, LT^{-1}

K_d, contaminant partitioning coefficient, $\mathrm{L}^3\mathrm{M}^{-1}$

K_{w0}, pore water bulk modulus, $\mathrm{ML}^{-1}\mathrm{T}^{-2}$

L, thickness of CCL, L

l_c, characteristic unit for length, L

n, current soil porosity

n^0, initial soil porosity

P_a, gauge air pressure, $ML^{-1}T^{-2}$

P_0, atmosphere air pressure, $ML^{-1}T^{-2}$

p^*, non-dimensional excess pore water pressure

p_c, characteristic unit of excess pore pressure, $ML^{-1}T^{-2}$

p^e, excess pore pressure, $ML^{-1}T^{-2}$

r_h, volumetric fraction of dissolved air

S, mass of contaminant sorbed onto the solid phase per unit mass of solid phase

S_r, degree of saturation

T_v, consolidation time factor in Terzaghi consolidation theory, T

t, time, T

t^*, non-dimensional time

t_c, characteristic unit for time, T

u, soil displacement, L

u^*, non-dimensional soil displacement

u_c, characteristic unit for soil displacement, L

v_f, average fluid velocity, LT^{-1}

v_s, solid velocity, LT^{-1}

z, vertical coordinate, L

z^*, non-dimensional vertical coordinate

Greek symbols:

ρ_w, density of pore water, ML^{-3}

ρ_s, density of soil gain, ML^{-3}

β, compressibility of pore water, LT^2M^{-1}

ν, Poisson's ratio

α_L, longitudinal dispersion, L

Abbreviation:

ADE, advection-dispersion equation

CCL, compacted clay liner

CPW, compressible pore water

REV, represent element volume

SVP, spatial variation of porosity

SW, self-weight of the clay liner

VOCs, volatile organic chemicals

Chapter 4

Solute Transport in Isothermal Deformable Soil: Finite Strain Model

4.1 Introduction

The VOC transit time was traditionally estimated using the diffusion equation (Rowe and Badv, 1996a; Fityus et al., 1999; Foose, 2002). However, several field tests have reported that the transit of VOCs is much earlier than theoretical predictions (Workman, 1993; Othman et al., 1997). Many researchers attribute this to consolidation and associated advective transport. Several theoretical models coupling mechanical consolidation with solute transport were constructed in recent years (Smith, 2000; Fox, 2007b; Lewis et al., 2009).

There are opposing opinions regarding the importance of consolidation-induced advection. Based on a model coupling finite deformation consolidation with solute transport, Lewis et al. (2009) claimed that consolidation is essentially complete before the VOC break though the clay liner, and its influence is further minimized in the presence of sorption. In their illustrative example, with linear sorption at the level of $K_d = 0.001$ l/g, the consolidation made no discernible difference to the concentration at the compacted clay liner (CCL) drainage base. Consequently, they concluded that the advective transport flux has less influence on solute migration than the combination of geometric and void ratio variation. With this assumption, Lewis et al. (2009) proposed several simplified models, such as the *instant deformation-diffusion only* model (calculates the final layer thickness and void ratio before performing a diffusion-only analysis), and the *no advection* model (ignores the advective

transport component in the coupled model), to approximate the coupled consolidation and transport model. It is noted that, in their model (Lewis et al., 2009), the boundary condition for the void ratio at the CCL base is constant, which is not consistent with Smith (2000). On the other hand, Fox (2007b) presented contrary simulation results and stated that the advective flux caused by consolidation has a lasting effect on transport even after the consolidation has completed, and that its relative importance does not diminish for a VOC sorption level up to 0.001 l/g.

In real environments, the clay barrier below the waste content is not fully saturated (Fityus et al., 1999). Soil parameters, such as hydraulic conductivity and effective diffusion depend on the degree of saturation. Based on the one-dimensional Biot consolidation theory, the previous chapter proposes an advection-diffusion equation that incorporates the degree of saturation, compressibility of the pore fluid (CPW) and dispersivity of the solute transport in an unsaturated deforming porous medium. Both CPW and dispersivity were found to significantly influence the solute migration within CCL in some circumstances. However, it makes an assumption of an infinitesimal strain, i.e., small deformation. Additionally, it neglects the material and geometric nonlinearity, factors that could be important in some circumstances (Lewis et al., 2009).

The study in this chapter is focused on extending the small deformation model for solute transport in an unsaturated medium (Zhang et al., 2012) to finite deformations, and clarifying the influence of consolidation on solute transport with a time-dependent boundary in terms of void ratio at the CCL base. The influence of unsaturation on the transit time of VOC in clay barriers will also be examined. To account for the geometric nonlinearity, a material coordinate system is used. Both CPW and dispersivity are considered in the new model. Further, the nonlinearity of the constitutive properties related to soil compressibility, the hydraulic conductivity and decreasing effective diffusion coefficient are incorporated. A parametric study is carried out to examine the influence of several dominant parameters on the process of solute transport in porous medium. Finally, the symbols utilized in this chapter are listed. This chapter forms the manuscript of "Solute transport in unsaturated porous media under landfill clay liners: A finite deformation approach" listed in the preface.

4.2 Model formulation

Recently, Lewis et al. (2009) and Peters and Smith (2002) developed a model coupling finite strain consolidation and solute transport in a fully saturated soil. Below, the CPW and dispersion in a *partially* saturated soil is included.

4.2.1 Coordinates systems

A Lagrangian coordinates system (z, t) is employed to derive the flow and transport equations. We define $\xi(z,t)$ as the particle displacement with $\xi(z,0) = z$. The relationship between Lagrangian and Eulerian (ξ, t) coordinate systems then implies that for any variable $F(z,t) = f(\xi(z,t),t)$

$$\frac{\partial F}{\partial z} = \frac{\partial f}{\partial \xi}\frac{\partial \xi}{\partial z}, \; \frac{\partial F}{\partial t} = \frac{\partial f}{\partial \xi}\frac{\partial \xi}{\partial t} + \frac{\partial f}{\partial t} = \frac{\partial f}{\partial \xi}v_s + \frac{\partial f}{\partial t}, \tag{4.1}$$

where $v_s = \partial\xi/\partial t$ is the solid velocity.

4.2.2 Consolidation equations

The equation describing changes in void ratio, $e(z,t)$, are derived from the continuity equations for solid and fluid phases together with Darcy's law. Based on the concept of representative element volume (REV), the mass balance equation of the solid phase in differential form is

$$\frac{\partial}{\partial t}\left[\rho_s\,(1-n)\,\frac{\partial \xi}{\partial z}\right] = 0, \tag{4.2}$$

where ρ_s is the soil grain density, $n = e/(1+e)$ is the current porosity, and $n_0 = n(z,0)$ is the initial porosity. Note that for constant ρ_s the Jacobian, M, for the coordinate transformation is

$$M = \frac{\partial \xi}{\partial z} = \frac{1-n_0}{1-n} = \frac{1+e}{1+e_0}, \tag{4.3}$$

where e_0 is the initial void ratio.

The continuity equation for the fluid phase (i.e., pore water) is

$$\frac{\partial}{\partial t}\left(nS_r\rho_f\frac{\partial \xi}{\partial z}\right) = -\frac{\partial}{\partial z}(\rho_f q), \tag{4.4}$$

where ρ_f is the pore fluid density.

According to Darcy's Law, the fluid flux is given by

$$q = -\frac{k_v}{\rho_f g}\frac{\partial p}{\partial \xi}, \tag{4.5}$$

where k_v is hydraulic conductivity and p is excess pore pressure. If the hydraulic gradient is zero, the Darcy equation in terms of total pressure can be transformed to this form (Peters and Smith, 2002).

Assuming ρ_f varies with pore pressure as $\partial\rho_f/\partial p = \beta\rho_f$, substituting Eq. (4.5) into Eq. (4.4), then the continuity equation for the fluid phase becomes

$$nS_r\beta\frac{\partial \xi}{\partial z}\frac{\partial p}{\partial t} + \frac{\partial}{\partial t}\left(S_r\frac{\partial \xi}{\partial z}\right) = \frac{1}{\rho_f g}\frac{\partial}{\partial z}\left(k_v\frac{\partial p}{\partial z}\frac{\partial z}{\partial \xi}\right), \tag{4.6}$$

where the compressibility of pore fluid (β) can be estimated by (Fredlund and Rahardjo, 1993)

$$\beta = \frac{S_r}{K_{w0}} + \frac{1 - S_r + r_h S_r}{P_a + P_0}, \tag{4.7}$$

in which K_{w0} is the pore water bulk modulus, r_h denotes volumetric fraction of dissolved air within pore water, P_a denotes gauge air pressure and P_0 represents the atmospheric pressure. In a nearly saturated soil, for example, $r_h = 0.02$, $S_r = 0.8 \sim 1.0$, β falls into the range of $2 \times 10^{-6} \sim 2 \times 10^{-7}$ Pa^{-1}.

Because n and n_0 (implicitly embedded in $\partial\xi/\partial z$) appear simultaneously, and n is unknown, Eq. (4.6) can not be directly solved in terms of p. In the following derivation, it

turns out that once the relationship between derivative of p (with respect to t and a) and the corresponding derivative of e is known, it is straightforward to convert Eq. (4.6) to an equation in terms of e.

Assuming self-weight is negligible due to the relatively small thickness of the CCL (Zhang et al., 2012), the vertical force equilibrium is

$$\frac{\partial \sigma}{\partial z} = 0, \tag{4.8}$$

where σ (now a function only of t) is the total normal stress of the soil and the z coordinate is vertically upwards. Assuming the compressive normal stress is positive, i.e., $\sigma = \sigma' + p$ (σ' is the effective normal stress), Eq. (4.8) leads to

$$\frac{\partial p}{\partial \xi} = \frac{\partial}{\partial z}(-\sigma' + \sigma)\frac{\partial z}{\partial \xi} = \frac{1+e_0}{1+e}\frac{1}{\alpha_v}\frac{\partial e}{\partial z}, \tag{4.9}$$

where $\alpha_v = -de/d\sigma'$ is the coefficient of soil compressibility.

In the absence of self-weight, the rate of change of total stress at an arbitrary location equals that of the external top loading,

$$\frac{\partial \sigma}{\partial t} = \frac{\partial Q}{\partial t}, \tag{4.10}$$

where Q is the external load. Therefore $Q(z,t) = g(z) + \sigma(t)$ for an arbitrary function $g(z)$. The rate of change of the excess pore water pressure in the time domain is

$$\frac{\partial p}{\partial t} = \frac{\partial}{\partial t}(\sigma - \sigma') = \frac{\partial Q}{\partial t} + \frac{1}{\alpha_v}\frac{\partial e}{\partial t}. \tag{4.11}$$

Substituting Eqs. (4.3, 4.9, 4.11) into Eq. (4.6) yields

$$\left(\frac{eS_r\beta}{(1+e_0)\alpha_v} + \frac{S_r}{1+e_0}\right)\frac{\partial e}{\partial t} - \frac{1+e_0}{\rho_f g}\frac{\partial}{\partial z}\left(\frac{k_v}{\alpha_v(1+e)}\frac{\partial e}{\partial z}\right) = -\frac{S_r\beta e}{1+e_0}\frac{\partial Q}{\partial t}. \tag{4.12}$$

For the fully saturated case and when the CPW is neglected, i.e., $\beta = 0$, Eq. (4.12) reduces to

$$\frac{1}{1+e_0}\frac{\partial e}{\partial t} = \frac{1+e_0}{\rho_f g}\frac{\partial}{\partial z}\left(\frac{k_v}{\alpha_v(1+e)}\frac{\partial e}{\partial z}\right), \tag{4.13}$$

which is identical to Eq. (1) of Lewis et al. (2009).

4.2.3 Solute transport equations

Solute transport occurs in both solid and fluid phases. The mass conservation equation for the solute in the solid phase is

$$\frac{\partial}{\partial t}\left[(1-n)\rho_s S\frac{\partial \xi}{\partial z}\right] = f'_{a\to s}, \tag{4.14}$$

where S is the mass of solute sorbed on or within the solid phase per unit mass of the solid phase and $f'_{a\to s}$ denotes rate of solute loss in the aquatic phase by solid phase sorption.

The mass conservation equation for solute in the fluid phase is

$$\frac{\partial}{\partial t}\left(nS_r c_f\frac{\partial \xi}{\partial z}\right) = -\frac{\partial J_f}{\partial z} - f'_{a\to s}, \tag{4.15}$$

where c_f is the concentration of the solute in the pore fluid. In Eq. (4.15), the term $\partial\xi/\partial z$ comes from the volumetric change (Peters and Smith, 2002) and J_f represents solute flux in the fluid phase, which is described by (Peters and Smith, 2002)

$$J_f(z,t) = nS_r(v_f - v_s)c_f - \frac{nS_r D}{M}\frac{\partial c_f}{\partial z}, \tag{4.16}$$

where D is the hydrodynamic dispersion coefficient. It is given by the sum of the effective diffusion coefficient (D_e) and the coefficient of mechanical dispersion (D_m)

$$D_m = \alpha_L\left(v_f - v_s\right), \tag{4.17}$$

where α_L is dispersion coefficient and v_f is the pore fluid velocity.

Based on Eq. (4.14-4.16), we have

$$\frac{\partial}{\partial t}\left\{\left[nS_r c_f + (1-n)\rho_s S\right]\frac{\partial \xi}{\partial z}\right\} = \frac{\partial}{\partial z}\left(\frac{nS_r D}{M}\frac{\partial c_f}{\partial z}\right) - \frac{\partial}{\partial z}\left[nS_r(v_f - v_s)c_f\right]. \tag{4.18}$$

The above equation can be further simplified with Darcy's Law, Eq. (4.5), and the mass balance equations for both solid and fluid phases, Eq. (4.2) and Eq. (4.4), then Eq. (4.18) can be expressed as

$$\begin{aligned} nS_r\frac{\partial \xi}{\partial z}\frac{\partial c_f}{\partial t} + (1-n)\rho_s\frac{\partial \xi}{\partial z}\frac{\partial S}{\partial t} =& \frac{\partial}{\partial z}\left(\frac{nS_r D}{M}\frac{\partial c_f}{\partial z}\right) + \frac{k_v}{\rho_f g}\frac{\partial p}{\partial \xi}\frac{\partial c_f}{\partial z} \\ &+ \left(nS_r\beta\frac{\partial \xi}{\partial z}\frac{\partial p}{\partial t} - \frac{\beta k_v}{\rho_f g}\frac{\partial p}{\partial \xi}\frac{\partial p}{\partial z}\right)c_f. \end{aligned} \tag{4.19}$$

Substituting Eq. (4.9) and Eq. (4.11) into Eq. (4.19) results in

$$\begin{aligned} \left(S_r\frac{e}{1+e_0} + \frac{\rho_s K_d}{1+e_0}\right)\frac{\partial c_f}{\partial t} =& S_r\frac{\partial}{\partial z}\left(\frac{e(1+e_0)}{(1+e)^2}D\frac{\partial c_f}{\partial z}\right) + \frac{k_v}{\rho_f g}\frac{1+e_0}{\alpha_v(1+e)}\frac{\partial e}{\partial z}\frac{\partial c_f}{\partial z} \\ &+ \beta\left[S_r\frac{e}{1+e_0}\left(\frac{\partial Q}{\partial t} + \frac{1}{\alpha_v}\frac{\partial e}{\partial t}\right) - \frac{k_v}{\rho_f g\alpha_v^2}\frac{1+e_0}{1+e}\left(\frac{\partial e}{\partial z}\right)^2\right]c_f, \end{aligned} \tag{4.20}$$

where, K_d describes the partitioning coefficient.

4.2.4 Special cases

In this section, three special cases of the present model are outlined.

A. Saturated soil with finite deformation

For a saturated soil, where $S_r = 1$, and incompressible pore fluid, i.e., $\beta = 0$, Eq. (4.20) reduces to

$$\left(\frac{e}{1+e_0} + \frac{\rho_s K_d}{1+e_0}\right)\frac{\partial c_f}{\partial t} = \frac{\partial}{\partial z}\left(\frac{e(1+e_0)}{(1+e)^2}D\frac{\partial c_f}{\partial z}\right) + \frac{k_v}{\rho_f g}\frac{1+e_0}{\alpha_v(1+e)}\frac{\partial e}{\partial z}\frac{\partial c_f}{\partial z}. \tag{4.21}$$

which is identical to (4) in Lewis et al. (2009) and (44) in Peters and Smith (2002) with their notations.

B. Small deformation model

Under the assumptions of negligible self-weight and small deformation (constant porosity, i.e., $n = n_0$), the coupled small deformation model is (Zhang et al., 2012)

$$S_r n_0 \beta \frac{\partial p}{\partial t} + S_r \frac{\partial^2 u}{\partial t \partial \xi} = \frac{1}{\rho_w g} \frac{\partial}{\partial \xi} \left(k_v \frac{\partial p}{\partial \xi} \right), \tag{4.22}$$

$$G \frac{2(1-\nu)}{(1-2\nu)} \frac{\partial^2 u}{\partial \xi^2} = \frac{\partial p}{\partial \xi}, \tag{4.23}$$

and

$$\begin{aligned} \left[S_r n_0 + (1-n_0) \rho_s K_d \right] \frac{\partial c_f}{\partial t} &= S_r n_0 D_e \frac{\partial^2 c_f}{\partial \xi^2} - \alpha_L \frac{k_v}{\rho_w g} \frac{\partial p}{\partial \xi} \frac{\partial^2 c_f}{\partial \xi^2} \\ &+ \frac{\partial c_f}{\partial \xi} \left\{ -\alpha_L S_r n_0 \beta \frac{\partial p}{\partial t} - \alpha_L S_r \frac{\partial^2 u}{\partial \xi \partial t} \right. \\ &+ \frac{\alpha_L \beta k_v}{\rho_w g} \left(\frac{\partial p}{\partial \xi} \right)^2 + S_r D_e (1-n_0) \frac{\partial^2 u}{\partial \xi^2} \\ &\left. + \frac{k_v}{\rho_w g} \frac{\partial p}{\partial \xi} - \left[S_r n_0 + (1-n_0) \rho_s K_d \right] \frac{\partial u}{\partial t} \right\} \\ &+ S_r n_0 \beta \frac{\partial p}{\partial t} c_f - \beta \frac{k_v}{\rho_w g} \left(\frac{\partial p}{\partial \xi} \right)^2 c_f + S_r n_0 \beta \frac{\partial u}{\partial t} \frac{\partial p}{\partial \xi} c_f, \end{aligned} \tag{4.24}$$

where u is the soil displacement, G the shear modulus and ν Poisson's ratio. Eqs. (4.22 and (4.24) are identical to Eqs. (3.1) and (3.13), respectively. Eq. (4.23) is modified from Eq. (3.2) by neglecting the self-weight of soil. The constant material coefficients can be described as

$$\begin{aligned} G = & \frac{c_v \rho_f g (1-2\nu)}{2 k_v (1-\nu)} = \frac{(1+e_p)(1-2\nu)}{2(1-\nu)\alpha_{vp}}, \\ & k_v = k_p, \quad D_e = D_{e0}, \end{aligned} \tag{4.25}$$

where c_v is the consolidation coefficient; k_s and k_p the saturated hydraulic conductivity and hydraulic conductivity of the soil corresponding to e_p (the void ratio corresponding to pre-consolidation stress), respectively.

C. Unsaturated soil with no deformation

For the partially saturated no deformation model, i.e., $e = e_0$, $\xi = z$, the overloading, Q, does not affect solute transport. In the spatial coordinate system (ξ, t), Eq. (4.20) reduces to the linear diffusion equation

$$\frac{\partial c_f}{\partial t} = D\left(1 + \frac{\rho_s K_d}{S_r e_0}\right)^{-1} \frac{\partial^2 c_f}{\partial \xi^2}. \tag{4.26}$$

4.3 Variations of parameters in consolidation and solute transport processes

Once the finite deformation model is established, it is possible to consider the effects of variations in the coefficients of consolidation and transport, such as the coefficient of compressibility (α_v), hydraulic conductivity (k_v) and hydrodynamic dispersion (D). Lewis et al. (2009) utilized void ratio-dependent functions for the related coefficients while Li and Liu (2006) used a fractal pore-space theory to develop fractal models of the water flow and the solute diffusion for rigid unsaturated soils, which allowed comparison of the dependence of these coefficients between fully saturated and unsaturated cases. Here, a combination of both models is employed so that the hydraulic conductivity and the effective diffusion depend on both the void ratio and the degree of saturation. Linear, reversible solute sorption is assumed in this study; however, the approach can be adapted for other sorption models.

4.3.1 Soil compressibility

The soil layer is assumed to be over-consolidated, and compression of the soil layer commences when the applied stress exceeds the pre-consolidation stress, i.e., deformation due to re-compression is neglected. In this case, the void ratio is idealized as a linear function of the logarithm of the effective stress: (Means and JV., 1964)

$$e = e_p - C_c \log\left(\frac{\sigma'}{\sigma'_p}\right), \tag{4.27}$$

where σ' is effective stress, σ'_p denotes the pre-consolidation stress and C_c is the compression index of the soil (defined by the absolute value of the slope of the idealized virgin compression line). The coefficient of compressibility in terms of void ratio can be obtained by differentiation of Eq. (4.27) with respect to effective normal stress (Lewis et al., 2009)

$$\alpha_v = \alpha_{vp}\exp\left[\ln 10\left(\frac{e - e_p}{C_c}\right)\right], \tag{4.28}$$

where α_{vp} is the coefficient of compressibility corresponding to σ'_p, i.e.,

$$\alpha_{vp} = \frac{C_c}{\sigma'_p \ln 10}. \tag{4.29}$$

4.3.2 Hydraulic characteristic

For hydraulic conductivity, an empirical relationship describing its variation with void ratio in saturated clay soils is given as (Mitchelll, 1993):

$$k_s = k_p\exp\left[\ln 10\left(\frac{e - e_p}{C_k}\right)\right], \tag{4.30}$$

where C_k is the hydraulic conductivity index.

The power law relationship equation for hydraulic conductivity versus water content θ ($= S_r n$) is (Li and Liu, 2006)

$$k_v = k_s\left(\frac{\theta}{\theta_s}\right)^{\alpha}, \tag{4.31}$$

where θ_s is saturated water content, and α falls in the range of 2.68 to 2.78 for clay loam.

4.3.3 Dispersion coefficient

In a saturated soil, the effective solute diffusion coefficient is defined as the product of the free diffusion coefficient of the solute in the pore fluid (D_f) and the tortuosity factor (τ_f), which accounts for the irregular path that diffusing molecules must take through the pore space (Acar and Haider, 1990). Lewis et al. (2009) claimed that it is rational to take D_e as constant, because uncertainty of the range of τ_f can be the same order of consolidation-induced change of D_e. Alternatively, the reduction of D_e can be expressed with a hypothetical relationship associated with the overall void ratio change as (Lewis et al., 2009)

$$D_e = \left(\frac{e_0 - e}{3(e_0 - e_f)} + \frac{e - e_f}{e_0 - e_f} \right) D_{e_0}, \tag{4.32}$$

where e_f denotes the final void ratio, and D_{e0} is the initial effective dispersion coefficient.

In variably saturated soils, the effective diffusion coefficient, D_e, depends on soil water content, bulk density, and soil type for soils with different textures. Regarding the water content, there is a threshold value under which solute diffusivity vanishes (Hunt and Ewing, 2003; Hamamoto et al., 2009). The impedance factor (Porter et al., 1960) (i.e., the ratio of solute diffusion coefficient in soil to product of solute diffusion coefficient in free water and volumetric soil water content), decreased with increasing bulk density for each soil type, but the effect of the overall bulk density on the impedance factor is minor compared with the effect of soil water content and soil type (Hamamoto et al., 2009). The effective diffusion coefficient was found to decrease with decreasing of the degree of saturation in the previous experiment (Barbour et al., 1996). The decrease was found to be quite rapid initially, followed by a near-linear decline for degree of saturation below 60%. Here, the soil diffusion coefficient is expressed as (Li and Liu, 2006):

$$D_e = 1.1 D_f \theta (\theta - \theta_t), \tag{4.33}$$

where θ_t denotes threshold water content, which was observed to become higher with increasing clay content and varies between 3% and 20% for clay soil.

4.3.4 Sorption

It has been reported that the effect of the degree of saturation on the adsorption coefficient is insignificant from full saturation to a degree of saturation of 10% (Barbour et al., 1996). A significant decrease in the adsorption coefficient only occurs in cases with a low degree of saturation. In this study the degree of saturation varies from 1 to 0.8, i.e., the effect on sorption can be neglected. Therefore, the concentration of solute in the solid phase, S, is expressed as

$$S = K_d c_f. \tag{4.34}$$

This assumption of a linear sorption is valid at the relatively low concentrations that are usually found in the municipal waste disposal sites (Mathur and Jayawardena, 2008).

4.4 Application to a landfill liner

4.4.1 Problem description

The same landfill bottom composite clay liner as in previous chapter is used here as an illustrative example. The model parameters employed in the following analyses are based on those used in recent studies of solute transport in composite liners (Foose, 2002; Lewis et al., 2009). Because of the unavailability of consolidation data in the literature, hypothetical values of the applied stress, pre-consolidation stress, compression index, hydraulic conductivity index, threshold moisture content and other parameters in calculating the D_e and k_v are used. As a primary parameter, the compression index covers a large range to account for the high-compressibility soil considered (Lewis et al., 2009). However, the related applied stress has been selected to avoid negative and unrealistically low void ratios. The parameters used are given in Table 4.1.

Table 4.1: Values of input parameters

Parameter	Value
Maximum applied stress (ramp loading for 2 years), σ_a	450 kPa
Preconsolidation stress, σ'_p	50 kPa
Compression index, C_c	0.2, 0.8
Preconsolidation hydraulic conductivity, k_p	10^{-9}, 2×10^{-10} m/s
Constant, α	2.7
Hydraulic conductivity index, C_k	0.585
Thickness of geomembrane, h	0.0015 m
Thickness of CCL, L	1.22 m
Mass transfer coefficient of geomembrane, P_G	4×10^{-11}m^2/s
Initial effective diffusion coefficient, D_{e0}	2×10^{-10} m^2/s
Free diffusion coefficient in the pore fluid, D_f	10^{-9} m^2/s
Threshold moisture content, θ_t	0.05
Partitioning coefficient, K_d	0, 0.2, 1 ml/g
Dispersion, α_L	0, 0.1 m
Initial void ratio, e_0 (= e_p)	1.17
Acceleration due to gravity, g	9.81 m/s^2
Initial density of pore water, ρ_f	10^3 kg/m^3
Density of the solid phase, ρ_s	2.7×10^3 kg/m^3
Degree of saturation of clay, S_r	1, 0.9, 0.8

4.4.2 Boundary conditions for consolidation

The following boundary conditions are introduced. Assuming there are no defects in the geomembrane, the top boundary ($z = 0$) is assumed to be impermeable, i.e., $q = 0$. Therefore, from Eq. (4.5) and Eq. (4.9),

$$\frac{\partial e}{\partial z} = 0 \text{ at } z = 0. \tag{4.35}$$

At the bottom drainage boundary ($z = L$), the excess pore pressure is zero and a Dirichlet-type boundary condition for void ratio (e) can be derived from the effective stress–void ratio equilibrium relationship Eq. (4.27):

$$e = e_p - C_c \log\left(\frac{\sigma'_L}{\sigma'_p}\right), \tag{4.36}$$

where σ'_L denotes the effective stress at bottom.

Since the excess pore pressure vanishes at the bottom boundary, $\sigma'_L = \sigma_a$, where σ_a is a time-varying stress due to the external overburden. It is noted that σ_a is the maximum loading in the model of Lewis et al. (2009). The void ratio rapidly approaches a steady value, which consequently leads to spurious higher fluid velocity and faster solute transportation. To distinguish the cases, we label the present boundary condition at the CCL bottom as 'BCC' and 'BCL' the boundary conditions used in Lewis et al. (2009).

4.4.3 Boundary conditions for solute transport

At the top of the CCL, diffusion of VOC through the geo-membrane is described by Fick's law (Booker et al., 1997), and the gradient of concentration is assumed proportional to the difference in concentrations because the geomembrane is sufficiently thin. In the material coordinate system the boundary condition is (Lewis et al., 2009):

$$\frac{\partial c_f}{\partial z}(0,t) = \frac{(1 + e(0,t))^2}{e_0(1 + e_0)} \frac{P_G}{hD_e} \left(c_f(0,t) - C_{f0}\right), \tag{4.37}$$

where C_{f0} is the constant concentration of solute at the top surface of the geo-membrane with the assumption that the landfill waste is of large volume (Peters and Smith, 2002); h and P_G are the thickness and the permeation coefficient for the solute in the geo-membrane respectively.

The lower boundary condition for the solute concentration (c_f) is (Peters and Smith, 2001):

$$\frac{\partial c_f}{\partial z} = 0, \text{ at } z = L, \tag{4.38}$$

which assumes negligible diffusion below the CCL base (Barry and Sposito, 1988).

4.5 Numerical results and discussions

A numerical solution was constructed using COMSOL 3.5a environments (COMSOL, 2010). It discretized the domain into unstructured Lagrange-linear elements with a maximum global element size of 10^{-2} m, and maximum local element size at the end boundaries (where the most rapid changes occur) of 10^{-4} m. The time step was 10^{-2} y. The tests concerning the mesh size and time step were conducted so that the simulation results are independent of them. To be easily interpreted, solution curves were plotted in the spatial coordinate x, described as:

$$\xi = z + \int_z^L \frac{e_0 - e(\zeta)}{1 + e_0} d\zeta. \tag{4.39}$$

Thus, the first-order PDE

$$\frac{\partial \xi}{\partial z} = 1 - \frac{e_0 - e(z)}{1 + e_0}, \tag{4.40}$$

with boundary conditions $\xi(0, t) = S_{mt}$ and $\xi(L, t) = L$ was constructed to find ξ, where the settlement S_{mt} is

Table 4.2: Governing equations (GEs) and constitutive relationship functions (CRFs) used in the models

Model	GEs	CRFs	Note
FD, D_e = const	Eq. (4.12), Eq. (4.20)	Eqs. (4.27-4.31), Eq. (4.34	Eq. (4.12), Eq. (4.20) can be solved separately
FD, Decreasing D_e	Eq. (4.12), Eq. (4.20)	Eqs. (4.27-4.31), Eq. (4.33) and Eq. (4.34	same as above
SD	Eqs. (4.22-4.24)	Eqs. (4.27-4.31), Eq. (4.34	Eq. (4.22-4.23) are coupled and Eq. (4.24) can be solved separately
ND	Eq. (4.26)	Eqs. (4.27-4.31), Eq. (4.34	

$$S_{mt} = \int_0^L \frac{e_0 - e(\zeta)}{1 + e_0} d\zeta. \tag{4.41}$$

The governing equations (GEs) and constitutive relationship functions (CRFs) employed in the various models are summarized in Table 4.2. The boundary conditions (BCs) are provided by Eqs. (4.35-4.38).

4.5.1 Model verification

Since there are no experimental data available in the literature, the present model was reduced to the full-saturation case using the same boundary condition at the CCL bottom for e as used by Lewis et al. (2009), i.e., σ_a is taken as the maximum loading; and $K_d = 0$, $\alpha_L = 0$, $C_c = 0.8$, $k_p = 10^{-9}$ m/s. A comparison between the present and previous models is illustrated in Fig. 4.1. In the figure, the results of the finite deformation with constant and decreasing hydrodynamic dispersion, Eq. (4.32), small deformation model (Zhang et al., 2012) and the pure diffusion model (i.e., no deformation model) are included. Both consolidation (i.e., void ratio, e, distribution) and relative concentration obtained from the present model are in excellent agreement with results of Lewis et al. (2009). As shown in Fig. 4.1, with the

constant effective diffusion coefficient, the small deformation model (Zhang et al., 2012) predicts a slower solute migration than the corresponding finite deformation model.

4.5.2 Correctness of the boundary condition at CCL base

To demonstrate the differences due to different boundary conditions of 'BCL' (used by Lewis et al. (2009)) and 'BCC' (used in the present model), a comparison is presented in Fig. 4.2, where $C_c = 0.8$ and $k_p = 10^{-9}$ m/s. Comparing Fig. 4.2(a) (BCC) with 4.1(a) (BCL), it is found that σ_a being taken as the maximum loading leads to a greater gradient of the void ratio and a faster consolidation process, although the final value of e is very close. This initially speeds up the solute transit slightly, and then slows it down in the long-term (Fig. 4.2(b)). The reason the trend reverses after consolidation completion for the 'BCL' case is that the higher solute concentration level during the consolidation phase of 'BCC' occurs later resulting in more advection flux. The separation is more obvious for the relatively soft and higher permeability cases. In the following sections all numerical results are based on the boundary condition 'BCC'.

4.5.3 Effect of consolidation

On basis of the 'BCL' boundary condition, Lewis et al. (2009) observed that there is no noticeable solute concentration at the CCL base when consolidation of the liner is completed even for the case of very high compressibility ($C_c = 0.8$). If the final level of void ratio can be considered in the transport equations, the pure diffusion model will be sufficient.

However, although the duration of consolidation may be short, it will change the distribution of solute concentration, which is the initial condition of a sequential process. Therefore, the advection transport due to consolidation may not be negligible. Figures 4.3 and 4.4 illustrate the consolidation processes and solute transport in a saturated soil for two cases with different compression index of soils (C_c) and hydraulic conductivity (k_v). Consolidation endures 2.2 and 34.5 years for $C_c = 0.2$ and $C_c = 0.8$, respectively. For the 'soft' case, a noticeable concentration difference from the no deformation model appears at the CCL base during consolidation, as shown in Fig. 4.4. The difference decreases with higher levels of

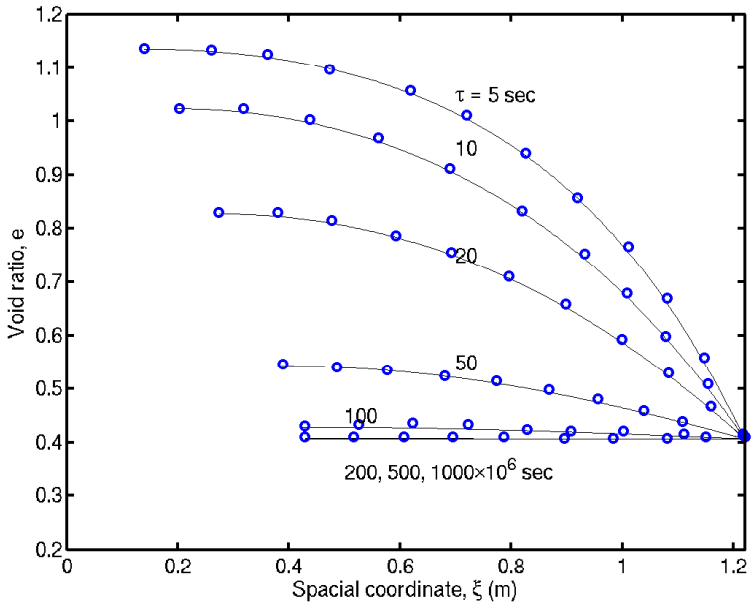

(a) void ratio evolution

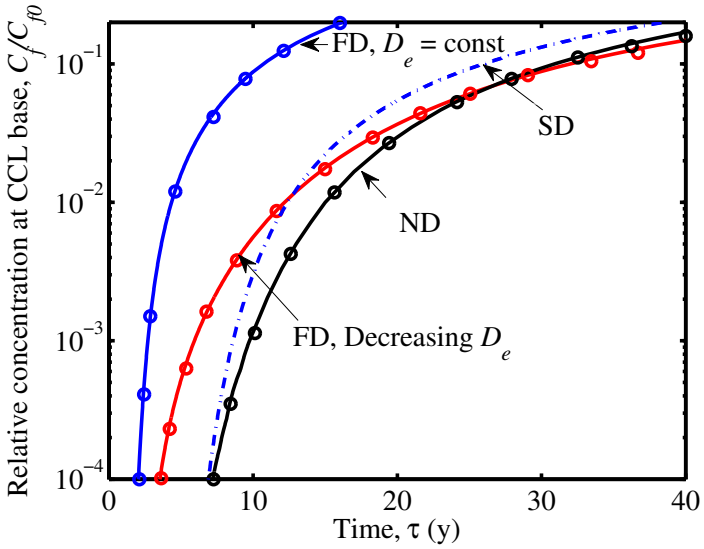

(b) breakthrough curves

Figure 4.1: Comparison of (a) void ratio evolution and (b) breakthrough curves between the present model (solid line) and Lewis et al. (2009) (circle). Notations: FD: finite deformation model, SD: small deformation model, ND: no deformation model.

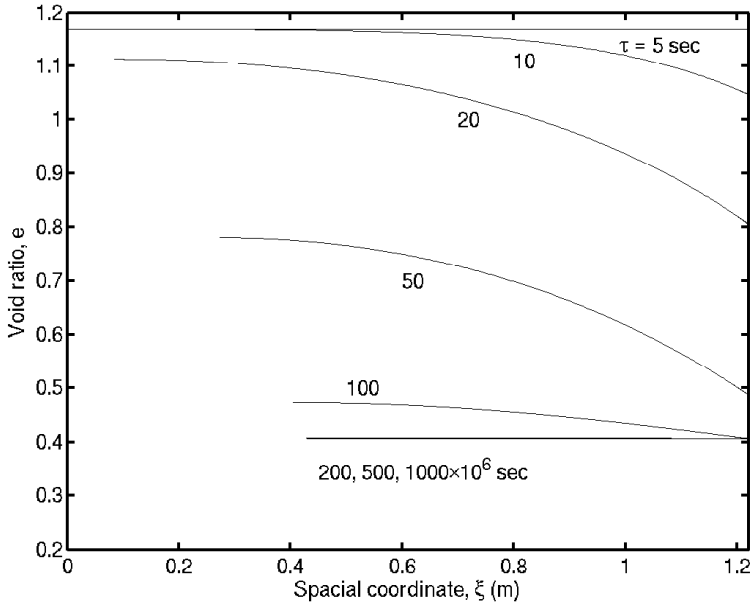

(a) void ratio evolution (BCC only)

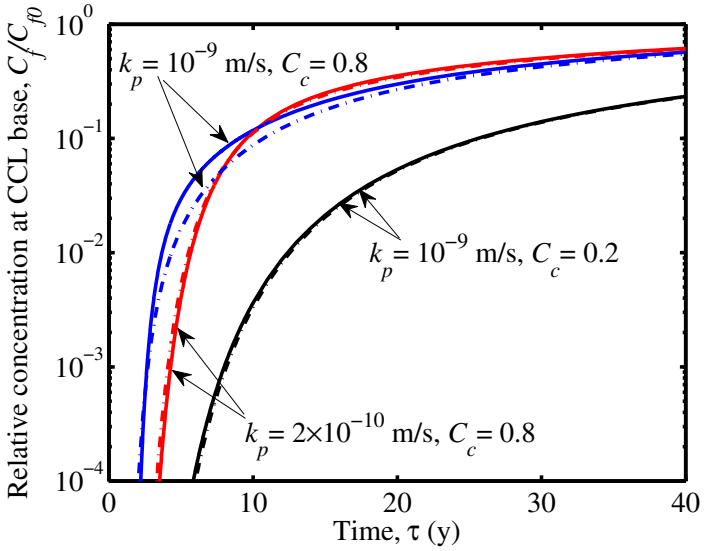

(b) breakthrough curves (BCC and BCL)

Figure 4.2: Influence of Boundary condition of void ratio (e) at CCL base (a) void ratio evolution (BCC only) and (b) breakthrough curves ($S_r = 1, \beta = 0, \alpha_L = 0$, constant D_e). In (b), solid line for 'BCC', and dash-dot line for 'BCL'.

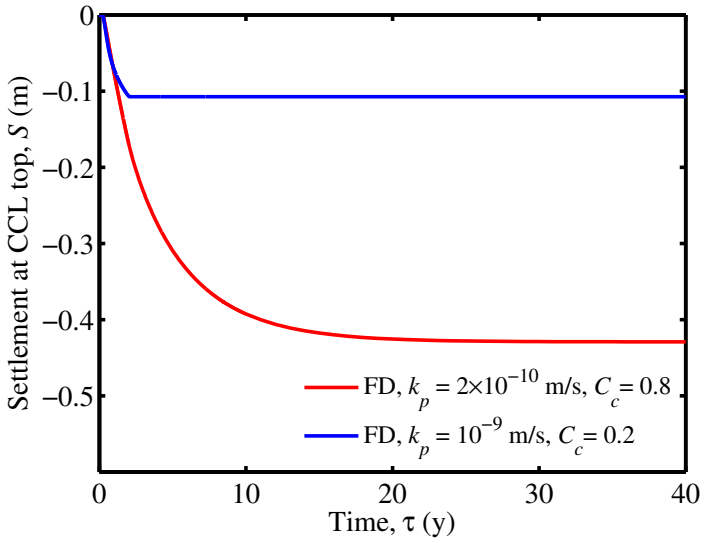

Figure 4.3: Consolidation settlements in a saturated soil ($S_r = 1$).

sorption (Fig. 4.4(b)). The effect of consolidation on transport exists during both the consolidation and post-consolidation stages, which is consistent with Fox (2007b). Since the advection results in a notable concentration level at the CCL base, simplification assumptions such as instant deformation, pure diffusion and finite deformation without advection modelling are not appropriate. The magnitudes of solute concentration c_f have large differences in Fig. 4.4(a) and Fig. 4.4(b). It indicates that the sorption is a controlling influence factor that drastically retards the solute transport.

Figures 4.5 and 4.6 present the results for an unsaturated soil. It shows again that soft clay has a more influential consolidation effect on solute transport (Fig. 4.5). However, since the effective diffusion D_e reduces with deformation, concentration of a pure diffusion model surpasses that of coupled models. This is obvious for the case with sorption level of $K_d = 1$ ml/g.

Consolidation effects are composed of the variation of void ratio and the occurrence of pore water flow, which in turn causes the advection flux in transport. As mentioned previously, Lewis et al. (2009) claimed the advection component can be ignored as long as the variation of void ratio is considered. Here, the finite deformation without advection model, i.e., eliminating advection in Eq. (4.20), was also included as shown in Fig. 4.7. It is

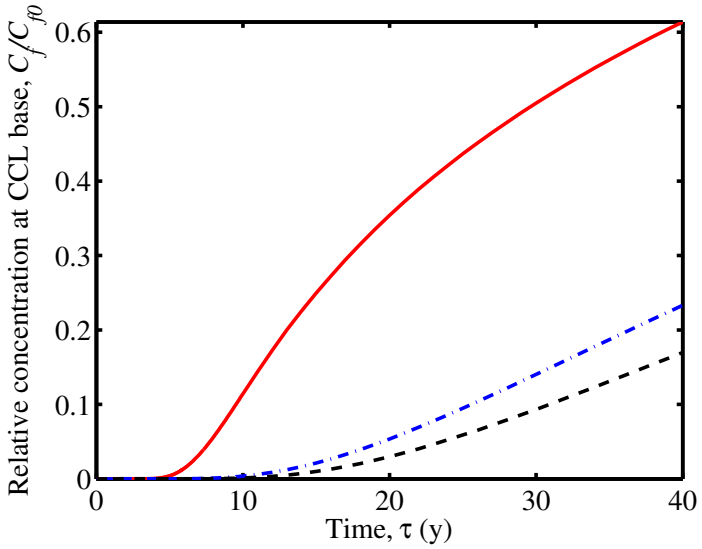

(a) $K_d = 0$

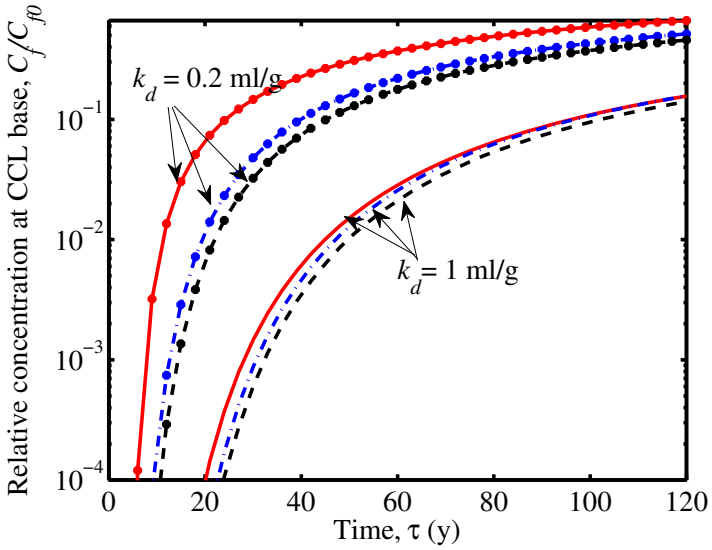

(b) $K_d \neq 0$

Figure 4.4: Effect of consolidation on relative concentration C_f/C_{f0} in a saturated soil (a) $K_d = 0$ and (b) $K_d \neq 0$ ($S_r = 1$, without CPW, $\alpha_L = 0$, constant D_e). Notations: solid line (FD, finite deformation model): $C_c = 0.8$, $k_p = 2 \times 10^{-10}$ m/s; dash-dot line (FD, finite deformation model): $C_c = 0.2$, $k_p = 10^{-9}$ m/s; and dashed line: no deformation model (ND).

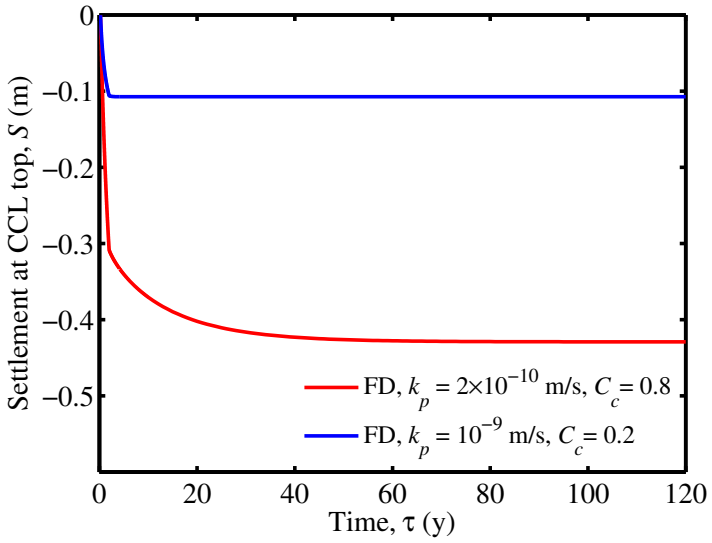

Figure 4.5: Consolidation settlement in partially saturated soils ($S_r = 0.8$).

found that exclusion of advection underestimates the concentration level and consequently leads to a longer transit time. In the absence of sorption, at the nominal 10% breakthrough, a nearly twofold change was made in the transit time, and this is even greater for the cases with sorption.

4.5.4 Effect of degree of saturation

Fig. 4.8 demonstrates that the higher saturation of the no-deformation (ND) model results in faster solute transport due to the saturation (S_r)-dependent effective diffusion, and the gap is larger in the presence of sorption. For the coupling deformation and solute transport models, the results of concentration are shown in Figures 4.9 and 4.10 (results of ND model also included here for comparison). For cases with parameters $C_c = 0.8$, $k_p = 10^{-9}$ m/s, consolidation lasts for approximately 12.8 years. Higher saturation results in faster solute transport because of greater effective diffusion, regardless of the sorption. When decreasing D_e is considered, the predicted transit time is longer. In the presence of sorption, finite deformation with $S_r = 0.8$ and constant D_e leads to almost the same level of concentration as the ND model (Fig. 4.10(b)). It demonstrates that the effect of unsaturation is more notable in the presence of sorption. Interestingly, with both sorption and decreasing D_e taken

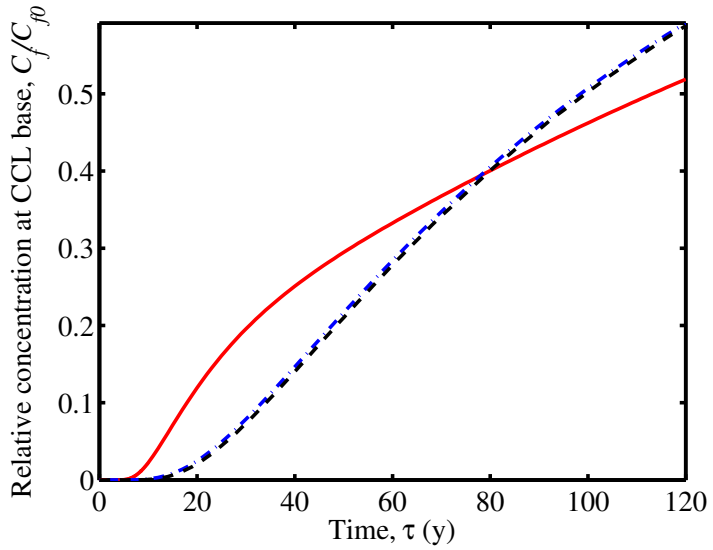

(a) $K_d = 0$

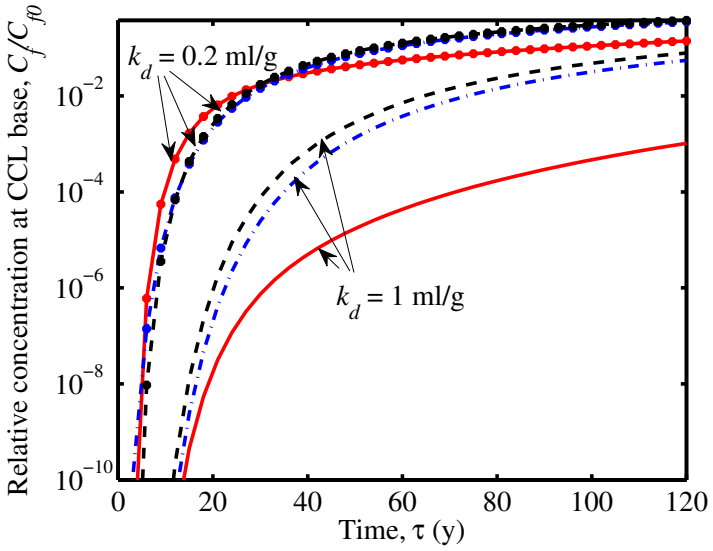

(b) $K_d \neq 0$

Figure 4.6: Effect of consolidation on relative concentration C_f/C_{f0} (a) $K_d = 0$ and (b) $K_d \neq 0$ in partially saturated soils ($S_r = 0.8$, with CPW, $\alpha_L = 0.1$ m, varying D_e as in Equation Eq. (4.33)). Notations: solid line (FD, finite deformation model): $C_c = 0.8$, $k_p = 2 \times 10^{-10}$ m/s; dash-dot line (FD, finite deformation model): $C_c = 0.2$, $k_p = 10^{-9}$ m/s; and dashed line: no deformation model (ND).

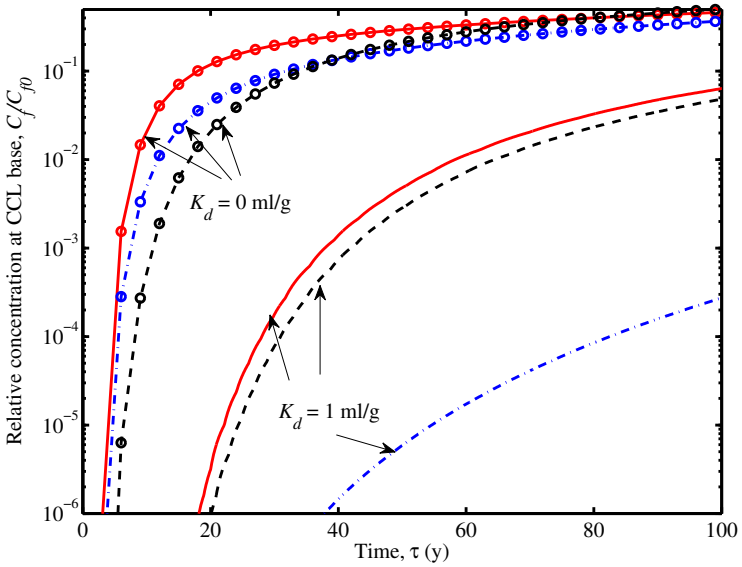

Figure 4.7: Effect of advection flux on concentration level at CCL base for partially saturated cases ($S_r = 0.8$, with CPW, $\alpha_L = 0.1$ m, varying D_e as in (4.33)). For finite deformation model, solid line: $C_c = 0.8$, $k_p = 2 \times 10^{-10}$ m/s; dash-dot line: without advection flux in transport, (4.20); dashed line: No deformation model.

into account, finite deformation (FD) models will not always produce a faster solute transport (Fig. 4.9(b)). During the progress of consolidation and in the early post-consolidation stage, the FD models have a faster transit, but then are surpassed by the ND model because the effective diffusion was reduced due to compaction. However, the decreasing D_e with compaction is an inevitable physical phenomenon, and an earlier appearance of VOC in the field than predicted by the pure diffusion model has been observed (Peters and Smith, 2002). The possible explanations are: (1) the constitutive relationships for soil parameters are not accurate enough; or (2) other factors, such as heat transfer, should be also included in the model. In this model, the degree of saturation, S_r is assumed to be constant in time and space. However, as discussed in section 3.3.4, S_r tends to increase during the consolidation, which will result in a slightly faster movement of solute.

4.5.5 Effects of compressibility of pore water (CPW)

As shown in Fig. 4.11, the effect of compressibility of pore water (CPW) is related to the coefficient, C_c. The influence of CPW on the relative concentration at the CCL becomes

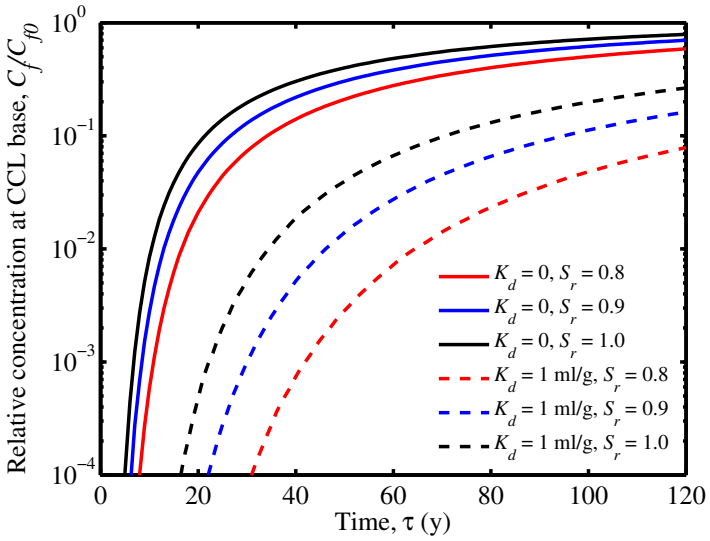

Figure 4.8: Effect of saturation S_r on transport for no-deformation model

more significant for the cases with smaller C_c. When the soil is relative soft ($C_c = 0.8$ and $k_p = 2 \times 10^{-10}$ m/s), CPW causes twofold longer transit times for the nominal 10% breakthrough. However, at the early stage during consolidation, the retarding effect of CPW is more pronounced for 'stiffer' soils and then the trend reverses (Fig. 4.11) after consolidation completion. These graphs are not shown as the numerical values are too small to present in the same figure. This can be explained by the slowing fluid flow and longer consolidation time due to CPW. Since the separation of curves at a relatively higher concentration level, i.e., absolute concentration difference, is of interest, it implies that the influence of CPW is more significant in softer soil.

To further investigate the influence of CPW, three models, in which the effect of each term involving β, are considered here.

- Model A: eliminate $\frac{eS_r\beta}{(1+e_0)\alpha_v}\frac{\partial e}{\partial t}$ from Eq. (4.12);
- Model B: eliminate $-\frac{S_r\beta e}{1+e_0}\frac{\partial Q}{\partial t}$ from Eq. (4.12);
- Model C: eliminate the term involving β from Eq. (4.20).

As shown in Fig. 4.12, all terms involving β should be retained for the cases considered.

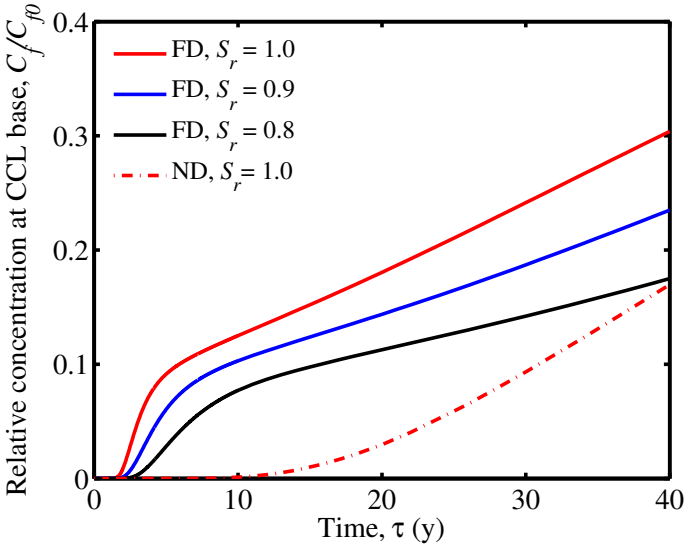

(a) $K_d = 0$

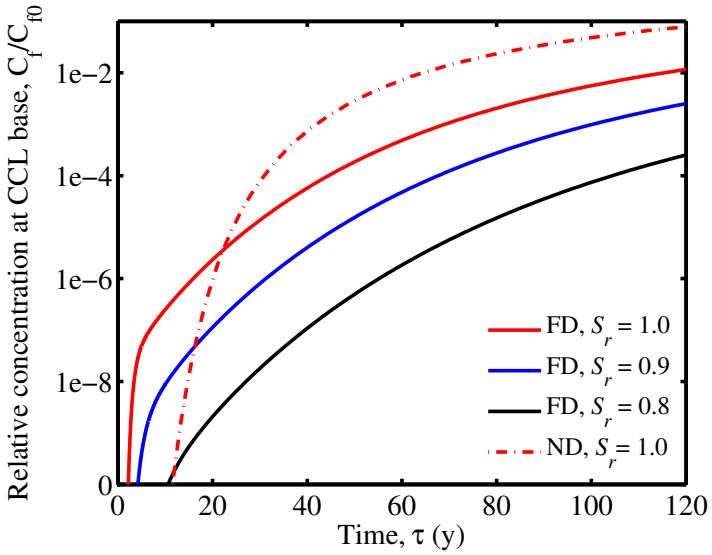

(b) K_d = 1 ml/g

Figure 4.9: Concentration level at CCL base for partially saturated cases with decreasing D_e. (C_c = 0.8, k_p = 10^{-9} m/s). Notation: FD: finite deformation model and ND: no deformation model.

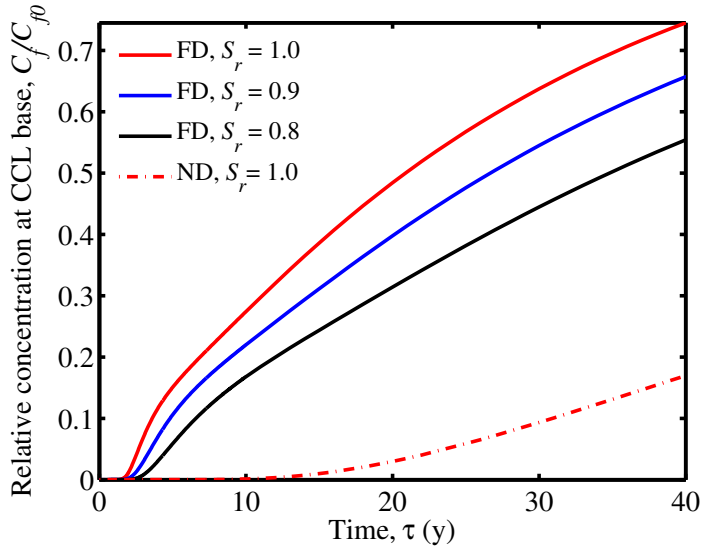

(a) $K_d = 0$

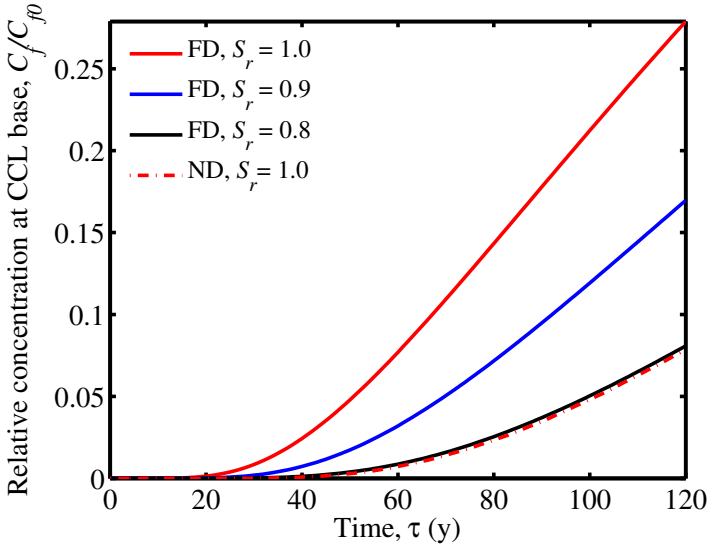

(b) $K_d = 1$ ml/g

Figure 4.10: Concentration level at CCL base for partially saturated cases with a constant D_e ($\theta = S_r n_0$ in (4.33)). ($C_c = 0.8$ and $k_p = 10^{-9}$ m/s). Notation: FD: finite deformation model and ND: no deformation model.

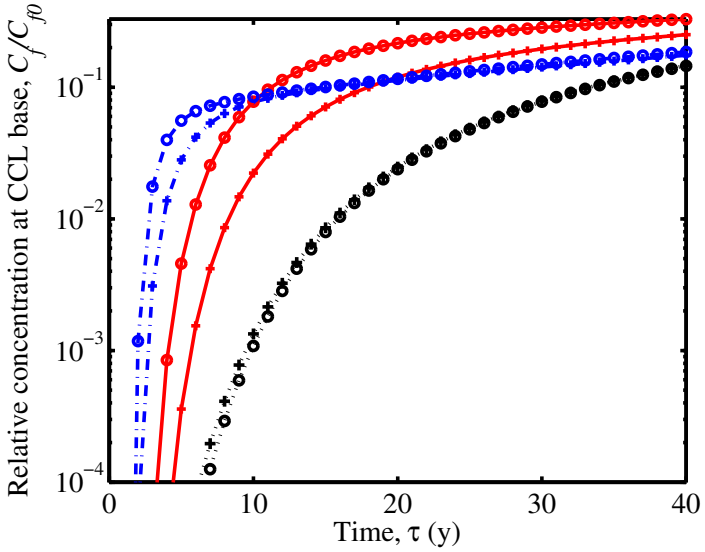

Figure 4.11: Effect of CPW on concentration level at CCL base for partially saturated cases ($S_r = 0.8$) with varying D_e and without sorption ($K_d = 0$). Solid lines: $C_c = 0.8$, $k_p = 2 \times 10^{-10}$ m/s; Dashdot lines: $C_c = 0.8$, $k_p = 10^{-9}$ m/s; Dotted lines: $C_c = 0.2$, $k_p = 10^{-9}$ m/s. Cross symbol: with CPW; circle symbol: without CPW ($\beta = 0$).

4.5.6 Effect of dispersion

Lewis et al. (2009) neglected mechanical dispersion on the assumption that the pore fluid velocity in fine-grain soil is less than 10^{-6} m^2/s. However, as shown in Fig. 4.13, its influence cannot be neglected when the clay is relatively soft, even when the maximum fluid average linear velocity is approximately 4.5×10^{-9} m/s for the case $C_c = 0.8$ and $k_p = 2 \times 10^{-10}$ m/s. Its influence becomes more significant as hydraulic conductivity increases with the same soil compressibility, C_c. This is because the decreasing D_e gradually increases the Péclet number, which is the ratio of the rate of advection to the rate of diffusion. Therefore, a rough estimate using pore fluid velocity as proposed by Lewis et al. (2009) is not always conservative.

Fig. 4.14 illustrates the individual influence of decreasing D_e, dispersion and CPW. The effect of reducing D_e causes slower transport, while dispersion cases a faster transit. Although the influence of CPW is not as significant as decreasing D_e and dispersion, it is not negligible, as shown in Fig. 4.14.

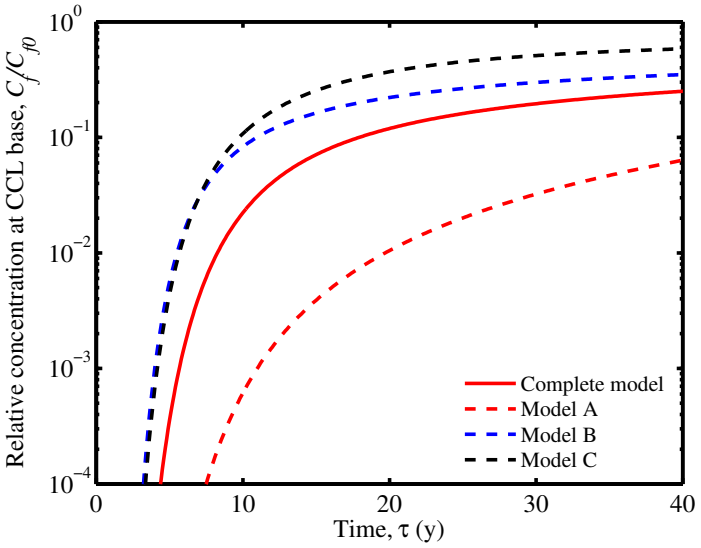

Figure 4.12: Significance of each term involving β on concentration level at CCL base for partially saturated cases ($S_r = 0.8$, $C_c = 0.8$, $k_p = 2 \times 10^{-10}$ m/s) with varying D_e and without sorption ($K_d = 0$).

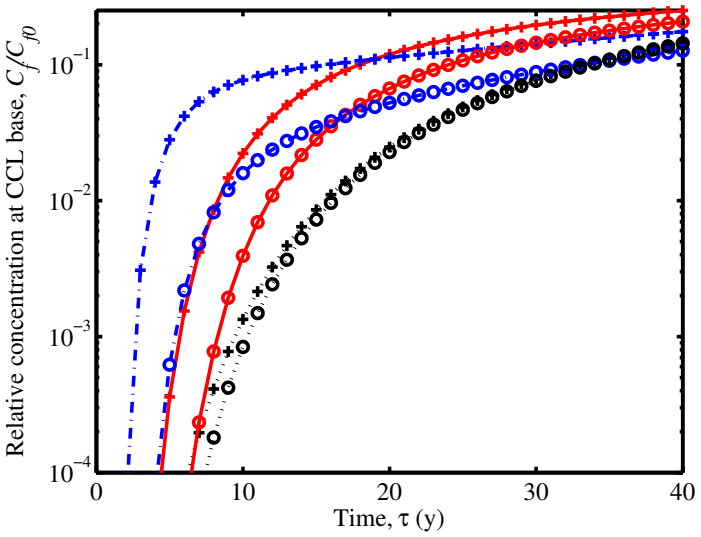

Figure 4.13: Effect of dispersion on concentration level at CCL base for partially saturated cases ($S_r = 0.8$) with varying D_e and without sorption ($K_d = 0$). Solid lines: $C_c = 0.8$, $k_p = 2 \times 10^{-10}$ m/s; Dashdot lines: $C_c = 0.8$, $k_p = 10^{-9}$ m/s; Dotted lines: $C_c = 0.2$, $k_p = 10^{-9}$ m/s. Cross symbol: $\alpha_L = 0.1$ m; circle symbol: $\alpha_L = 0$ (no dispersion).

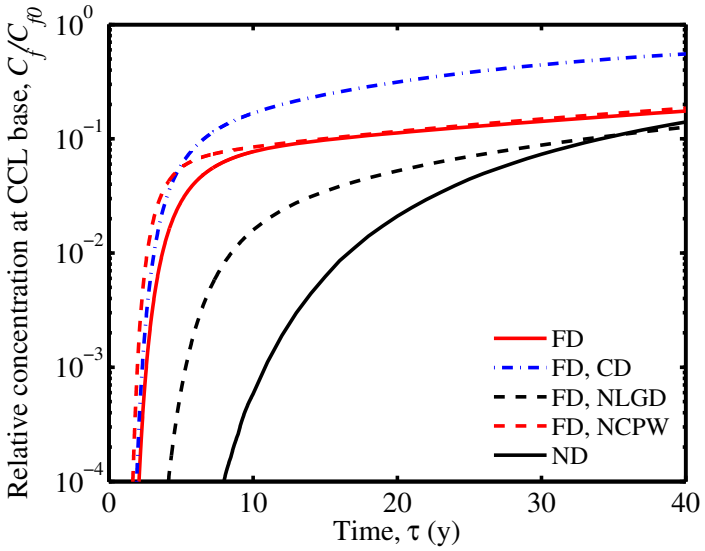

(a) $K_d = 0$

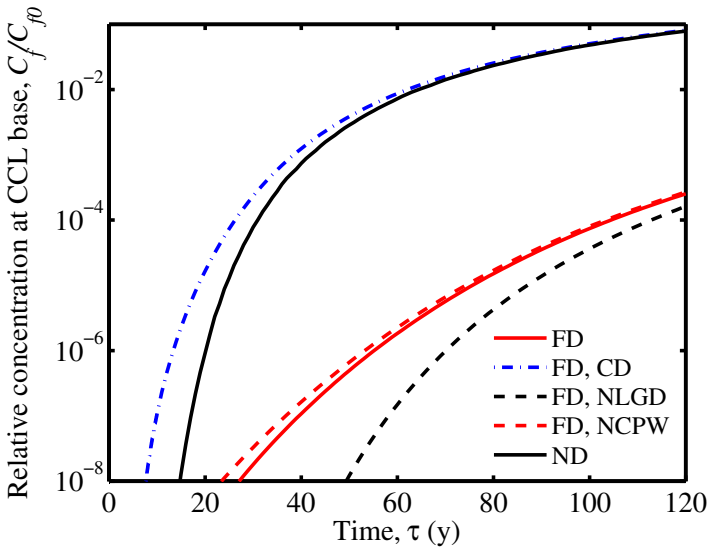

(b)K_d = 1 ml/g

Figure 4.14: Comparison of the concentration level at CCL base for various variables involved in the partially saturated soils ($S_r = 0.8$, $C_c = 0.8$, $k_p = 10^{-9}$ m/s). Notation: FD: finite deformation model; CD: constant D_e; NLGD: excluding the dispersion; NCPW: excluding the CPW; ND: no deformation model.

4.5.7 Effect of finite deformation

For the soil without sorption (see Fig. 4.1b, 4.9a, 4.10a, 4.14a), the ND model always leads to a longer transit time than the finite deformation model. In the presence of sorption (as shown in Fig. 4.10b), the difference between the ND model and the finite deformation model is negligibly small. However, when the decrease of the effective diffusion coefficient due to deformation is also considered (Fig. 4.9b and 4.14b), the results of the two models differ.

Compared with the finite deformation model, the small deformation model can overestimate the transit time of contaminants in a liner undergoing large consolidation (see Fig. 4.1b). This demonstrates that the significance of geometric nonlinearity is noticeable for relatively soft soil. This finding is consistent with that of Peters and Smith (2002) and Lewis et al. (2009). Regarding the consolidation, the small deformation model can predict settlement that is non-physical for soft soil (i.e., larger than the total soil thickness) for soft soil. Therefore, for a relatively compressible soil, where the consolidation effect is more significant, a finite deformation consolidation model is necessary when being coupled with the solute transport model.

4.6 Summary

In this paper, a finite deformation model for coupling consolidation and solute transport processes in partially saturated soil has been presented. It was applied to predict the VOC breakthrough in a landfill clay liner. CPW, dispersion, the nonlinear variation of soil compaction, hydraulic conductivity and effective diffusion are included in the model. Based on the numerical simulation results, these conclusions are drawn:

1. Consolidation-induced advection has a lasting effect on solute transport during and after the deformation for relatively compressible soil regardless of the sorption level, though the sorption could dramatically slow the solute transport process rate.

2. After an initial acceleration effect on transport, the finite-deformation coupled model with decreasing effective diffusion and sorption produces a lower concentration at the CCL base than the pure diffusion model.

3. A lower degree of saturation leads to a slower pore fluid flow and solute transport due to a narrower channel. The CPW associated with unsaturated conditions cannot be ignored when the consolidation is required to be coupled with solute transport. CPW-involving terms exist in both the consolidation and transport equations, none of them can be neglected for simplification. Effective diffusion decreases during consolidation and consequently the relative importance of mechanical dispersion becomes profound. For a long-term prediction, mechanical dispersion could cause significant solute transport. Therefore, it should be included to provide a reliable prediction of solute transport.

4. Generally speaking, reducing soil compressibility and improving sorption levels of clay are the most effective ways to retard contaminant migration. At the same level of stiffness and sorption, the lower hydraulic conductivity and lower degree of saturation can lengthen the time for contaminants to break through the protective liner.

4.7 Notation

The following notation is used in Chapter 4:

Roman Letters:

z, material coordinate, L

C_c, compression index of the soil

C_k, hydraulic conductivity index

c_{f0}, solute mass concentration at top of geo-membrane, ML^{-3}

c_f, concentration of the solute in the fluid phase, ML^{-3}

c_s, concentration of the solute in the solid phase, ML^{-3}

D, hydrodynamic dispersion coefficient, L^2T^{-1}

e, void ratio

e_0, initial void ratio

e_p, void ratio corresponding to the pre-consolidation stress

P_G, mass transfer coefficient of geomembrane, L^2T^{-1}

D_e, effective diffusion coefficient, L^2T^{-1}

D_{e0}, initial effective dispersion coefficient, L^2T^{-1}

D_f, free diffusion coefficient of the solute in the pore fluid, L^2T^{-1}

D_m, coefficient of mechanical dispersion, L^2T^{-1}

$f_{a\to s}$, rate of solute loss in aquatic phase by sorption onto solid phase, $ML^{-3}T^{-1}$

G, shear modulus of soil, $ML^{-1}T^{-2}$

g, gravity acceleration, LT^{-2}

h, thickness of geomembrane, L

J_f, solute flux in fluid phase, $M^2L^{-3}T^{-1}$

k_p, hydraulic conductivity corresponding to e_p, LT^{-1}

k_s, saturated hydraulic conductivity, LT^{-1}

k_v, hydraulic conductivity, LT^{-1}

K_d, contaminant partitioning coefficient, L^3M^{-1}

K_{w0}, pore water bulk modulus, $ML^{-1}T^{-2}$

L, thickness of CCL, L

M, Jacobian of coordinate transformation

n, current soil porosity

n_0, initial soil porosity

P_a, atmospheric pressure, $ML^{-1}T^{-2}$

P_0, atmosphere air pressure, $ML^{-1}T^{-2}$

p, excess pore pressure, $ML^{-1}T^{-2}$

r_h, volumetric fraction of dissolved air

q, Darcy flow velocity, LT^{-1}

Q, external load, $ML^{-1}T^{-2}$

S, mass of contaminant sorbed onto the solid phase per unit mass of solid phase

S_r, degree of saturation

t, time, T

u, soil displacement, L

u', arbitrary variable

U, arbitrary variable

v_f, average fluid velocity, LT^{-1}

v_s, solid velocity, LT^{-1}

x, spatial coordinate, L

Greek symbols

ξ, spatial coordinate, L

τ_f, the tortuosity factor

σ, total soil stress, $\mathrm{ML}^{-1}\mathrm{T}^{-2}$

$\sigma^{'}$, effective soil stress, $\mathrm{ML}^{-1}\mathrm{T}^{-2}$

σ_a, the time varying stress due to external overburden, $\mathrm{ML}^{-1}\mathrm{T}^{-2}$

$\sigma^{'}_L$, the effective stress at bottom, $\mathrm{ML}^{-1}\mathrm{T}^{-2}$

$\sigma^{'}_p$, effective soil stress corresponding to the pre-consolidation stress

ρ_f, density of pore water, ML^{-3}

ρ_s, density of soil gain, ML^{-3}

β, compressibility of pore water, $\mathrm{LT}^2\mathrm{M}^{-1}$

ν, Poisson's ratio

α, coefficient in calculating k_v

α_L, longitudinal dispersion, L

α_v, coefficient of compressibility, $\mathrm{LT}^2\mathrm{M}^{-1}$

α_{vp}, coefficient of compressibility corresponding to $\sigma^{'}_p$, $\mathrm{LT}^2\mathrm{M}^{-1}$

θ, water content

θ_s, saturated water content

θ_t, threshold water content

Abbreviation:

ADE, advection-dispersion equation

BCs, boundary conditions

CCL, compacted clay liner

CRFs, constitutive relationship functions

CPW, compressible pore water

GEs, governing equations

ICs, initial conditions

REV, represent element volume

SVP, spatial variation of porosity

VOCs, volatile organic chemicals

Chapter 5

Multi-phase Solute Transport in Non-isothermal Deformable Soil

5.1 Introduction

Solid waste landfills pose a potential major environmental threat to the groundwater resource. Unlike the inorganic compounds, VOCs can diffuse through the geomembrane, then breakthrough the underlying barrier and finally impair the quality of surrounding groundwater. Therefore, understanding the progress and minimizing the migration of VOCs in landfill liner is of great importance to design a effective barrier.

Numerous researches have been done in this area and most of them focused on the mechanism of liquid phase transport for either completely saturated (Kim, 1997; Nguyen et al., 2011) or unsaturated soil liner (Fityus et al., 1999). However, VOCs can reside in gaseous phase in addition to the solid and liquid phases (Jury et al., 1990) when the unsaturation prevails in soil liners. Therefore, the pore air motion in an unsaturated soil liner and its contribution to VOCs migration should be incorporated.

On the other hand, the temperature gradient has been confirmed to affect transport of VOCs significantly (Nassar et al., 1999). The temperature at top of basal liner may reach 30 °C to 60 °C (Rowe, 2005) due to biodegration of solid waste in a landfill.

An analytical solution is available for volatile organic contamination (VOC) transport in porous medium (Shan and Stephens, 1995), but it is not able to deal with the transient fluid and gas velocity due to the consolidation and temperature gradient. Regarding the numerical

solution, a few relevant works have been made to couple the non-isothermal moisture flow with solute or toxic gas transport in an unsaturated soil (Nassar and Horton, 1997; Thomas and Ferguson, 1999). Unfortunately, the deformation has been ignored.

As for the non-isothermal moisture transport in an unsaturated landfill liner, the soil deformation has been incorporated in a small deformation frame (Thomas and He, 1997; Zhou and Rowe, 2005). However, the compressive stress change due to external filling could be in the range of MPa and a sigmificant deformation may takes place. In this case, the assumption of small deformation will be inadequate and both the geometric and material non-linearity should be considered (Lewis et al., 2009).

The study in this chapter proposes a mathematical model for non-isothermal multi-phase moisture and VOC transport (in solid, liquid and gaseous phases) model for unsaturated soil in the frame of finite deformation. Prior to be used in a landfill liner, the model is benchmarked against a non-isothermal moisture transport in soil column and an analytical solution of multi-phase VOCs transport in an unsaturated soil. Then the breakthrough of VOCs in a unsaturated CCL was examined. Influences of various factors such as the mechanical consolidation, temperature gradient, soil velocity, finite deformation, mechanical dispersion and water vapor diffusivity in presence of VOCs vapor are investigated. The contribution of dispersion (diffusion and mechanical dispersion) in gas phase is also examined. Furthermore, there is no consensus regarding the sources of VOCs sorption onto soil solid. In this chapter, the disagreement in expression of total VOCs concentration in soil is discussed. In the end, the symbols used in this chapter are summarized. This chapter forms the manuscript of "Organic contamination transport through non-isothermal un-saturated deforming clay liner" listed in the preface.

5.2 Model Formulations

To establish the force equilibrium equation as well as mass conservation equations for water, gas, heat and VOCs, the following assumptions are made:

1. Pore fluid flow in both liquid and gas phases is driven by pressure, viscosity and gravity forces;

2. Water vapor moves through mechanism of diffusion and convection;

3. Heat flow occurs by conduction and convection and the temperature of individual soil phase are equal. In the range of temperature considered in this study, the phenomenas such as boiling, freezing and thawing are not considered (Nassar and Horton, 1997).

4. Soil liner is intact and no chemical reaction occurs except sorption of VOCs.

5.2.1 Coordinates systems

A Lagrangian coordinates system (z, t) is employed to derive the flow and transport equations. We define $\xi(z,t)$ as the particle displacement with $\xi(z,0) = z$. The relationship between Lagrangian and Eulerian (ξ, t) coordinate systems then implies that for any variable $F(z,t) = f(\xi(z,t),t)$

$$\frac{\partial F}{\partial z} = \frac{\partial f}{\partial \xi}\frac{\partial \xi}{\partial z}, \quad \frac{\partial F}{\partial t} = \frac{\partial f}{\partial \xi}\frac{\partial \xi}{\partial t} + \frac{\partial f}{\partial t} = \frac{\partial f}{\partial \xi}v_s + \frac{\partial f}{\partial t}, \tag{5.1}$$

where $v_s = \partial\xi/\partial t$ is the solid velocity.

Here, a fixed representative element volume (REV) is selected in the Lagrangian coordinates system. Therefore, the same amount of solid remains in each REV of soil, the continuity equation for solid phase takes the form

$$\rho_s(z,0)(1-n_0)\Delta z = \rho_s(1-n)\Delta\xi, \tag{5.2}$$

where ρ_s is the soil grain density, $n = e/(1+e)$ is the current porosity, and $n_0 = n(z,0)$ is the initial porosity. For Δz and $\Delta\xi$ approaching zero, with definition of partial derivative, rearranging above equation yields the Jacobian, M, for the coordinate transformation

$$M = \frac{\partial \xi}{\partial z} = \frac{1-n_0}{1-n} = \frac{1+e}{1+e_0}, \tag{5.3}$$

where e_0 is the initial void ratio.

5.2.2 Force equilibrium

Lateral soil pressure, σ_l is related to the vertical pressure, σ_v by the earth pressure coefficient at rest, K_0 (Boyd and Sivakumar, 2011; Fredlund and Rahardjo, 1993; Ishihara, 1993)

$$(\sigma_l + p_a) = K_0(\sigma_v + p_a), \tag{5.4}$$

Hence, the net mean stress is:

$$\sigma^* = \frac{\sigma_v + 2\sigma_l}{3} + p_a = \frac{1 + 2K_0}{3}\sigma_v + p_a. \tag{5.5}$$

Here the tension stresses are taken as positive and p_a is pore air gauge pressure.

For the compaction-induced soil lateral pressure, the value of K_0 increases rapidly with degree of saturation around optimum water content and may exceed 0.9 when the water content is above the optimum (Ishihara, 1993). In engineering practice, the landfill clay liner is usually compacted with the water content above the optimum (Edil, 2003). Therefore, in this study K_0 is taken as 0.9.

The force equilibrium of soil is described in terms of vertical soil stress σ_v as:

$$\frac{\partial \sigma_v}{\partial z} - b\frac{\partial \xi}{\partial z} = 0, \tag{5.6}$$

where b denotes the body force given by:

$$b = \{[\theta\rho_l + (n - \theta)\rho_v + (1 - n)\rho_s] - [\theta_0\rho_l + (n_0 - \theta_0)\rho_v + (1 - n_0)\rho_s]\}\, g_i. \tag{5.7}$$

in which θ and θ_0 represent current and initial water volume fraction, respectively. ρ_l denotes density of liquid water and ρ_v is water vapor. g_i is gravitational acceleration (equals 9.8 m^2/s when the vertical coordinate, z is in the opposite direction from gravity). The mass of dry air is negligibly small and is ignored.

5.2.3 Moisture and heat energy transfer in spatial coordinate system (ξ, t)

5.2.3.1 Mass balance for water

The expressions for liquid water and water vapor mass flux in unsaturated media can be written as

$$q_l = \rho_l \theta v_{li} - \rho_l D_T \frac{\partial T}{\partial \xi}, \tag{5.8}$$

$$q_v = -D^* \frac{\partial \rho_v}{\partial \xi} + \rho_v (n - \theta) v_{ai}. \tag{5.9}$$

The second term on RHS of (5.8) represents the water flux due to thermal gradient. D_T denotes the phenomenological coefficient relating water flux to temperature gradient. T is the absolute temperature increase and D^* is the effective molecular diffusivity of water vapor. The intrinsic, or linear average velocity of each individual liquid phase in soil is:

$$v_{li} = -\frac{k_l}{\theta} \frac{\partial}{\partial \xi} (p_c + p_a + \rho_l g_i \xi) + v_s, \tag{5.10}$$

$$v_{ai} = -\frac{k_a}{n - \theta} \frac{\partial p_a}{\partial \xi} + v_s, \tag{5.11}$$

where k_l and k_a are the mobility coefficient for liquid pore water and continuous air phase, respectively. $k_l = K_l/(\rho_l g)$, in which K_l is hydraulic conductivity of the soil medium. ξ is vertical spatial coordinate and its direction is downward positive. v_{li} and v_{ai} denote the intrinsic phase average velocity with respect to a fixed coordinate system (Bear and Cheng, 2010) for liquid and vapor water, respectively. The gravitational contribution to v_{ai} is neglected because the density of air ρ_a is negligibly small (Zhou and Rajapakse, 1998).

The importance of compressibility of pore water has been demonstrated in prediction of solute break through the partially saturated landfill liner (Zhang et al., 2012). The solute was

assumed to exist in solid and liquid phases. For the multi-phase VOCs transport model in this study, the density of both liquid and vapor water are taken as functions of temperature and capillary pressure:

$$\rho_l = \rho_{l0}\left[1 + \beta_l\left(p_c + p_a\right) - \alpha_l T\right], \tag{5.12}$$

where the initial density of liquid water, $\rho_{l0} = 998$ kg/m^3, pore water compressibility coefficient, $\beta_l = 3.3 \times 10^9$ Pa^{-1}, $\alpha_l = 3.0 \times 10^{-4}$ K^{-1} (Zhou and Rajapakse, 1998).

$$\rho_v = \rho_0 h = \rho_0 \exp\left[\frac{p_c}{\rho_l R_v\left(T + T_0\right)}\right], \tag{5.13}$$

in which ρ_0 is density of vapor at saturation (kg/m^3) given by (Thomas et al., 1996)

$$\rho_0 = \frac{1}{194.4}\exp\left[a_0 T' + b_0\left(T'\right)^2\right], \tag{5.14}$$

where R_v is the specific gas constant and $a_0 = 0.06374$, $b_0 = -0.1634\times10^{-3}$, $T' = T + T_0 - 273$ (T_0 is the initial temperature).

In the previous non-isothermal moisture transport models (Azad et al., 2012; Thomas et al., 1996; Thomas and He, 1997; Zhou and Rajapakse, 1998; Zhou and Rowe, 2005), the solid velocity was not included in expression of water flux in deformable media. It is probably due to the direct borrowing of the expressions for the rigid porous medium. In this study, the solid velocity is incorporated in both mass and heat fluxes, and in the liquid linear average velocity as well for the purpose of theoretical self-consistent. When converted to the material coordinate system in the sequential section, all terms involving v_s disappear and no extra complexity in formulas is introduced.

The mass conservation equation for the moisture in a deformable unsaturated soil can be expressed by

$$\frac{\partial}{\partial t}\left[\rho_l\theta + \rho_v\left(n - \theta\right)\right] = -\frac{\partial}{\partial \xi}\left(q_l + q_v\right). \tag{5.15}$$

Regarding D_T, Zhou et al. Zhou and Rajapakse (1998) takes it as 2.4×10^{-10} $m^2/(s\ K)$ in the simulation example of an non-isothermal unsaturated soil column, whilst other researchers attributed the influence of temperature on liquid water flux to its effect on capillary potential head and expressed it as (Nassar and Horton, 1997; Philip and de Vries, 1957)

$$D_T = k_l \rho_l g \frac{\partial \Psi}{\partial T}. \tag{5.16}$$

The temperature-corrected potential head which is assumed to be a function of capillary potential head, Ψ and temperature is given by (Milly, 1984)

$$\Psi = p_c/(\rho_l g)\exp(-C_\psi T), \tag{5.17}$$

where C_ψ is the temperature coefficient of water retention. It can be taken as -0.0068 K^{-1} (Scanlon and Milly, 1994; Zhou and Rowe, 2003).

Considering the gaseous mixture of dry air and water vapor, the effective molecular diffusivity of water vapor, D^* can be expressed as (Philip and de Vries, 1957; Zhou and Rajapakse, 1998)

$$D^* = D_{atm} \nu_m \tau (n - \theta) \tag{5.18}$$

where τ is the dimensionless tortuosity factor to account for complexities in pore geometry and boundary conditions that influence vapor transport at the microscopic scale (Zhou and Rajapakse, 1998). Its typical value is less than 1.0 for intact soil, and it is temperature-dependent. In the validation of non-isothermal moisture transport, τ is assumed to be a constant. The mass flow factor, $\nu_m = p_a/(p_a - p_v)$. D_{atm} is the molecular diffusion coefficient of water vapor in air (m^2/s), and is expressed in terms of absolute temperature and air pressure (here, p_a is in the unit of Pa) (Thomas et al., 1996):

$$D_{atm} = 5.893 \times 10^{-6} \left[(T + T_0)^{2.3} / p_a \right] \tag{5.19}$$

Alternatively, the vapor diffusion flow which is assumed to be driven by a vapor density gradient (Thomas and He, 1997) can be described by an extended vapor velocity equation proposed by (Thomas and King, 1994)

$$D^* \frac{\partial \rho_v}{\partial \xi} = n D_{atm} \nu_m \left[\frac{\partial \rho_v}{\partial p_c} \frac{\partial p_c}{\partial \xi} + \frac{(\nabla T)_a}{\nabla T} \frac{\partial \rho_v}{\partial T} \frac{\partial T}{\partial \xi} \right], \tag{5.20}$$

where $(\nabla T)_a / \nabla T$ is ratio of the microscopic temperature gradient to macroscopic temperature gradient. It is introduced to consider that the microscopic temperature gradients in the fluid filled pores much higher than macroscopic gradients across the sample as a whole. Thomas and Ferguson (1999) employed (5.20) to describe the water vapor diffusivity even in presence of VOCs gas.

When the concentration of VOC in liquid phase increases to a critical level, its effect on Ψ may not be neglected and can be considered via the surface tension model (Smith and Gillham, 1994):

$$\Psi = \Psi(T_r)(\gamma_m / \gamma_w), \tag{5.21}$$

where T_r is an arbitrary reference temperature, $\Psi(T_r)$ is the capillary pressure head at the reference temperature, γ_w is the surface tension of a free-water system at the reference temperature (J/m^2), and γ_m is surface tension (J/m^2) at VOC concentration of c_l. In view of (5.17), the capillary pressure head can eventually be expressed as

$$\Psi = p_c / (\rho_l g) \exp(-C_\psi T)(\gamma_m / \gamma_w), \tag{5.22}$$

The effect of organic chemical concentration on the surface tension, γ_m / γ_w, can be calculated for nonionized organic solute by (Nassar and Horton, 1999; Reid et al., 1987a)

$$\gamma_m / \gamma_w = \left[\Gamma_w + \Gamma_0 \left(\gamma_0 / \gamma_w \right)^{1/4} \right]^4 \tag{5.23}$$

where γ_0 is the surface tension of VOC (J/m^2), Γ_w and Γ_0 represent the superficial volume fraction of water and VOC in the surface layer, whose data are very rare in literature. Therefore, effect of VOCs on surface tension of mixture liquid is included by specifying a constant reduce factor for (γ_m/γ_w). In contrary to inorganic species, organic compounds typically decrease the surface tension of water. The reduce factor falls in the range of 0.6 to 1 for the organic concentration lower than 10 mg/ml or less than 1×10^{-3} mol/ml in terms of molar concentration (Tuckermann, 2007; Tuckermann and Cammenga, 2004).

In case of gaseous mixture composed of water vapor, dry air and VOC vapor, the water vapor diffusion may be influenced by presence of VOC vapor especially when its mole fraction is relatively large. It can be described as (Nassar and Horton, 1999; Welty et al., 1984)

$$D^* = \left[(n-\theta)^{5/3}\right] D_{wm} \tag{5.24}$$

where, the molecular diffusivity of water vapor in a gas mixture (m^2/s), D_{wm} is

$$D_{wm} = 1/\left(y'_2/D_{i-2} + y'_3/D_{i-3} + ... + y'_n/D_{i-n}\right) \tag{5.25}$$

in which D_{i-n} denotes the molecular diffusivity for the binary pair, i.e., water vapor diffusive through components n. y'_n is the mole fraction of component n in the gas mixture evaluated on a component-water-vapor-free basis, that is,

$$y'_2 = y_2/\left(y_2 + y_3 + ... + y_n\right) \tag{5.26}$$

For a gaseous mixture that obeys the ideal gas law, the mole fraction equals the ratio of corresponding partial pressure (Welty et al., 1984).

5.2.3.2 Mass balance for dry air

Air flow occurs as bulk flow and diffusion flow of dry air and dissolved air within the pore water. Assuming the diffusion flow of dry air is very small relative to bulk flow and can be ignored (Thomas and He, 1997; Zhou and Rajapakse, 1998), the mass balance for air in a deformable unsaturated soil can be written as

$$\frac{\partial}{\partial t}\left\{\rho_{da}\left[n-(1-H)\,\theta\right]\right\}=-\frac{\partial q_{da}}{\partial \xi}, \tag{5.27}$$

where ρ_{da} is density of dry air and H is the dimensionless coefficient of solubility defined by Henry's law (Thomas and Sansom, 1995). The dry air flux, q_{da}, is described as

$$q_{da}=H\rho_{da}\left(\theta v_{li}-D_T\frac{\partial T}{\partial \xi}\right)+\rho_{da}\,(n-\theta)\,v_{ai}, \tag{5.28}$$

In this study, the variation of pore air pressure from atmosphere pressure is far less than 1 bar except when the degree of saturation exceeds 0.985. Furthermore, the temperature falls in the range of 10 to 60 Celcius. Therefore, the background condition for pore air is close to the condition of standard temperature and pressure (STP). It is satisfactorily accurate for technical calculation to make the assumption that the mixture of gases obey the ideal gas law and Dalton's law (Thomas and Sansom, 1995; Thomas and He, 1997). Therefore, we have

$$\rho_{da}=\frac{p_{da}}{R_{da}\,(T+T_0)}, \tag{5.29}$$

$$p_v=\rho_v R_v\,(T+T_0)\,. \tag{5.30}$$

where $R_i(i=da,v)$ is the specific gas constant (ideal gas constant divided by the molecular weight).

When the volume fraction of VOC in gaseous phase is sufficiently small (Challa et al., 1997; Hodgson et al., 1992; Soltani-Ahmadi, 2000), the first approximation can be made that the presence of VOC may not significantly alter the density and pressure of dry air and water

vapor. Applying Dalton's law to the pore air mixture, the pore air pressure p_a is sum of dry air pressure p_{da} and vapour pressure p_v

$$p_a = p_{da} + p_v. \tag{5.31}$$

Substitution of equation (5.30) and (5.31) into (5.29) leads to

$$\rho_{da} = \frac{p_a}{R_{da}\left(T + T_0\right)} - \frac{R_v}{R_{da}}\rho_v, \tag{5.32}$$

where the specific gas constant, $R_{da} = 287.1$ J/kg K, $R_v = 461.5$ J/kg K.

The above approach is applicable for the case with relatively large VOC mole fraction in the gas mixture. Since density of VOCs vapor (ρ_{VOC}) can be expressed in terms of adsorption coefficient H and liquid concentration of VOCs, c_l, as $\rho_{VOC} = Hc_l$, this additional compound does not add extra unknown. Considering Dalton's law of partial pressure yields

$$p_{VOC} = \rho_{VOC} R_{VOC}\left(T + T_0\right), \tag{5.33}$$

$$p_a = p_{da} + p_v + p_{VOC}, \tag{5.34}$$

$$\rho_{da} = \frac{p_a}{R_{da}\left(T + T_0\right)} - \frac{R_v}{R_{da}}\rho_v - -\frac{R_{VOC}}{R_{da}}\rho_{VOC}, \tag{5.35}$$

where R_{VOC} is the specific gas constant for VOCs.

5.2.3.3 Heat energy balance

For a unit volume of a deformable unsaturated medium, the conservation of heat energy can be written as

$$\frac{\partial \Phi}{\partial t} = -\frac{\partial q_T}{\partial \xi}, \tag{5.36}$$

where Φ and q_T are the heat capacity of the soil and the total heat flux per unit volume, respectively. Besides heat content in individual phase, considering the contributions of latent heat of vaporization and exothermic process of wetting of the porous medium, Φ can be defined as (Zhou and Rajapakse, 1998)

$$\begin{aligned}\Phi = &\left[\rho_s(1-n)C_s + \rho_l\theta C_l + \rho_v\left(n-\theta\right)C_v + \rho_{da}\left(n-\left(1-H\right)\theta\right)C_{da}\right]T \\ &+ L_0\rho_v\left(n-\theta\right) + \rho_l\theta W,\end{aligned} \tag{5.37}$$

where C_i $(i = s, l, v, da)$ is the specific heat capacity of each constituent in soil, L_0 is the latent heat of vaporization and W (J/kg), the differential heat of wetting given by (Milly, 1984) (quoted by Zhou and Rajapakse (1998))

$$W = \frac{H_w}{\rho_l\delta}\exp(-\theta/\delta S') \tag{5.38}$$

in which $S' = 1.0\times10^7$ m^{-1} is specific surface of the material and material constants $H_w = 1$ J/m^2, $\delta = 1.0\times10^{-9}$ m in accordance to Zhou and Rajapakse (1998). The alternative form of expression for W can be found in de Vries (1958).

In this study, heat transfer mechanisms includes conduction, convection, vaporization of heat, gradient of water potential and differential heat of wetting flux. When expressing the gradient of differential heat of wetting flux as liquid water flux multiplying the coefficient of differential heat of wetting, W, q_T can be written as (Prunty, 2002),

$$\begin{aligned}q_T = &-\lambda\frac{\partial T}{\partial \xi} + \left(\rho_s\left(1-n\right)v_sC_s + q_lC_l + q_vC_v + q_{da}C_{da}\right)T + q_lW \\ &+ L_0q_v - D_c^*\frac{\partial}{\partial \xi}\left(p_c + p_a + \rho_l g\xi_i\right)\end{aligned} \tag{5.39}$$

where $\lambda = (1 - S_l)\lambda_{dry} + S_l\lambda_{sat}$ is thermal conductivity (where the degree of saturation $S_l = \theta/n$, $\lambda_{dry} = 0.5$ J/(s m K), $\lambda_{sat} = 2.0$ J/(s m K) (Zhou and Rajapakse, 1998)). $D_c^* = (T + T_0)D_T$ is to relate water potential gradient to heat flux phenomenologically (Kay and Groenevelt, 1974; Milly, 1982b). For the case with relatively large VOCs concentration in three-phases within soil, the heat transfer parameters employed should be measured specifically to incorporate the effect of VOCs.

5.2.3.4 Organic solute transfer

VOCs may reside in liquid, gaseous and solid phase of soil (Jury et al., 1990), and its movement can be caused by diffusion and advection in both liquid and vapor phases. Ignoring the degradation of VOCs in soil, its mass conservation is written as

$$\frac{\partial c_{mt}}{\partial t} = -\frac{\partial q_{ct}}{\partial \xi}, \tag{5.40}$$

where c_{mt} denotes the mass of contaminants in unit volume of soil matrix and q_{ct} represents the total VOCs flux. In accordance to Nassar and Horton (1999), we have

$$c_{mt} = (1 - n)\,\rho_s S + \theta c_l + (n - \theta)c_g, \tag{5.41}$$

where S is adsorbed concentration (mass per mass soil) and can be divided into two parts (Poulsen et al., 1998)which are sorbed from water phase and air phase, respectively. In the present study, local chemical equilibrium is assumed between each phase, i.e., concentration of VOCs in one phase can be evaluated from that in another phase. Assuming a linear partitioning coefficient between soil phases i and j, H_{ij} (Nassar and Horton, 1999; Nassar et al., 1999), we have

$$\begin{aligned} S &= H_{sl}c_l + H_{sg}c_g, \\ c_g &= H_{gl}c_l \end{aligned} \tag{5.42}$$

where $c_i (i = l, g)$ denotes mass of VOCs in unit volume of liquid and gas phase, respectively. They are related by $H_{ij}(i, j = s, l, g)$, the linear partitioning coefficients between individual soil phase. Nassar et al. Nassar et al. (1999) provided that the liquid-solid partitioning coefficient, $H_{sl} = 0.343 \times 10^{-3} \mathrm{m}^3/\mathrm{kg}$ (depends on water mass content, kg water per kg soil), and dimensionless Henry's constant, $H_{gl} = 0.2$ (depends on the temperature and relative humidity level). Sorption of VOC from the vapor phase onto soil minerals, namely, H_{sg}, is strongly dependent upon pore water content, soil type, and on the chemical properties of the sorbing VOC (Nassar et al., 1999; Petersen et al., 1995). It can be around 1,000 times of H_{sl} for dry soil (Ho, 2006). H_{gl} for benzene is taken as 0.191 (Staudinger and Roberts, 2001). The partitioning coefficients are assumed to be functions of σ^*, p_c, p_a and T for sake of generality in the derivation of related equations and coefficients. The linear sorption relationship employed here is valid because VOCs concentrations in landfill liner are normally very low (Poulsen et al., 1996, 1998).

For the VOCs transport mechanism, advection is caused by moisture transport (liquid and vapour) and solid grain motion for the deformable porous medium considered, whilst dispersion is caused by mechanical dispersion and molecular diffusion,

$$\begin{aligned} q_{ct} = & -\theta D_{lc}\frac{\partial c_l}{\partial \xi} - (n-\theta)D_{gc}\frac{\partial c_g}{\partial \xi} + (1-n)\rho_s v_s S + \frac{q_l}{\rho_l}c_l \\ & + (n-\theta)\left(v_{ai} + v_g\right)c_g \end{aligned} \tag{5.43}$$

where $D_{ic}(i = l, g)$ is the hydrodynamic dispersion coefficient and thermal diffusion effect is represented through temperature-dependent diffusion coefficient in each phase. Here the VOCs advective flux in gas phase consists of two parts. v_{ai} is driven by air pressure gradient and the equivalent vapor diffusion velocity, v_g is due to water vapor density gradient. In literature, Thomas and Ferguson (1999) only accounted for the first part while Nassar and Horton Nassar and Horton (1999) considered only the second part. However, both of them should be incorporated in analogy to the derivation of water vapor transport equation.

When defining the total VOCs concentration in Eq. (5.41) and flux in Eq. (5.43), the bulk density of soil, ρ_{sb}, is often used to express solute mass sorbed onto solid phase (Nassar

and Horton, 1999; Shan and Stephens, 1995). However, ρ_{sb} varies due to the change of porosity. Therefore, ρ_s is employed herein for the convenience in describing the varying porosity explicitly.

The hydrodynamic dispersion coefficient for VOCs in liquid phase, D_{lc} is given by (Nassar and Horton, 1999):

$$D_{lc} = 0.001 D_0 \exp(10\theta)/\theta + D_{hw}, \tag{5.44}$$

where $D_{hw} = \alpha_{Lw}|v_{li}|$ (α_{Lw} is the longitudinal dispersivity parameter, which equals 0.004 m (Yong et al., 1992)) is mechanical dispersion coefficient of VOC (m^2/s). D_0 is mass diffusivity of organic chemical through water (m^2/s), which can be expressed through the Wilke-Chang equation (Welty et al., 1984) (which is also quoted by Nassar and Horton (1999)):

$$D_0 = \frac{7 \times 10^{-12} (\phi M_w)^{0.5} (T + T_0)}{\mu_w V_i^{0.6}}, \tag{5.45}$$

where ϕ is dimensionless association factor of solvent. It can be chosen as 2.6 for water solvent (Nassar and Horton, 1999). M_w is the molecular weight of water (g/mol). V_i is the molal volume of organic solute at the normal boiling point (cm^3/mol), which can be estimated from the addictive methods (Reid et al., 1987a) as 224 cm^3/mol and 98 cm^3/mol for toluene and benzene, respectively.

The dynamic viscosity of water, μ_w (mPa·s) is (Zhou and Rajapakse, 1998)

$$\mu_w = 661.2 \, (T + T_0 - 229)^{-1.562} \, . \tag{5.46}$$

The existing liquid state theories for calculating the diffusion coefficients are quite idealized and none is satisfactorily accurate. Here, Eq. (5.45) is one of the methods commonly used to estimate the binary liquid diffusion coefficient of liquid at infinite dilution. The error induced by this method is around 10% (Reid et al., 1987b).

The hydrodynamic dispersion coefficient for VOCs in gaseous phase, D_{gc} is (Nassar and Horton, 1999)

$$D_{gc} = \Omega D_{gm} + D_{hg}, \tag{5.47}$$

where $D_{hg} = \alpha_{Lg}|v_{ai}|$ (α_{Lg} is the mechanical dispersion coefficient and it is taken as 1 cm following Cann et al. (2004) in this study) is dispersion coefficient of VOC in gaseous phase. The molecular-diffusion coefficient of an organic compound in a gaseous mixture (water vapor, air and vapor of the VOC), D_{gm}, can be calculated via Eq. (5.25). $\Omega = (n-\theta)^{2/3}$, is a factor representing the tortuosity. The binary diffusion diffusivity (m^2/s) for gas i through gas n in the vapor phase can be calculated as (Fuller et al., 1966; Welty et al., 1984; Reid et al., 1987b),

$$D_{i-n} = \frac{0.00143\,(T+T_0)^{1.75}}{P\,(M_{i-n})^{1/2}\left[(\Sigma_v)_i^{1/3} + (\Sigma_v)_n^{1/3}\right]^2} 10^{-4}, \tag{5.48}$$

where $M_{i-n} = 2\,(1/m_i + 1/m_n)^{-1}$. $m_j (j = i, n)$ (g/mol) is the molecular weight for gases ($j = i, n$). Σ_v (no unit) is the sum of atomic diffusion volumes for each gas component (Reid et al., 1987b) (18 for water vapor, 19.7 for dry air, 90.96 for benzene). P is air pressure (=p_a) with unit in atmospheres.

Since each VOC compound has a different specific gas constant (due to the unique molecular weight) and partitioning coefficients, one mass conservation equation can be written for each individual component when VOCs is a multicomponent mixture. There is no extra theoretical complexity except that more computational effort is required. In this study, a single compound is considered.

5.2.4 Moisture and heat energy transfer in material coordinate system (z, t)

Mass balance equation for moisture is

$$\frac{\partial}{\partial t}\left\{\left[\rho_l\theta+\rho_v\left(n-\theta\right)\right]M\right\}=-\frac{\partial}{\partial z}\left[-\rho_l k_l\frac{\partial}{\partial\xi}\left(p_c+p_a+\rho_l g\xi_i\right)-\rho_l D_T\frac{\partial T}{\partial\xi}-D^*\frac{\partial\rho_v}{\partial\xi}-\rho_v k_a\frac{\partial p_a}{\partial\xi}\right] \tag{5.49}$$

M at left hand side (LHS) is to address the deformation of representative element volume (REV) relative to the spatial grid. The spatial gradient involved in the water flux on right hand side (RHS) is implemented by transformation to material coordinate, i.e., $\partial(\cdot)/\partial\xi = 1/M\partial(\cdot)/\partial z$.

Mass balance equation for dry air is

$$\frac{\partial}{\partial t}\left\{\rho_{da}\left[n-\left(1-H\right)\theta\right]M\right\}=-\frac{\partial}{\partial z}\left\{H\rho_{da}\left[-k_l\frac{\partial}{\partial\xi}\left(p_c+p_a+\rho_l g\xi_i\right)-D_T\frac{\partial T}{\partial\xi}\right]+\rho_{da}\left(-k_a\frac{\partial p_a}{\partial\xi}\right)\right\} \tag{5.50}$$

Heat energy conservation is

$$\begin{aligned}\frac{\partial}{\partial t}\left(\Phi M\right)=-\frac{\partial}{\partial z}\Bigg\{&-\lambda\frac{\partial T}{\partial\xi}+\left(-\rho_l k_l\frac{\partial}{\partial\xi}\left(p_c+p_a+\rho_l g\xi_i\right)-\rho_l D_T\frac{\partial T}{\partial\xi}\right)C_l T\\&+\left(-D^*\frac{\partial\rho_v}{\partial\xi}-\rho_v k_a\frac{\partial p_a}{\partial\xi}\right)C_v T+H\rho_{da}\left(-k_l\frac{\partial}{\partial\xi}\left(p_c+p_a+\rho_l g\xi_i\right)-D_T\frac{\partial T}{\partial\xi}\right)C_{da}T\\&+\rho_{da}\left(-k_a\frac{\partial p_a}{\partial\xi}\right)C_{da}T+\left[-\rho_l k_l\frac{\partial}{\partial\xi}\left(p_c+p_a+\rho_l g\xi_i\right)-\rho_l D_T\frac{\partial T}{\partial\xi}\right]W\\&+L_0\left(-D^*\frac{\partial\rho_v}{\partial\xi}-\rho_v k_a\frac{\partial p_a}{\partial\xi}\right)-D_c^*\frac{\partial}{\partial\xi}\left(p_c+p_a+\rho_l g\xi_i\right)\Bigg\}\end{aligned} \tag{5.51}$$

Mass conservation for VOCs is

$$\begin{aligned}\frac{\partial}{\partial t}\left(c_{mt}M\right)=-\frac{\partial}{\partial z}\Bigg\{&-\theta D_{lc}\frac{\partial c_l}{\partial\xi}-\left(n-\theta\right)D_{gc}\frac{\partial c_g}{\partial\xi}\\&-\left[k_l\frac{\partial}{\partial\xi}\left(p_c+p_a+\rho_l g\xi_i\right)+D_T\frac{\partial T}{\partial\xi}\right]c_l-k_a\frac{\partial p_a}{\partial\xi}c_g+\frac{D^*}{\rho_v}\frac{\partial\rho_v}{\partial\xi}c_g\Bigg\}\end{aligned} \tag{5.52}$$

The above equations (5.49-5.52) can also be developed via coordinate transformation. The method in tackling v_s is in analogy with that used in appendix C of Peters and Smith (2002). The procedure is demonstrated in Appendix 5B. When $M = 1$, the equations can be reduced to the geometric linear model without considering soil velocity. Expanding the terms on LHS of each equation obtains:

$$\begin{aligned} & E_{11}\frac{\partial \sigma_v}{\partial t} + E_{12}\frac{\partial p_c}{\partial t} + E_{13}\frac{\partial p_a}{\partial t} + E_{14}\frac{\partial T}{\partial t} \\ &= -\frac{\partial}{\partial z}\left[-\rho_l k_l \frac{\partial}{\partial \xi}(p_c + p_a + \rho_l g \xi_i) - \rho_l D_T \frac{\partial T}{\partial \xi} - D^* \frac{\partial \rho_v}{\partial \xi} - \rho_v k_a \frac{\partial p_a}{\partial \xi}\right] \end{aligned} \tag{5.53}$$

$$\begin{aligned} & E_{21}\frac{\partial \sigma_v}{\partial t} + E_{22}\frac{\partial p_c}{\partial t} + E_{23}\frac{\partial p_a}{\partial t} + E_{24}\frac{\partial T}{\partial t} \\ &= -\frac{\partial}{\partial z}\left\{H\rho_{da}\left[-k_l \frac{\partial}{\partial \xi}(p_c + p_a + \rho_l g \xi_i) - D_T \frac{\partial T}{\partial \xi}\right] + \rho_{da}\left(-k_a \frac{\partial p_a}{\partial \xi}\right)\right\} \end{aligned} \tag{5.54}$$

$$\begin{aligned} & E_{31}\frac{\partial \sigma_v}{\partial t} + E_{32}\frac{\partial p_c}{\partial t} + E_{33}\frac{\partial p_a}{\partial t} + E_{34}\frac{\partial T}{\partial t} \\ &= -\frac{\partial}{\partial z}\left\{-\lambda \frac{\partial T}{\partial \xi} + \left[-\rho_l k_l \frac{\partial}{\partial \xi}(p_c + p_a + \rho_l g \xi_i) - \rho_l D_T \frac{\partial T}{\partial \xi}\right] C_l T \right. \\ &\quad + \left(-D^* \frac{\partial \rho_v}{\partial \xi} - \rho_v k_a \frac{\partial p_a}{\partial \xi}\right) C_v T + H\rho_{da}\left[-k_l \frac{\partial}{\partial \xi}(p_c + p_a + \rho_l g \xi_i) - D_T \frac{\partial T}{\partial \xi}\right] C_{da} T \\ &\quad + \rho_{da}\left(-k_a \frac{\partial p_a}{\partial \xi}\right) C_{da} T + \left[-\rho_l k_l \frac{\partial}{\partial \xi}(p_c + p_a + \rho_l g \xi_i) - \rho_l D_T \frac{\partial T}{\partial \xi}\right] W \\ &\quad \left. + L_0\left(-D^* \frac{\partial \rho_v}{\partial \xi} - \rho_v k_a \frac{\partial p_a}{\partial \xi}\right) - D_c^* \frac{\partial}{\partial \xi}(p_c + p_a + \rho_l g \xi_i)\right\} \end{aligned} \tag{5.55}$$

$$\begin{aligned} & E_{41} c_l \frac{\partial \sigma_v}{\partial t} + E_{42} c_l \frac{\partial p_c}{\partial t} + E_{43} c_l \frac{\partial p_a}{\partial t} + E_{44} c_l \frac{\partial T}{\partial t} + E_{45}\frac{\partial c_l}{\partial t} \\ &= -\frac{\partial}{\partial z}\left\{\left[\theta D_{lc} + (n-\theta) D_{gc} H_{gl}\right] \frac{\partial c_l}{\partial \xi} - (n-\theta) D_{gc} \frac{\partial H_{gl}}{\partial \xi} c_l \right. \\ &\quad \left. - \left[k_l \frac{\partial}{\partial \xi}(p_c + p_a + \rho_l g \xi_i) + D_T \frac{\partial T}{\partial \xi}\right] c_l - k_a \frac{\partial p_a}{\partial \xi} H_{gl} c_l - \frac{D^*}{\rho_v} \frac{\partial \rho_v}{\partial \xi} H_{gl} c_l\right\} \end{aligned} \tag{5.56}$$

Coefficients, E_{ij} ($i = 1, 2, 3, 4,\ j = 1, 2, 3, 4, 5$) used in the above equations of Eq. (5.53) to Eq. (5.56) are formulated in detail in the Appendix 5A. Spatial coordinate, ξ can be determined by

$$\xi = z + \int_z^L \frac{e_0 - e(\zeta)}{1 + e_0} d\zeta. \tag{5.57}$$

Thus, the first-order PDE

$$\frac{\partial \xi}{\partial z} = 1 - \frac{e_0 - e(z)}{1 + e_0}, \tag{5.58}$$

with boundary conditions $\xi(L, t) = L$ was constructed to find solution of ξ.

5.2.5 Constitutive relationships

A non-linear elastic soil model is used here. Generally, both state surfaces for void ratio and liquid water content can be postulated as (Zhou and Rajapakse, 1998)

$$e = f_e(\sigma^*, p_c, T), \tag{5.59}$$

$$\theta = f_\theta(\sigma^*, p_c, T). \tag{5.60}$$

Considering (5.5), e and θ actually depend on the four primary variables. Thus we have

$$e = f_e(\sigma_v, p_c, p_a, T), \tag{5.61}$$

$$\theta = f_\theta(\sigma_v, p_c, p_a, T). \tag{5.62}$$

Lloret and Alonso Lloret and Alonso (1985) made a extensive review of a number of forms of state surfaces and concluded that the following formulation gives the best description of soil behavior (also employed by Zhou and Rowe (2005)):

$$e = a_e + b\ln(-\sigma^*) + c\ln(-p_c) + d\ln(-\sigma^*)\ln(-p_c) + (1 + e_0)\alpha_T T \tag{5.63}$$

where a_e, b, c and d are model parameters. The thermal coefficient of volume change, α_T, can be expressed as (Thomas et al., 1996)

$$\alpha_T = \alpha_0 + \alpha_2 T + (\alpha_1 + \alpha_3 T)\ln\left(\frac{\sigma^*}{\sigma_0^*}\right) \tag{5.64}$$

where σ_0^* is the reference net mean stress and $\alpha_i (i = 0, 1, 2, 3)$ are the model parameters.

The water retention curve and hydraulic conductivity for a clay liner at a reference temperature T_r can be described by (Lloret and Alonso, 1985) (employed by Azad et al. (2012))

$$\theta = \{a' - [1 - \exp(-b' p_c)](c' - d'\sigma^* \times 10^{-3})\}\frac{e}{1 + e} \tag{5.65}$$

where a', b', c' and d' are model parameters.

The unsaturated hydraulic conductivity of the deformable soil under isothermal conditions, K_l, is given by (Alonso et al., 1988)

$$K_l = k_l \rho_l g = A\left[\frac{S_l - S_{lu}}{1 - S_{lu}}\right]^3 10^{\alpha_k e} \tag{5.66}$$

where S_l is degree of saturation and A, S_{lu}, and α_k are the related constants. And the mobility coefficient of continuous air phase, k_a, is (Alonso et al., 1988)

$$k_a = \frac{B}{\mu_a}[e\,(1 - S_l)]^\beta \tag{5.67}$$

where μ_a is dynamic viscosity of the pore air. B and β are model constants.

5.3 Validation of the proposed model

In this section, the present model was reduced in order to be validified against the benchmark problems in literature.

5.3.1 Non-isothermal moisture transport in deformable soil column

Infiltration of an unsaturated soil column 1.0 m high in Zhou and Rajapakse (1998) is considered. The initial conditions of the soil are uniform capillary pressure, $p_{c0} = -200$kPa, uniform air pressure, $p_{a0} = 1$ bar and zero temperature increase, i.e., $T(t = 0) = 0$ K with a uniform background temperature of $T_0 = 293$ K. At the top ($z = 0$) of soil column, a constant capillary pressure increase of 150 kPa is applied. The soil is free to deform and both air pressure and temperature are kept constant. At the fixed bottom ($z = 1$), each quantity stays at the initial state. The comparison results are shown in Fig. 5.1, which indicates an excellent agreement.

5.3.2 Multi-phase VOCs transport

Here, an analytical solution of multi-phase VOCs transport in Shan and Stephens (1995) is adopted as a benchmark case. Consider the problem of Trichloroethylene (TCE) transport in a vadose zone with a thickeness of 10 m. Initially, there is a uniform concentration of 100 μ g /cm^3 between 700 cm to 710 cm. The boundary conditions are a zero concentration at the soil surface, and a zero concentration gradient at the bottom. The effects of mechanical dispersion and bio-degradation are neglected and the gas advection velocity was assumed to zero. As shown in Fig. 5.2, the present model accurately reproduces the analytical solution.

5.4 Application: VOCs transport through intact compacted clay liner (CCL)

5.4.1 Problem description

The liner system investigated here is the same as used in the Chapter 3 and Chapter 4. Initially the VOCs-free CCL has a uniform of pore air pressure (1 bar) and temperature T_0. To account for the initial steady liquid distribution resulting from gravity, a linear variation of pore water pressure is assumed as (Thomas et al., 1996)

$$p_c(z, t = 0) = p_{cr} + \rho_{l0} g_i (L - z), \tag{5.68}$$

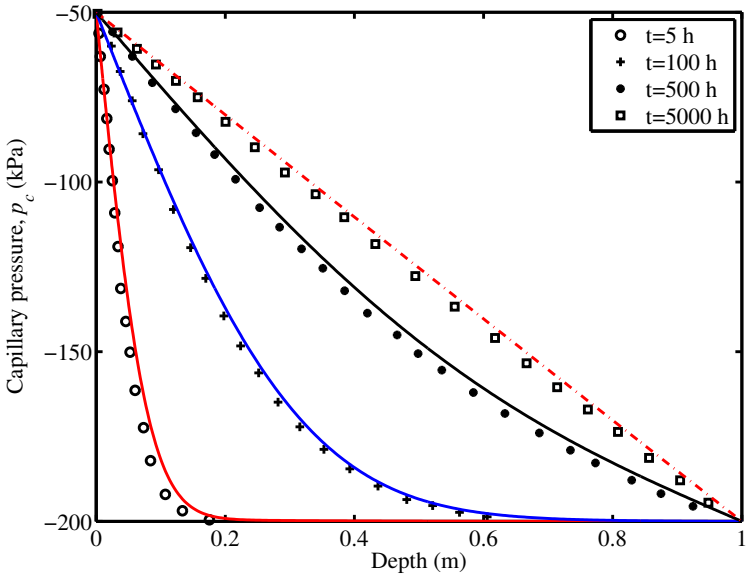

(a)

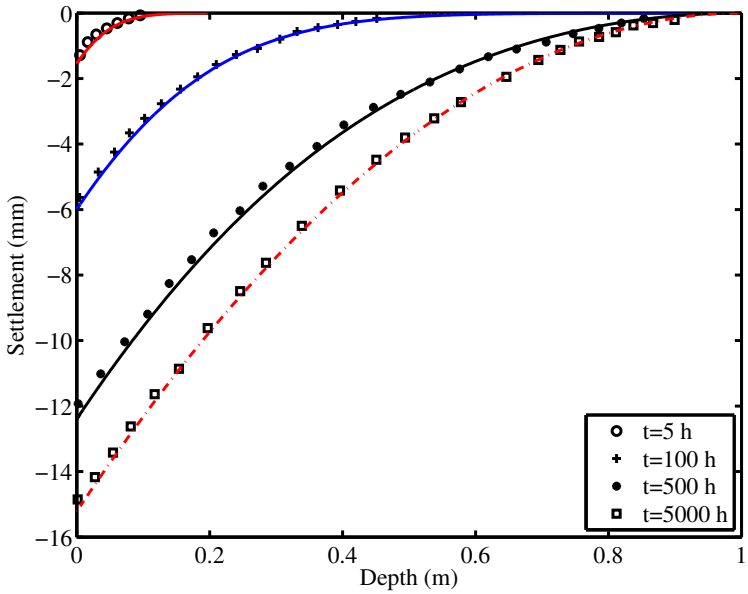

(b)

Figure 5.1: Comparison of capillary pressure and displacement due to infiltration: symbols are for results in Zhou and Rajapakse (1998) and solid line are for the present model.

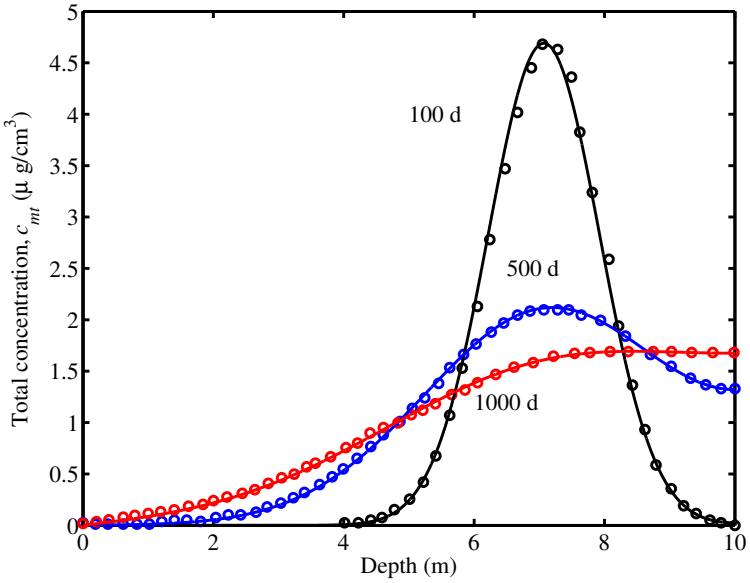

Figure 5.2: Comparison of total concentration distribution at three time instants (100, 500, 1000 days): circles are for results in Zhou and Rajapakse (1998) and solid line are for the present model.

where p_{cr} is the reference capillary pressure and L is thickness of CCL. The initial uniform net mean stress is σ_0^*.

At top of CCL, a time-dependent temperature increase is imposed. It has a rapid increase followed by a steady state, and finally decreases gradually to zero.

$$T(z=0,t)=\begin{cases} t/t_1\Delta T, & 0\le t\le t_1 \\ \Delta T, & t_1\le t\le t_2 \\ \left[1-(t-t_2)/(t_3-t_2)\right]\Delta T, & t_2\le t\le t_3 \\ 0, & t\ge t_3. \end{cases}, \tag{5.69}$$

where ΔT is the maximum temperature increase and $t_i (i=1,2,3)$ is the time instants used to describe the change of temperature due to waste degradation.

The waste filling process is approximated as a linear ramp loading (Peters and Smith, 2002)

$$\sigma_v(z=0,t)=\begin{cases} t/t'\Delta Q, & 0\le t\le t' \\ \Delta Q. & t\ge t' \end{cases}, \tag{5.70}$$

where ΔQ is the maximum surcharge and t' is the time taken by landfill to reach its full capacity.

The impervious geomembrane dictates that liquid water mass flux equals zero, $q_l(z = 0, t) = 0$ and pore air pressure gradient vanishes, i.e., $\partial p_a(z = 0, t)/\partial z = 0$.

VOCs vapor can permeate through non-porous geomembrane at a molecular level and the process occurs at three steps (Pierson and Barroso, 2002; Stark and Choi, 2005). First, the permeant dissolves and partitions at the geomembrane surface. Second, it diffuses through the geomembrane in the direction of lower chemical potential. Finally, it evaporate or desorb onto the ambient receiving medium.

The VOCs diffuse through the thin (relative to CCL) geomembrane at the top boundary, and the solute flux can be approximated as

$$f(0^-, t) = -P_G \frac{c_l(0^+, t) - c_0}{h}, \tag{5.71}$$

where c_0 is the concentration of VOCs in liquid phase at top side of the geomembrane, which is of the thickness h. P_G is the product of diffusion coefficient for solute in the geomembrane (D_G) and the partitioning coefficient of solute between the geomembrane and adjacent fluid (S_G) (Lewis et al., 2009). A good contact between the geomembrane and CCL is assumed and $c_l(0^+, t)$ is same as the concentration at the bottom surface of the geomembrane consequently. The flux in the CCL at the interface is

$$f(0^+, t) = -\theta D_{lc} \frac{\partial c_l}{\partial z}(0^+, t). \tag{5.72}$$

Equating Eq. (5.71) and Eq. (5.72) (Peters and Smith, 2002), a Neumann boundary condition for solute concentration can be obtained as

$$\frac{\partial c_l}{\partial z}(0, t) - \frac{P_G}{\theta(0^+, t) h D_{lc}} c_l(0, t) = -\frac{P_G}{\theta(0^+, t) h D_{lc}} c_0. \tag{5.73}$$

At the bottom of CCL, the second leachate collecting system is often made of gravel material with high conductivity. Therefore, it is assumed that liquid drains freely and the gradient of solute concentration is assumed to be zero (Danckwerts boundary condition, Danckwerts (1953)), although different interpretations of this condition are possible (e.g., Barry and Sposito (1988)):

$$\begin{aligned} &p_c(z = L, t) = p_c(z = L, t = 0), \\ &p_a(z = L, t) = 1 \text{ bar}, \\ &T(z = L, t) = T_0, \\ &\frac{\partial c_l}{\partial z} = 0. \end{aligned} \tag{5.74}$$

The model parameters employed in the following analyses are based on recent studies of solute transport in clay liners (Foose, 2002; Lewis et al., 2009). The values of parameters used are shown in Table 5.1-5.4 unless stated otherwise.

The coupled non-linear equations are solved numerically by the FEM scheme. The codes were constructed using the multiphysics modeling software package COMSOL 3.5a COMSOL (2010), which is capable of solving equations (5.6), (5.53) to (5.56) and (5.58) simultaneously. Consequently, the two-way coupling of moisture and VOCs transport is implemented. In the FEM analysis, the system was discretized into unstructured Lagrange-linear elements with a maximum global element size of 10^{-2} m, and maximum local element size at the end boundaries (where the most rapid changes occur) of 10^{-3} m. The time step was set to 10^{-2} year in the simulation of the first 2 years. Then, it was increased to 1 year in the following simulation period. The mesh size and time step have been tested so that the following numerical simulation results are independent of them.

5.4.2 Results and discussion

Based on the present model, effects of variety of factors involved in the multi-phase moisture and VOC transport on VOC transit are examined in this section. The governing equations (GEs) and constitutive relationship functions (CRFs) employed in the various models are

Table 5.1: Soil parameters employed in numerical simulations

Parameter	Value
Concentration in landfill, c_0	100 mg/dm^3
Maximum waste loading, ΔQ	2×10^5 Pa
Loading period, t'	2 yr
Thickness of geomembrane, h (Lewis et al., 2009)	0.0015 m
Mass transfer coefficient of geomembrane, P_G (Lewis et al., 2009)	4×10^{-11}m^2/s
Thickness of CCL, L	1 m
Acceleration due to gravity, g	9.81 m/s^2
Initial compressive stress, σ_{v0} (Zhou and Rowe, 2005)	-200 kPa
Reference capillary pressure, p_{cr} (Zhou and Rowe, 2005)	-2.8 kPa
Earth pressure coefficient at rest, K_0	0.9
Temperature coefficient of water retention, C_ψ (Scanlon and Milly, 1994)	-0.0068 K^{-1}
Temperature increase at top boundary, ΔT	30 K
Initial temperature in liner, T_0	288 K
Other temperature associative parameters, $t_i (i = 1, 2, 3)$	1 yr, 10 yr and 10 yr respectively

Table 5.2: Soil components properties

Parameter	Value
Soil solids	
Density of the solid phase, ρ_s	2.7×10^3 kg/m^3
Specific heat capacity, $C_{p,s}$ (Lewis et al., 2009)	800 J kg^{-1} K^{-1}
Soil liquid water	
Initial density of pore water, ρ_{l0} (Lewis et al., 2009)	0.998×10^3 kg/m^3
Phenominlogical coefficient to relate liquid flux to temperature, D_T (Zhou and Rajapakse, 1998)	2.7×10^{-10} m^2/(s K)
Reduction factor of surface tension due to VOC, γ_m/γ_w	0.8
Specific heat capacity, $C_{p,f}$ (Lewis et al., 2009)	4180 J kg^{-1} K^{-1}
Soil air	
Henry's solubility coefficient for air, H (Lewis et al., 2009)	0.02
VOCs transport	
Specific gas constant for VOC, R_{VOC}	8.3144621/MW J/(kg K), where MW is molar weight of VOC (78.114 g/mol for Benzene)
Partitioning coefficient, H_{sg}	1.8×10^{-3} m^3/kg
Longitudinal mechanical dispersion coefficient for liquid phase, α_{Lw}	0.004 m

Table 5.3: State surface functions for unsaturated soil (Zhou and Rowe, 2005)

void ratio	a_e	b	c	d	α_T (K^{-1})
	5.5	-0.4	-0.25	0.02	2.5×10^{-4}
water volumetric content	a′	b′	c′	d′	
	0.9	-0.8	-1×10^{-8}	1×10^{-5}	

Table 5.4: Liquid mobility in unsaturated soil (Zhou and Rowe, 2005)

Hydraulic conductivity	A (m/s)	S_{lu}	α_k
	6.0×10^{-14}	0.05	5
Conductivity of air	B (m/s)	μ_a (N·s/m^2)	β_k
	1.8×10^{-12}	1.0×10^{-5}	4

summarized in Table 5.5. The boundary conditions (BCs) and initial conditions (ICs) are provided by Eqs. (5.68-5.70) and Eqs. (5.73-5.74).

5.4.2.1 Geometric non-linearity and soil velocity

One of the important features of the present model (FD) is the finite deformation modeling with soil velocity being included. Two other models were constructed for comparison. First one is small deformation model (SD1) without soil velocity occurrence in both mass flux and linear average velocity of liquid phase v_{li} and v_{ai}; The second one (SD2) is small deformation model but considering soil velocity.

As illustrated in Fig. 5.3, small deformation model underestimates transport of contaminant. Relative to the finite deformation model (FD), small deformation models, SD1 and SD2 assume that the thickness of soil is unchanging even though the consolidation does cause a soil contraction. As a result, the in artificially thicker soil column it takes the VOCs a longer time to break through. In the previous literature on non-isothermal moisture transport in deformable soil, solid velocity is conventionally neglected based on the assumption that it is relatively small. However, Fig. 5.3 demonstrates that including soil mobility can accelerate VOCs transport. The reason is that the VOCs flux term related to solid particle carrying, $(1-n)\rho_s v_s S$ may become non-negligible because of the relatively large solid grain

Table 5.5: Governing equations (GEs) and constitutive relationship functions (CRFs) used in the models

Model	GEs	CRFs	Note
FD, WVD1	Eq. (5.6), Eqs. (5.53-5.56) and Eq. (5.58)	Eqs. (5.12-5.14), Eq. (5.22, Eqs. (5.33-5.35), Eq. (5.38), Eqs. (5.44-5.47), Eqs. (5.63-5.67 and Eqs. (5.24, 5.25, 5.48)	All GEs are solved simultaneously
WVD2	Eq. (5.6), Eqs. (5.53-5.56) and Eq. (5.58)	Eqs. (5.12-5.14), Eq. (5.22, Eqs. (5.33-5.35), Eq. (5.38), Eqs. (5.44-5.47), Eqs. (5.63-5.67 and Eqs. (5.18-5.19)	Eqs. (5.53-5.55) and Eq. (5.58) are coupled while Eq. (5.56) can be solved separately
SD1	Eq. (5.6), Eqs. (5.53-5.56) and Eq. (5.58)	Eqs. (5.12-5.14), Eq. (5.22, Eqs. (5.33-5.35), Eq. (5.38), Eqs. (5.44-5.47), Eqs. (5.63-5.67 and Eqs. (5.24, 5.25, 5.48)	E'_{ij} are used
SD2	Eq. (5.6), Eqs. (5.15, 5.27, 5.36 and 5.40)	Eqs. (5.12-5.14), Eq. (5.22, Eqs. (5.33-5.35), Eq. (5.38), Eqs. (5.44-5.47), Eqs. (5.63-5.67 and Eqs. (5.24, 5.25, 5.48)	$M = 1$ in Eq. (5.6)

density with even a small solid velocity. Therefore, the present model is not only theoretically consistent because it considers the soil velocity, but it also accommodates the geometric non-linearity.

Since the advective VOCs flux is significant (especially when temperature increase, ΔT is higher), the VOCs concentration level at exiting boundary may exceed that in its vicinity. With the temperature decrease and advective flux gradually vanish, the VOCs concentration at bottom boundary will see a gradual decrease due to dispersion of mass to the adjacent zone until a steady state is reached.

5.4.2.2 Two-way coupling coefficient D^* and ρ_{da}

The water vapor diffusivity, D^* can be calculated by using Eqs. (5.24, 5.25, 5.48). Here, we name it as method WVD1. This approach requires two-way coupling of moisture, heat and VOCs transport to provide real time value of VOCs concentration when determining D^*. Alternatively, D^* can be approximated by Eq. (5.18) and Eq. (5.19) (method WVD2), in which way solving of VOCs transport can be decoupled and be solved sequentially after moisture and heat transport. However, Fig. 5.4 demonstrates that WVD2 overestimates

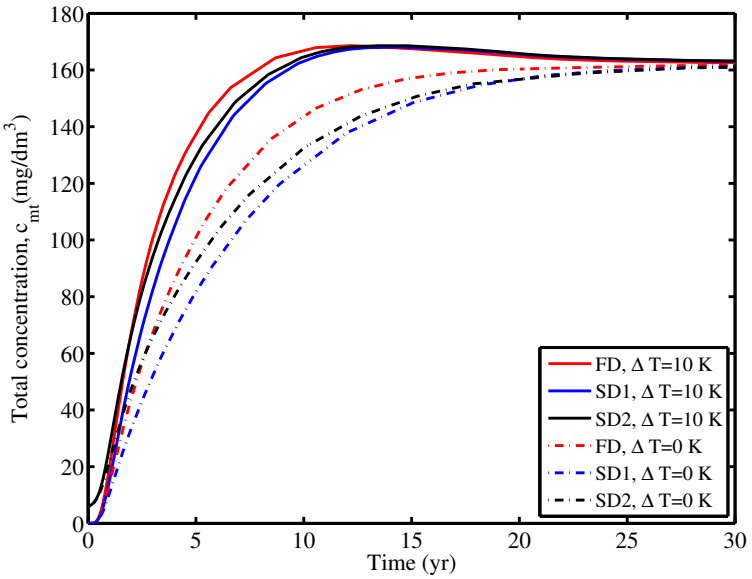

Figure 5.3: Effect of geometric non-linearity and soil velocity on VOCs breakthrough.

water vapor diffusivity and predict a faster contaminant migration as a result. For either WVD1 or WVD2, the final levels of total VOC concentration are identical regardless the temperature gradient. As explained in the last section, the concentration level at existing boundary undergoes a decrease especially for a greater temperature gradient. There is a un-smooth part on the curve of WVD2, $\Delta T = 30$ K due to the numerical dispersion. This is probably caused by the relatively larger ratio of advection to effective dispersion in the advection-dispersion-equation. On the other hand, either considering VOCs or not when calculating density of dry air, ρ_{da} does not make discernible difference on the VOCs transport progress (not shown here).

5.4.2.3 Total VOCs concentration constitution

In the literature, there is no concenus on the expression of total VOCs concentration in un-saturated soil. While Thomas and Ferguson (1999) only focused on retention of VOCs in aqueous and gaseous phase, most researchers agree that the VOCs also reside in solid phase due to adsorption. However, different opinion exists on its description. For example, some described the absorbed concentration as originating from either aqueous phase or gaseous

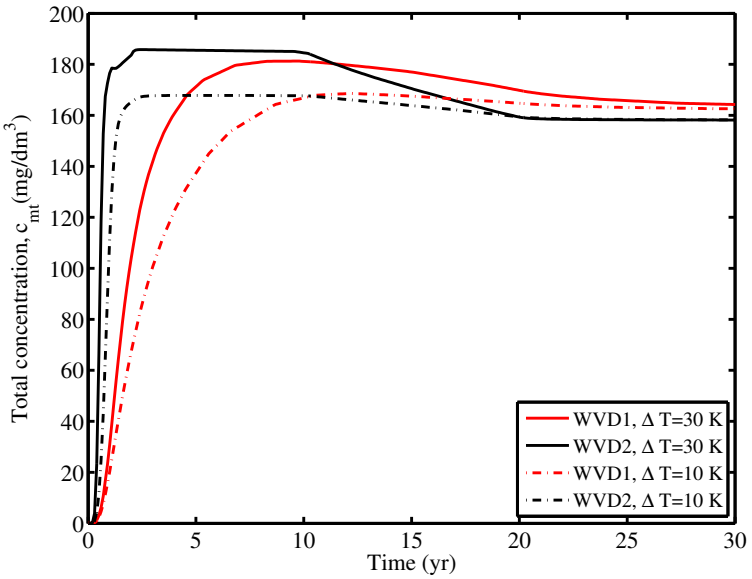

Figure 5.4: Effect of VOCs presence on water vapor diffusivity.

phase (Lin and Hildemann, 1995; Nassar and Horton, 1999), but others included adsorption from both phases (Poulsen et al., 1998; Shan and Stephens, 1995).

Fig. 5.5 illustrates the liquid phase concentration and total concentration level at bottom boundary. 'ExpCtoti' represents three kinds of model: expression of total concentration used in the present model (i = 1), excluding contribution of adsorption from gaseous phase (i = 2) and no adsorption onto solid phase (i = 3), respectively. As expected, more complete adsorption mechanism results in slower VOCs transport due to the retardation effect. The different final total concentrations in Fig. 5.5(b) are caused by their different constitution. Higher temperature increase at top boundary leads to larger carrying capacity of both liquid and gaseous phase. Consequently, the migration of VOCs is accelerated. More discussions on influence of temperature increase will be presented in the later section.

5.4.2.4 Longitudinal mechanical dispersion (D_{hw} and D_{hg})

Based on the assumption that the pore water flow velocity in fine-grained soils due to mechanical consolidation is low (less than 10^{-6} m/s), mechanical dispersion can be neglected (Acar and Haider, 1990; Lewis et al., 2009). However, Zhang et al. (Zhang et al., 2012) have confirmed that mechanical dispersion could double the final advective emission at bottom of

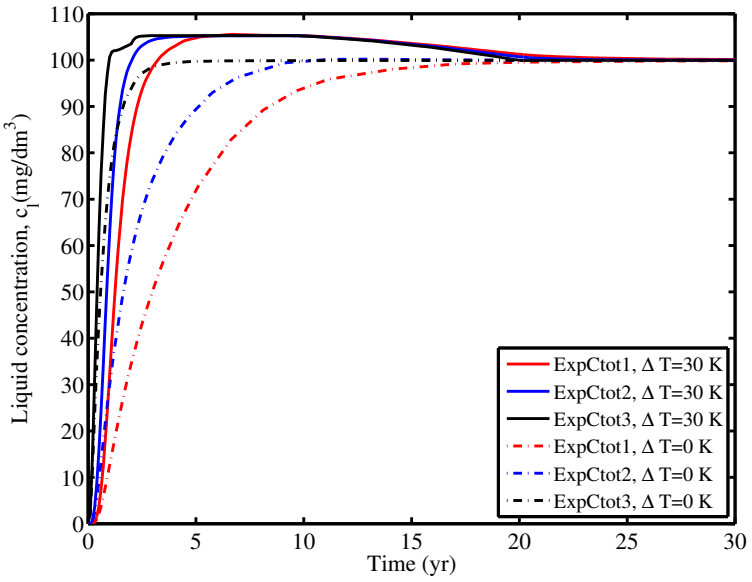

(a) Liquid phase concentration level at bottom boundary

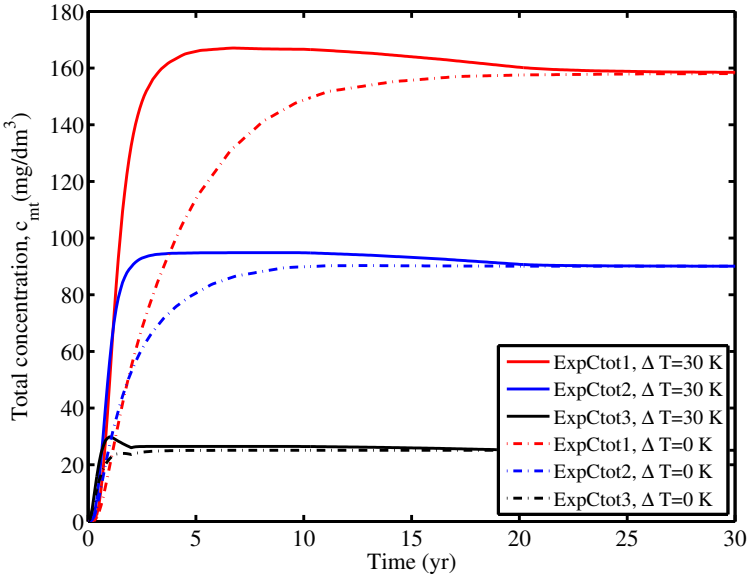

(b) Total concentration level at bottom boundary

Figure 5.5: Comparison of VOCs concentration expression on its breakthrough

a partially saturated CCL when the molecular diffusion decreases within a practical range. In this section, the effect of mechanical dispersion on VOCs transport will be re-examined in a multi-phase frame.

The transport parameter of mechanical dispersivity is often obtained experimentally by fitting measured breakthrough curves with analytical solutions of the advection-dispersion equation. Yule and Gardner Yule and Gardner (1978) conducted a experiment using a vertical unsaturated plainfield sand column and measured the longitudinal dispersion coefficient, $\alpha_{Lw} = 0.216$ m. However, there is the so-called dispersion-scale effect, namely, the dispersivity changes with the distance over which contaminants travel. A good first approximation is to use a value of one-tenth of the transport distance for the longitudinal dispersivity if there is a lack of enough information (Anderson, 1984). In this section, $\alpha_{Lw} = 0.1$ m was used to examine the effect of mechanical dispersion.

Fig. 5.6 illustrates the distribution of VOCs dispersive flux in both aqueous and gaseous phase. For the unsaturated soil considered here, the gas molecular diffusion coefficient is four orders greater than the gas mechanical dispersivity coefficient, so the mechanical dispersive flux is too small compared with the dominant diffusion flux through gas phase (which is at the scale of 10^{-6} g/(m^2 s)). Therefore, the mechanical dispersion in unsaturated CCL in the considered cases can be neglected (shown in Fig. 5.7).

5.4.2.5 Mechanical consolidation and temperature increase

When the waste filling is exerted on the top boundary, the clay liner will experience a mechanical consolidation, which can cause advective pore flow and thus is expected to help accelerate VOCs transport. To investigate the contribution of mechanical consolidation in the unsaturated CCL, the present model was reduced to 'NoSV', which does not integrate variation of vertical stress. Comparison was made between the NoSV and the present model (Model Cpt). Fig. 5.8a and the case with $\Delta T = 30$ K in Fig. 5.8b demonstrate that including of vertical compressive stress, namely, the mechanical consolidation seems to predict a slower VOCs transport, which is contrary to the conclusion for VOCs transport (in solid-lquid phases) within a saturated or partially saturated CCL. This can be explained from

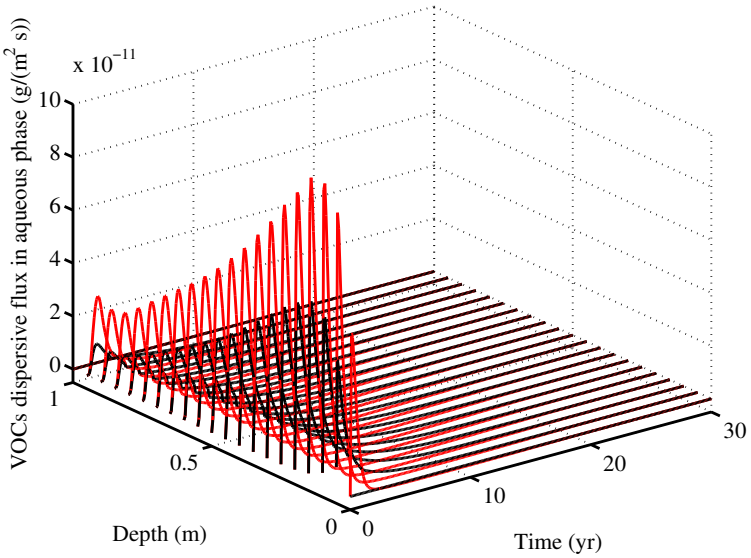

(a) Aqueous phase flux

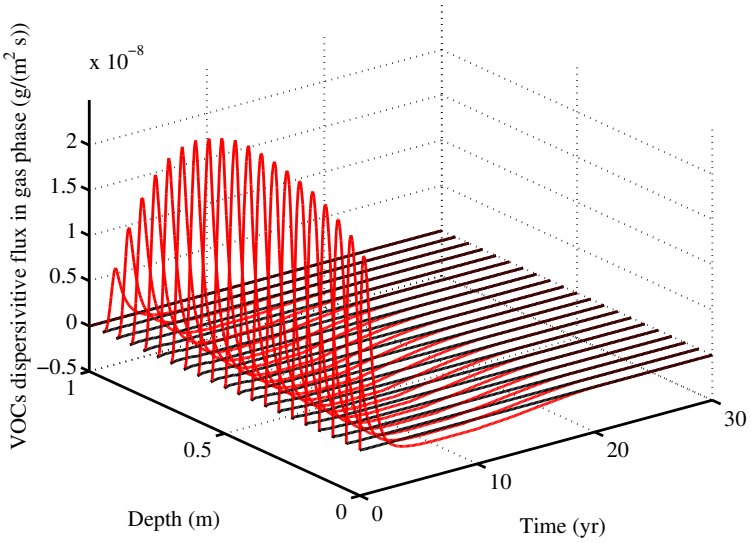

(b) Gaseous phase flux

Figure 5.6: Distribution of VOCs dispersive flux (α_{Lw} = 0.1 m): red curves for T = 30 K and black curves for T = 0 K.

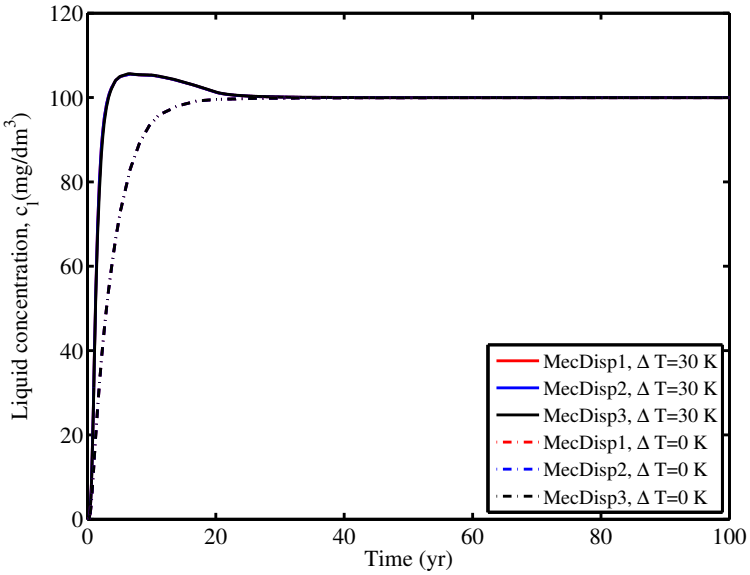

Figure 5.7: Effect of mechanical dispersion on VOCs breakthrough (α_{Lw} = 0.1 m).

two aspects: Firstly, the gaseous phase diffusion dominates the transport progress for unsaturated soil instead of the advective flux in liquid phase for saturated soil; Secondly, the mechanical consolidation compacts the soil column and reduces the effective gas diffusion due to the lower void ratio. For the cases with greater temperature gradient, the effect of soil contraction due to mechanical consolidation is balanced by the swelling due to heating. Thus, the influence made by mechanical consolidation on VOCs movement is limited. Further, both the liquid phase concentration and total concentration of VOCs corresponding to higher temperature gradient have higher peak values than the cases with lower temperature gradient. This phenomenon is a result of the advection transport due to the higher temperature. Gradually, the concentration level decreases with the decreasing of advective VOCs fluxes. In Fig. 5.8b, the total concentration for 'Model Cpt' surpasses that of 'Model NoSV' for cases with ΔT = 0 K after a certain period. This is because the capacity of 'carrying VOCs' for a unit volume of solid is greater than unit value of pore fluid. When the soil is compressed and void fluid is expelled, a unit volume of soil can carry more VOCs. Therefore, the mechanical consolidation does not always lead to a faster transit of multi-phase VOCs within an unsaturated soil.

Fig. 5.9 indicates that the lower pre-consolidation stress and the consequent larger initial void can speed the VOCs migration. Three pre-consolidation stress levels are assumed here: PS1 with $\sigma_{v0} = -200$ kPa, PS2 with $\sigma_{v0} = -100$ kPa and PS3 with $\sigma_{v0} = -50$ kPa. The values of associative initial void ratio are 0.628 (0.646), 0.775 (0.815) and 0.920 (0.980) respectively. The values in brackets are the void ratio at the soil column bottom (the void ratio increase linearly from top to bottom due to the distribution of initial capillary pressure).

Higher temperature increase on top boundary was observed to significantly shorten the breakthrough time required. This is because the gaseous phase VOCs diffusion increases rapidly with the increasing temperature and dominates the migration progress.

5.4.2.6 Contribution of gaseous phase

In this section, a model (NoGas) without VOCs flux in gaseous phase was established by letting $H_{gl} = H_{sg} = 0$ in the present model. As illustrated in Fig. 5.10, incorporating gas phase can dramatically speed up migration of VOCs for both non-isothermal and isotermal soil. This is attributed to the huge magnitude of diffusion coefficient (at scale of 10^{-7} m^2/s) for gaseous phase relative to that for fluid aqueous phase (at scale of 10^{-10} m^2/s).

Since gaseous phase diffusion depends on the gas saturation, $S_g = 1 - \theta/n$, a parametric study on initial volume water content, θ was performed to examine the influence of degree of saturation on VOCs migration. Fig. 5.11 shows that lower water content leads to a faster VOCs migration in unsaturated soil predicted by three-phase transport model, which is opposite to the trend for two-phase (aqueous and solid phases) model (NoGas). In the former model, lower water content means larger gas saturation and larger gas flow pathway. In contrast, it results in smaller pore water fraction which decrease the VOCs transit for model NoGas.

Therefore, gaseous phase transport is proved to play a crucial role in the VOCs transport within unsaturated soil. It helps answer the question why the field-measured VOCs move far faster than that predicted by a conventional liquid-phase diffusion model.

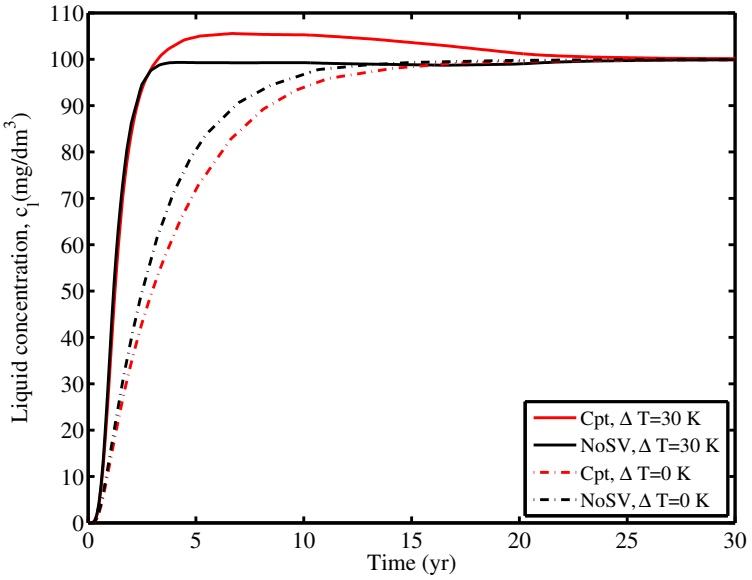

(a) Liquid concentration level at bottom boundary

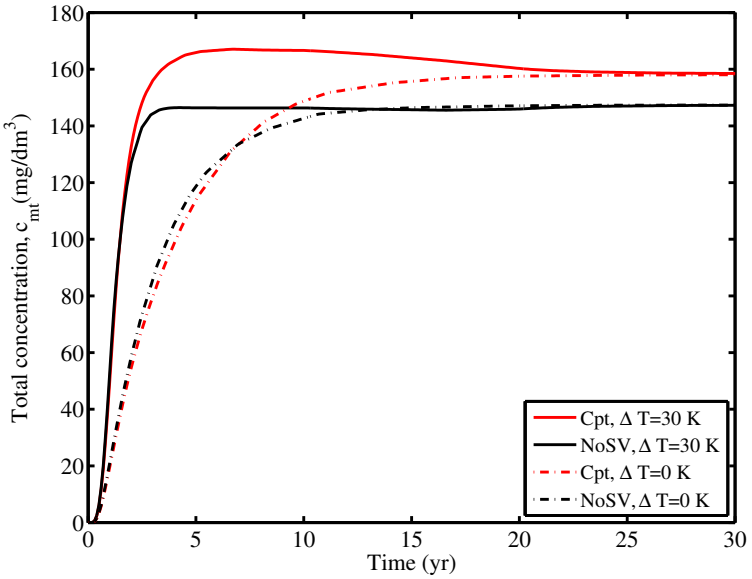

(b) Total concentration level at bottom boundary

Figure 5.8: Effect of mechanical consolidation and temperature increase on VOCs breakthrough.

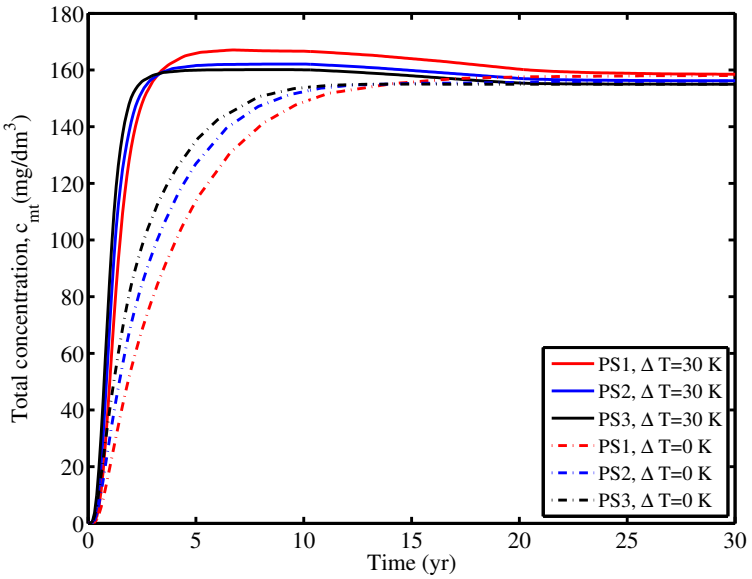

Figure 5.9: Effect of pre-consolidation stress (σ_{v0}) and temperature increase on VOCs breakthrough ($a' = 0.9$).

5.5 Summary

A one-dimensional non-isothermal multi-phase (solid, liquid and gas phases) moisture and VOCs transport model in finite deformation frame has been developed. The model proposed in this study is theoretically consistent for a deformable soil column because it integrates the soil velocity in the linear average pore fluid (liquid and gas) velocities and considers the mass flux due to soil motion. Based on the present model, benzene migration in solid waste landfill CCL under top surcharge and temperature gradient condition was investigated. The following conclusions can be drawn:

1. The assumption of small deformation (neglecting change of soil column) and ignoring soil velocity leads to underestimated VOCs transport;

2. A two-way coupling approach is essential for getting an accurate evaluation of water vapor diffusion coefficient with presence of VOCs vapor;

3. Considering adsorption of VOCs from both gas and fluid phase in the composition of total concentration can considerably slow down the migration progress;

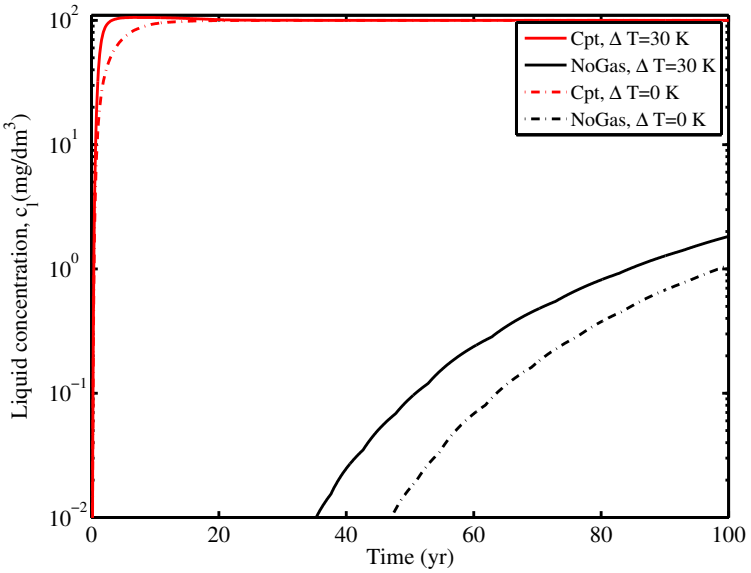

Figure 5.10: Contribution of gaseous phase on VOCs breakthrough ($a' = 0.9$).

4. The mechanical dispersion of fluid phase can be neglected because the related VOCs dispersion fluxes are several orders of magnitude lower than the diffusion flux in gas phase.

5. Shrinking of pores in soil due to mechanical consolidation helps to prevent VOCs breakthrough while higher environmental temperature will increase the VOCs gas phase diffusion, which plays a predominant role in unsaturated soil liner.

6. Furthermore, deviation of saturation from fully saturated state can significantly speed up the VOCs motion. Therefore, a non-isothermal multi-phase moisture and VOCs transport modeling is essential for obtaining a reliable prediction of VOCs migration in unsaturated soil liner exposed to condition of heating and compression.

5.6 Appendices

5.6.1 Appendix 5A: Coefficients used in governing equations

Coefficients E_{ij} ($i = 1 \sim 4$, $j = 1 \sim 5$) used in equations (5.53) to (5.56) are described as follows:

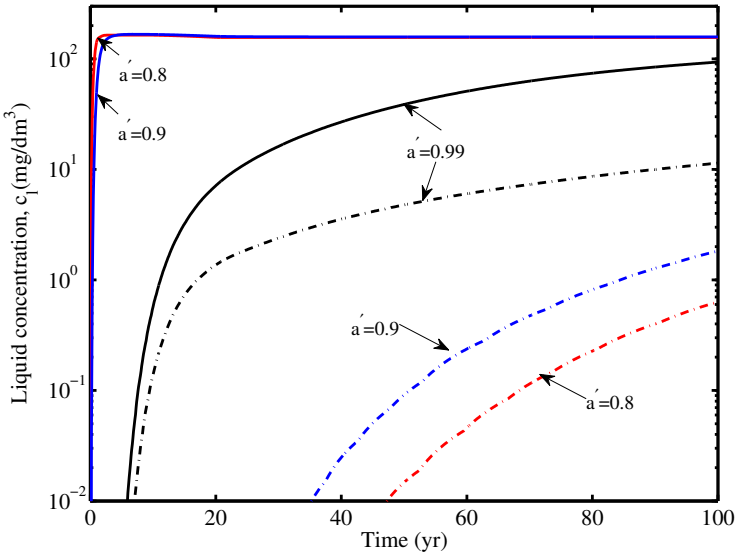

Figure 5.11: Effect of water content on VOCs breakthrough: solid line is the present model and dashdot line is for the NoGas model.

Finite deformation, i.e., $M \neq 1$:

$$E_{11} = \frac{1+2K_0}{3}\left(\frac{1+e}{1+e_0}\left(\rho_l - \rho_v\right)\frac{\partial\theta}{\partial\sigma^*} + \frac{1}{1+e_0}\left(\rho_l\theta + \rho_v - \rho_v\theta\right)\frac{\partial e}{\partial\sigma^*}\right) \tag{5.75}$$

$$\begin{aligned} E_{12} = {} & \theta\frac{1+e}{1+e_0}\frac{\partial\rho_l}{\partial p_c} + \left(\frac{e}{1+e_0} - \theta\frac{1+e}{1+e_0}\right)\frac{\partial\rho_v}{\partial p_c} \\ & + \frac{1+e}{1+e_0}\left(\rho_l - \rho_v\right)\frac{\partial\theta}{\partial p_c} + \frac{1}{1+e_0}\left(\rho_l\theta + \rho_v - \rho_v\theta\right)\frac{\partial e}{\partial p_c} \end{aligned} \tag{5.76}$$

$$E_{13} = \theta\frac{1+e}{1+e_0}\frac{\partial\rho_l}{\partial p_a} + \left(\frac{e}{1+e_0} - \theta\frac{1+e}{1+e_0}\right)\frac{\partial\rho_v}{\partial p_a} + E_{11}\frac{3}{1+2K_0} \tag{5.77}$$

$$\begin{aligned} E_{14} = {} & \theta\frac{1+e}{1+e_0}\frac{\partial\rho_l}{\partial T} + \left(\frac{e}{1+e_0} - \theta\frac{1+e}{1+e_0}\right)\frac{\partial\rho_v}{\partial T} \\ & + \frac{1+e}{1+e_0}\left(\rho_l - \rho_v\right)\frac{\partial\theta}{\partial T} + \frac{1}{1+e_0}\left(\rho_l\theta + \rho_v - \rho_v\theta\right)\frac{\partial e}{\partial T} \end{aligned} \tag{5.78}$$

$$E_{21} = \frac{1+2K_0}{3}\left(-(1-H)\rho_{da}\frac{1+e}{1+e_0}\frac{\partial\theta}{\partial\sigma^*} + \frac{\rho_{da}}{1+e_0}\left[1-(1-H)\theta\right]\frac{\partial e}{\partial\sigma^*}\right) \tag{5.79}$$

$$\begin{aligned} E_{22} = &\left(\frac{e}{1+e_0} - (1-H)\theta\frac{1+e}{1+e_0}\right)\frac{\partial\rho_{da}}{\partial p_c} - (1-H)\rho_{da}\frac{1+e}{1+e_0}\frac{\partial\theta}{\partial p_c} \\ &+ \frac{\rho_{da}}{1+e_0}\left[1-(1-H)\theta\right]\frac{\partial e}{\partial p_c} \end{aligned} \tag{5.80}$$

$$E_{23} = \left(\frac{e}{1+e_0} - (1-H)\theta\frac{1+e}{1+e_0}\right)\frac{\partial\rho_{da}}{\partial p_a} + E_{21}\frac{3}{1+2K_0} \tag{5.81}$$

$$\begin{aligned} E_{24} = &\left(\frac{e}{1+e_0} - (1-H)\theta\frac{1+e}{1+e_0}\right)\frac{\partial\rho_{da}}{\partial T} - (1-H)\rho_{da}\frac{1+e}{1+e_0}\frac{\partial\theta}{\partial T} \\ &+ \frac{\rho_{da}}{1+e_0}\left[1-(1-H)\theta\right]\frac{\partial e}{\partial T} \end{aligned} \tag{5.82}$$

$$E_{31} = \frac{1+2K_0}{3}\left(E_{311}\frac{\partial e}{\partial\sigma^*} + E_{312}\frac{\partial\theta}{\partial\sigma^*}\right) \tag{5.83}$$

$$\begin{aligned} E_{311} = &L_0\frac{\rho_v}{1+e_0} - L_0\frac{\rho_v\theta}{1+e_0} + W\rho_l\frac{\theta}{1+e_0} + C_lT\rho_l\frac{\theta}{1+e_0} \\ &+ C_vT\frac{\rho_v}{1+e_0} - C_vT\frac{\rho_v\theta}{1+e_0} + C_{da}T\frac{\rho_{da}}{1+e_0}[1-(1-H)\theta] \end{aligned} \tag{5.84}$$

$$\begin{aligned} E_{312} = &-L_0\frac{\rho_v(1+e)}{1+e_0} + W\rho_l\frac{1+e}{1+e_0} + C_lT\rho_l\frac{1+e}{1+e_0} \\ &- C_vT\frac{\rho_v(1+e)}{1+e_0} - C_{da}T(1-H)\rho_{da}\frac{1+e}{1+e_0} \\ &+ \rho_l\theta\frac{1+e}{1+e_0}\frac{\partial W}{\partial\theta} \end{aligned} \tag{5.85}$$

$$\begin{aligned} E_{32} = &E_{321}\frac{\partial\rho_v}{\partial p_c} + E_{322}\frac{\partial\rho_l}{\partial p_c} + C_{da}T\left[\frac{e}{1+e_0} - (1-H)\theta\frac{1+e}{1+e_0}\right]\frac{\partial\rho_{da}}{\partial p_c} \\ &+ E_{311}\frac{\partial e}{\partial p_c} + E_{312}\frac{\partial\theta}{\partial p_c} \end{aligned} \tag{5.86}$$

$$E_{321} = L_0\frac{e}{1+e_0} - L_0\frac{(1+e)\theta}{1+e_0} + C_vT\frac{e}{1+e_0} - C_vT\frac{(1+e)\theta}{1+e_0} \tag{5.87}$$

$$E_{322} = W\frac{(1+e)\theta}{1+e_0} + C_lT\frac{(1+e)\theta}{1+e_0} + \rho_l\theta\frac{1+e}{1+e_0}\frac{\partial W}{\partial \rho_l} \tag{5.88}$$

$$\begin{aligned} E_{33} =& E_{321}\frac{\partial \rho_v}{\partial p_a} + E_{322}\frac{\partial \rho_l}{\partial p_a} + C_{da}T\left[\frac{e}{1+e_0} - (1-H)\theta\frac{1+e}{1+e_0}\right]\frac{\partial \rho_{da}}{\partial p_a} \\ &+ E_{31}\frac{3}{1+2K_0} \end{aligned} \tag{5.89}$$

$$\begin{aligned} E_{34} =& E_{321}\frac{\partial \rho_v}{\partial T} + E_{322}\frac{\partial \rho_l}{\partial T} + C_{da}T\left[\frac{e}{1+e_0} - (1-H)\theta\frac{1+e}{1+e_0}\right]\frac{\partial \rho_{da}}{\partial T} \\ &+ E_{311}\frac{\partial e}{\partial T} + E_{312}\frac{\partial \theta}{\partial T} + C_s\frac{\rho_s}{1+e_0} \\ &+ \left[C_l\rho_l\theta\frac{1+e}{1+e_0} + C_v\rho_v\left(\frac{e}{1+e_0} - \theta\frac{1+e}{1+e_0}\right)\right] + C_{da}\frac{\rho_{da}}{1+e_0}[e-(1-H)\theta(1+e)] \end{aligned} \tag{5.90}$$

$$\begin{aligned} E_{41} =& \frac{1+2K_0}{3}\left(E_{411}\frac{\partial e}{\partial \sigma^*} + E_{412}\frac{\partial \theta}{\partial \sigma^*} + \frac{\rho_s}{1+e_0}c_l\frac{\partial H_{sl}}{\partial \sigma^*}\right. \\ &\left. + \frac{1}{1+e_0}\rho_s c_l\frac{\partial\left(H_{sg}H_{gl}\right)}{\partial \sigma^*} + \frac{\partial \xi}{\partial z}(n-\theta)\,c_l\frac{\partial H_{gl}}{\partial \sigma^*}\right) \end{aligned} \tag{5.91}$$

where,

$$E_{411} = \frac{\theta}{1+e_0}c_l + H_{gl}c_l\frac{1-\theta}{1+e_0} \tag{5.92}$$

$$E_{412} = \frac{\partial \xi}{\partial z}c_l - H_{gl}c_l\frac{\partial \xi}{\partial z} \tag{5.93}$$

$$\begin{aligned} E_{42} =& E_{411}\frac{\partial e}{\partial p_c} + E_{412}\frac{\partial \theta}{\partial p_c} + \frac{\rho_s}{1+e_0}c_l\frac{\partial H_{sl}}{\partial p_c} \\ &+ \frac{\rho_s}{1+e_0}c_l\frac{\partial\left(H_{sg}H_{gl}\right)}{\partial p_c} + \frac{\partial \xi}{\partial z}(n-\theta)\,c_l\frac{\partial H_{gl}}{\partial p_c} \end{aligned} \tag{5.94}$$

$$E_{43} = \frac{3}{1+2K_0} E_{41} \tag{5.95}$$

$$\begin{aligned} E_{44} =& E_{411}\frac{\partial e}{\partial T} + E_{412}\frac{\partial \theta}{\partial T} + \frac{\rho_s}{1+e_0} c_l \frac{\partial H_{sl}}{\partial T} \\ &+ \frac{\rho_s}{1+e_0} c_l \frac{\partial \left(H_{sg} H_{gl}\right)}{\partial T} + \frac{\partial \xi}{\partial z}(n-\theta)\, c_l \frac{\partial H_{gl}}{\partial T} \end{aligned} \tag{5.96}$$

$$E_{45} = \frac{\rho_s}{1+e_0}\left(H_{sl} + H_{sg}H_{gl}\right) + \theta\frac{\partial \xi}{\partial z} + (n-\theta)\frac{\partial \xi}{\partial z} H_{gl} \tag{5.97}$$

Small strain deformation, i.e., $M = 1$:

$$E'_{11} = \frac{1+2K_0}{3}\left[(\rho_l - \rho_v)\frac{\partial \theta}{\partial \sigma^*} + \rho_v (1+e)^{-2}\frac{\partial e}{\partial \sigma^*}\right] \tag{5.98}$$

$$E'_{12} = \theta\frac{\partial \rho_l}{\partial p_c} + (n-\theta)\frac{\partial \rho_v}{\partial p_c} + (\rho_l - \rho_v)\frac{\partial \theta}{\partial p_c} + \rho_v (1+e)^{-2}\frac{\partial e}{\partial p_c} \tag{5.99}$$

$$E'_{13} = \theta\frac{\partial \rho_l}{\partial p_a} + (n-\theta)\frac{\partial \rho_v}{\partial p_a} + E'_{11}\frac{3}{1+2K_0} \tag{5.100}$$

$$E'_{14} = \theta\frac{\partial \rho_l}{\partial T} + (n-\theta)\frac{\partial \rho_v}{\partial T} + (\rho_l - \rho_v)\frac{\partial \theta}{\partial T} + \rho_v (1+e)^{-2}\frac{\partial e}{\partial T} \tag{5.101}$$

$$E'_{21} = \frac{1+2K_0}{3}\left[-(1-H)\rho_{da}\frac{\partial \theta}{\partial \sigma^*} + \rho_{da}(1+e)^{-2}\frac{\partial e}{\partial \sigma^*}\right] \tag{5.102}$$

$$E'_{22} = [n-(1-H)\theta]\frac{\partial \rho_{da}}{\partial p_c} - (1-H)\rho_{da}\frac{\partial \theta}{\partial p_c} + \rho_{da}(1+e)^{-2}\frac{\partial e}{\partial p_c} \tag{5.103}$$

$$E'_{23} = [n - (1 - H)\theta] \frac{\partial \rho_{da}}{\partial p_a} + E'_{21} \frac{3}{1 + 2K_0} \tag{5.104}$$

$$E'_{24} = [n - (1 - H)\,\theta] \frac{\partial \rho_{da}}{\partial T} - (1 - H)\,\rho_{da} \frac{\partial \theta}{\partial T} + \rho_{da}\,(1 + e)^{-2} \frac{\partial e}{\partial T} \tag{5.105}$$

$$E'_{31} = \frac{1 + 2K_0}{3} \left(E'_{311} \frac{\partial e}{\partial \sigma^*} + E'_{312} \frac{\partial \theta}{\partial \sigma^*} \right) \tag{5.106}$$

$$E'_{311} = T\,(1 + e)^{-2}\,(\rho_v C_v + \rho_{da} C_{da}) + L_0 \rho_v\,(1 + e)^{-2} \tag{5.107}$$

$$E'_{312} = T\,[\rho_l C_l - \rho_v C_v - \rho_{da} C_{da}\,(1 - H)] - L_0 \rho_v + W \rho_l + \rho_l \theta \frac{\partial W}{\partial \theta} \tag{5.108}$$

$$\begin{aligned} E'_{32} =& E'_{321} \frac{\partial \rho_v}{\partial p_c} + E'_{322} \frac{\partial \rho_l}{\partial p_c} + C_{da} T\,[n - (1 - H)\,\theta] \frac{\partial \rho_{da}}{\partial p_c} \\ &+ E'_{311} \frac{\partial e}{\partial p_c} + E'_{312} \frac{\partial \theta}{\partial p_c} \end{aligned} \tag{5.109}$$

where,

$$E'_{321} = (n - \theta)\,(L_0 + C_v T) \tag{5.110}$$

$$E'_{322} = (W + T C_l)\,\theta + \rho_l \theta \frac{\partial W}{\partial \rho_l} \tag{5.111}$$

$$\begin{aligned} E'_{33} =& E'_{321} \frac{\partial \rho_v}{\partial p_a} + E'_{322} \frac{\partial \rho_l}{\partial p_a} + C_{da} T\,[n - (1 - H)\,\theta] \frac{\partial \rho_{da}}{\partial p_a} \\ &+ E'_{31} \frac{3}{1 + 2K_0} \end{aligned} \tag{5.112}$$

$$\begin{aligned} E'_{34} =& E'_{321}\frac{\partial \rho_v}{\partial T} + E'_{322}\frac{\partial \rho_l}{\partial T} + C_{da}T\left[n-(1-H)\,\theta\right]\frac{\partial \rho_{da}}{\partial T} \\ &+ E'_{311}\frac{\partial e}{\partial T} + E'_{312}\frac{\partial \theta}{\partial T} + C_s\rho_s\,(1-n) \\ &+ C_l\rho_l\theta + C_v\rho_v\,(n-\theta) + C_{da}\rho_{da}\left[n-(1-H)\,\theta\right] \end{aligned} \tag{5.113}$$

$$\begin{aligned} E'_{41} =& \frac{1+2K_0}{3}\left(E'_{411}\frac{\partial e}{\partial \sigma^*} + E'_{412}\frac{\partial \theta}{\partial \sigma^*} + E'_{413}\frac{\partial H_{sl}}{\partial \sigma^*}\right. \\ &\left. + E'_{413}\frac{\partial\left(H_{sg}H_{gl}\right)}{\partial \sigma^*} + E'_{414}\frac{\partial H_{gl}}{\partial \sigma^*}\right) \end{aligned} \tag{5.114}$$

where,

$$E'_{411} = c_l\,(1+e)^{-2}\left[\rho_s\left(H_{sl}+H_{sg}H_{gl}\right)+H_{gl}\right] \tag{5.115}$$

$$E'_{412} = c_l\left(1-H_{gl}\right) \tag{5.116}$$

$$E'_{413} = c_l\,(1-n)\,\rho_s \tag{5.117}$$

$$E'_{414} = c_l\,(n-\theta) \tag{5.118}$$

$$E'_{42} = E'_{411}\frac{\partial e}{\partial p_c} + E'_{412}\frac{\partial \theta}{\partial p_c} + E'_{413}\frac{\partial H_{sl}}{\partial p_c} + E'_{413}\frac{\partial\left(H_{sg}H_{gl}\right)}{\partial p_c} + E'_{414}\frac{\partial H_{gl}}{\partial p_c} \tag{5.119}$$

$$E'_{43} = \frac{3}{1+2K_0}E'_{41} \tag{5.120}$$

$$E'_{44} = E'_{411}\frac{\partial e}{\partial T} + E'_{412}\frac{\partial \theta}{\partial T} + E'_{413}\frac{\partial H_{sl}}{\partial T} + E'_{413}\frac{\partial\left(H_{sg}H_{gl}\right)}{\partial T} + E'_{414}\frac{\partial H_{gl}}{\partial T} \tag{5.121}$$

$$E'_{45} = (1-n)\,\rho_s\left(H_{sl}+H_{sg}H_{gl}\right)+\theta+(n-\theta)\,H_{gl} \tag{5.122}$$

5.6.2 Appendix 5B: Coordinate conversion for governing equations

As an example, consider the transformation of moisture mass balance equation (5.15) from (ξ, t) to (z, t). Inserting Eqs. (5.8-5.11) into Eq. (5.15) yields

$$\begin{aligned}\frac{\partial}{\partial t}\left[\rho_l\theta+\rho_v\left(n-\theta\right)\right]=-\frac{\partial}{\partial\xi}\Bigg[-\rho_l k_l\frac{\partial}{\partial\xi}\left(p_c+p_a+\rho_l g\xi_i\right)-\rho_l D_T\frac{\partial T}{\partial\xi}+\rho_l\theta v_s\\ -D^*\frac{\partial\rho_v}{\partial\xi}-\rho_v k_a\frac{\partial p_a}{\partial\xi}+\rho_v\left(n-\theta\right)v_s\Bigg].\end{aligned} \tag{5.123}$$

Apply the transformation formula (5.1) and multiply both sides by M to get

$$\begin{aligned}&\frac{\partial\xi}{\partial z}\frac{\partial}{\partial t}\left[\rho_l\theta+\rho_v\left(n-\theta\right)\right]-v_s\frac{\partial}{\partial\xi}\left[\rho_l\theta+\rho_v\left(n-\theta\right)\right]\frac{\partial\xi}{\partial z}\\ =&-\frac{\partial}{\partial z}\Bigg[-\rho_l k_l\frac{\partial}{\partial\xi}\left(p_c+p_a+\rho_l g\xi_i\right)-\rho_l D_T\frac{\partial T}{\partial\xi}\\ &-D^*\frac{\partial\rho_v}{\partial\xi}-\rho_v k_a\frac{\partial p_a}{\partial\xi}\Bigg]-\left[\rho_l\theta+\rho_v\left(n-\theta\right)\right]\frac{\partial v_s}{\partial z}-v_s\frac{\partial}{\partial z}\left[\rho_l\theta+\rho_v\left(n-\theta\right)\right].\end{aligned} \tag{5.124}$$

The first term on LHS and the second term on RHS can be simplified using the product rule of differentiation,

$$\begin{aligned}\frac{\partial}{\partial t}\left[\rho_l\theta+\rho_v\left(n-\theta\right)\frac{\partial\xi}{\partial z}\right]=-\frac{\partial}{\partial z}\Bigg[-\rho_l k_l\frac{\partial}{\partial\xi}\left(p_c+p_a+\rho_l g\xi_i\right)-\rho_l D_T\frac{\partial T}{\partial\xi}\\ -D^*\frac{\partial\rho_v}{\partial\xi}-\rho_v k_a\frac{\partial p_a}{\partial\xi}\Bigg],\end{aligned} \tag{5.125}$$

which is exactly identical with (5.49).

5.7 Notation

The following notation is used in Chapter 5:

Roman Letters:

a_0, constant used in calculating density of vapor at saturation

A, constant used in calculating hydraulic conductivity

b_0, constant used in calculating density of vapor at saturation

B, constant used in calculating mobility coefficient for pore air

b, soil body force, $ML^{-2}T^{-2}$

C_l, specific heat capacity of pore liquid in soil, $L^2T^{-2}K^{-1}$

C_{da}, specific heat capacity of dry air in soil, $L^2T^{-2}K^{-1}$

C_v, specific heat capacity of water vapor in soil, $L^2T^{-2}K^{-1}$

C_ψ, the temperature coefficient of water retention, K^{-1}

c_{mt}, mass of contaminants in unit volume of soil matrix, ML^{-3}

c_l, VOCs concentration in liquid phase

c_g, VOCs concentration in gaseous phase

D_{atm}, the molecular diffusion coefficient of water vapor in air, L^2T^{-1}

D_0, mass diffusivity of organic chemical through water, L^2T^{-1}

D^*, effective molecular diffusivity of water vapor, L^2T^{-1}

D_{hg}, mechanical dispersion coefficient of gaseous phase, L^2T^{-1}

D_{hw}, mechanical dispersion coefficient of VOC, L^2T^{-1}

D_{lc}, hydrodynamic dispersion coefficient for VOCs in liquid phase, L^2T^{-1}

D_{gc}, hydrodynamic dispersion coefficient for VOCs in gas phase, L^2T^{-1}

D_{i-n}, molecular diffusivity for the binary pair, L^2T^{-1}

D_T, phenomenological coefficient relating water flux to temperature gradient, $L^2T^{-1}K^{-1}$

D_{wm}, molecular diffusivity of water vapor in a gas mixture, L^2T^{-1}

e, void ratio

e_0, initial void ratio

P_G, mass transfer coefficient of geomembrane, L^2T^{-1}

g, gravity acceleration, LT^{-2}

g_i, gravity acceleration vector, LT^{-2}

h, thickness of geomembrane, L

K_l, hydraulic conductivity, LT^{-1}

k_a, mobility coefficient for gas, L^2TM^{-1}

k_l, mobility coefficient for liquid, L^2TM^{-1}

H, dimensionless coefficient of solubility

$H_{ij}(i, j = s, l, g)$, linear partitioning coefficients between individual soil phase

H_w, constant in calculating heat of wetting, MT^{-2}

K_0, earth pressure coefficient at rest

L_0, latent heat of vaporization, $\mathrm{L}^2\mathrm{T}^{-2}$

L, thickness of CCL, L

M, Jacobian of coordinate transformation

M_{i-n}, equivalent molecular weight, Mmol^{-1}

$m_j(j = i, n)$, molecular weight for gaseous component, Mmol^{-1}

n, current soil porosity

n_0, initial soil porosity

P, air pressure with unit in atmospheres

p_a, gauge pore air pressure, $\mathrm{ML}^{-1}\mathrm{T}^{-2}$

p_c, capillary pressure, $\mathrm{ML}^{-1}\mathrm{T}^{-2}$

p_{cr}, reference capillary pressure in CCL, $\mathrm{ML}^{-1}\mathrm{T}^{-2}$

ΔQ, maximum surcharge, $\mathrm{ML}^{-1}\mathrm{T}^{-2}$

q_{ct}, total VOCs flux, $\mathrm{ML}^{-2}\mathrm{T}^{-1}$

q_l, liquid water flux, $\mathrm{ML}^{-2}\mathrm{T}^{-1}$

q_T, heat flux, MT^{-3}

q_v, vapor water flux, $\mathrm{ML}^{-2}\mathrm{T}^{-1}$

R_{da}, specific gas constant for dry air, $\mathrm{L}^2\mathrm{T}^{-2}\mathrm{K}^{-1}$

R_v, specific gas constant for water vapor, $\mathrm{L}^2\mathrm{T}^{-2}\mathrm{K}^{-1}$

R_{VOC}, specific gas constant for VOCs vapor, $\mathrm{L}^2\mathrm{T}^{-2}\mathrm{K}^{-1}$

S, VOCs concentration adsorbed to soild phase

S', specific surface of the material, L^{-1}

S_l, degree of saturation

t, time, T

T, temperature increase, K

ΔT, maximum temperature increase, K

T_r, an arbitrary reference temperature, K

T_0, initial temperature, K

v_{ai}, average air velocity, LT^{-1}

v_g, equivalent vapor diffusion velocity, LT^{-1}

v_{li}, average fluid velocity, LT^{-1}

v_s, solid velocity, LT^{-1}

W, differential heat of wetting, L^2T^{-2}

y'_n, the mole fraction of component n in the gas mixture

z, material coordinate, L

Greek Symbols:

ξ, spatial coordinate, L

λ, equivalent thermal conductivity of unsaturated soil, $MLT^{-3}K^{-1}$

λ_{dry}, thermal conductivity of completely dry soil, $MLT^{-3}K^{-1}$

λ_{sat}, thermal conductivity of fully saturated soil, $MLT^{-3}K^{-1}$

Γ_0, superficial volume fraction of water in the surface layer

Γ_w, superficial volume fraction of VOC in the surface layer

γ_0, surface tension of VOC, $ML^{-3}T^{-2}$

γ_w, surface tension of a free-water system at the reference temperature, $ML^{-3}T^{-2}$

γ_m, surface tension of pore water at presence of VOCs, $ML^{-3}T^{-2}$

σ^*, net mean soil stress, $ML^{-1}T^{-2}$

σ^*_0, initial uniform net mean stress in CCL, $ML^{-1}T^{-2}$

σ_l, lateral soil stress, $ML^{-1}T^{-2}$

σ_v, vertical soil stress, $ML^{-1}T^{-2}$

ρ_{da}, density of dry air, ML^{-3}

ρ_0, density of vapor at saturation, ML^{-3}

ρ_l, density of pore liquid, ML^{-3}

ρ_{l0}, initial density of pore liquid, ML^{-3}

ρ_s, density of soil gain, ML^{-3}

ρ_v, density of water vapor, ML^{-3}

ρ_{VOC}, density of VOCs vapor, ML^{-3}

α_k, constant to calculate hydraulic conductivity

α_l, thermal expansion coefficient for pore water, K^{-1}

α_{Lg}, longitudinal dispersivity parameter for gas phase, L

α_{Lw}, longitudinal dispersivity parameter for liquid phase, L

β, constant used in calculating mobility coefficient for pore air

β_l, pore water compressibility coefficient, Pa^{-1}

δ, constant in calculating heat of wetting, L

ν_m, the mass flow factor

τ, the dimensionless tortuosity factor

θ, volume water content

θ_0, initial volume water content

Ψ, capillary potential head, L

$\Psi(T_r)$, the capillary pressure head at the reference temperature, L

Φ, heat capacity of the soil, $ML^{-1}T^{-2}$

ϕ, dimensionless association factor of solvent

μ_a, dynamic viscosity of pore air, MT^{-1}

μ_w, dynamic viscosity of pore water, MT^{-1}

Ω, factor representing the tortuosity in calculating dispersion coefficient of VOCs in gaseous phase

Σ_v, sum of atomic diffusion volumes for each gas component

Abbreviation:

ADE, advection-dispersion equation

BCs, boundary conditions

CCL, compacted clay liner

CPW, compressible pore water

CRFs, constitutive relationship functions

GEs, governing equations

ICs, initial conditions

REV, represent element volume

SVP, spatial variation of porosity

VOCs, volatile organic chemicals

Chapter 6

Conclusions and Recommendations

Based on the current literature, this thesis investigated the VOCs transport in partially saturated landfill soil liner theoretically. Despite its limitations, it assists in understanding more the processes and mechanisms controlling VOCs migration. In this chapter, conclusions will be made on the works presented in this thesis. Also, recommendations for the future study will be given.

6.1 Conclusions

The first specific objective to establish a model for VOCs movement in a nearly-saturated clay liner was implemented in two steps: small deformation and finite deformation models. Since the soil air phase exists in the form of occluded air bubbles and dissolved air in liquid phase, the mixture of pore water (with dissolved air) and occluded air bubbles can be taken as homogeneous pore fluid. In this case, VOCs solute moves in solid and liquid phases for a deformable porous medium.

Based on the mass conservation of pore fluid, a storage equation was derived with considering of the compressibility of the pore fluid and reduction in cross-section through which water flows in Chapter 3. Additionally, the well-known advection-dispersion equation conventionally used to describe the solute transport in rigid porous medium was modified to incorporate unsaturated conditions, compressibility of the pore fluid and longitudinal dispersivity of the solute transport in an unsaturated, deforming porous medium. The newly proposed advection-dispersion equation took into account carrying of solute by moving soil

solid. Thus, the solute advective flux includes advection due to velocities of both solid grain and pore water and hydro-dispersion which consists of effective molecular diffusion and mechanical dispersion. The deformation of soil was assumed to be caused by mechanical consolidation alone. The consolidation and porous flow can be solved by combining the fluid storage and force equilibrium equation. Then, the information of transient deformation and flow were input into the advection-dispersion equation. The solute mass concentration was assumed to be negligibly small and have no impact on the soil materials. Therefore, the one-way coupling consolidation and solute transport model for a quasi-saturated deformable porous medium was set up.

The presented coupled model was applied to a hypothetical landfill CCL. To understand the influence of each term in the governing equations, a non-dimensional analysis was performed. On the basis of the assessment of relative importance of each term involved, a simplified model was proposed for the case of a landfill liner. Using the simplified model, the effect of degree of saturation S_r and loading progress on the contaminant breakthrough and advective emission were examined. The following findings were confirmed:

- The non-dimensional analysis revealed that the effect of self-weight of CCL and spatial variation of porosity were negligible while the longitudinal dispersivity and compressibility of the pore fluid can be significant. Under the conditions of relatively small deformation, the soil porosity was approximated to be constant. In addition, molecular diffusivity, hydraulic conductivity and shear modulus were assumed to be temporally and spacially invariable. However, it is worthwhile to note that these assumptions can be relaxed in a dimensional analysis. The derivations presented in appendixes have given the expression for variation of soil porosity. Providing constitutive formulas with respect to molecular diffusivity, hydraulic conductivity and shear modulus are known, the nonlinearity of material is readily to be incorporated.

- The lower saturation led to more advective emission due to greater fluid velocity, and that the slow loading rate of surcharge increased the total advective emission significantly. Nevertheless, the variation of degree of saturation and different waste implace-

ment rates had little influence on the solute relative concentration evolution at landfill liner bottom, i.e., the time for VOCs break through CCL.

Chapter 4 continued to extend the one-dimensional model developed in Chapter 3 to account for both geometric and material nonlinearity. Lagrangian coordinate system was employed to address the finite deformation, which implies that the transient reduction of soil thickness is considered during the consolidation. Utilizing the concept of effective stress and vertical force equilibrium, these derivatives of excess pore pressure were expressed instead in term of the corresponding derivatives of void ratio. Therefore, a new non-linear consolidation equation for quasi-saturated porous medium was established. Similarly, the advection-dispersion equation derived in Chapter 3 was recast in Lagrangian coordinate. And hence coupling the non-linear consolidation and solute transport equations can solve the time-dependent void ratio and solute concentration. Soil displacement and excess pore pressure can also be obtained indirectly. The application of the model to a hypothetical landfill CCL led to the main findings as listed below:

- The total stress at top of CCL increases with implacement of landfill waste. When it was mistakenly taken as the maximum loading in literature, a greater gradient of the void ratio and a faster consolidation process were resulted in, although the final value of void ratio was very close. The improper use of this boundary leads to conclusion that a pure diffusion is sufficient if the final level of void ratio can be considered in the transport equations.

- A noticeable concentration difference from the no deformation model appeared at a relatively soft clay liner base during consolidation. Although the duration of consolidation may be short, it will change the distribution of solute concentration, which is the initial condition of a sequential process. Consolidation-induced advection had a lasting effect on solute transport during and after the deformation for relatively compressible soil regardless of the sorption level, though the sorption could dramatically slow down the solute transport process rate. Therefore, the advection transport due to consolidation may not be negligible. In other words, the approximation of pure diffusion with void ratio at final level is not appropriate.

- The effective diffusion plays a important role in solute migration. When considering the decreasing of effective diffusion due to unsaturation and soil contraction, the finite-deformation coupled model produces a lower concentration at the CCL base than the pure diffusion model. The acceleration effect of mechanical consolidation advection on solute transport only occurs at an initial stage.

- For both no-deformation and finite deformation models, results predicted for higher saturation had a faster solute transport because of greater effective diffusion. With both sorption and decreasing effective diffusion taken into account, finite deformation models will not always predict a faster solute transport. During the progress of consolidation and in the early post-consolidation stage, the finite deformation models have a faster transit, but then are surpassed by the no-deformation model because the effective diffusion was reduced due to compaction. However, the decreasing diffusion with compaction is an inevitable physical phenomenon, and an earlier appearance of VOC in the field than predicted by the pure diffusion model has been observed.

- The CPW associated with unsaturated conditions cannot be ignored when the consolidation is required to be coupled with solute transport. CPW-involving terms exist in both the consolidation and transport equations, none of which can be neglected for simplification.

- Effective diffusion decreases during consolidation and consequently the relative importance of mechanical dispersion becomes profound. For a long-term prediction, mechanical dispersion could cause significant solute transport. Therefore, it should be included for the sake of conservation.

- The small deformation model can predict settlement that is non-physical for soft soil (i.e., larger than the total soil thickness) for soft soil. Therefore, for a relatively compressible soil, where the consolidation effect is more significant, a finite deformation consolidation is necessary when being coupled with the solute transport.

- In general, reducing soil compressibility and improving sorption levels of clay are the most effective ways to retard contaminant migration. At the same level of stiffness and sorption, the lower hydraulic conductivity and lower degree of saturation can lengthen the time for contaminants to break through the protective liner. However, the air phase will becomes continuous if the desaturation is large enough. In this case, VOCs will also transport in gaseous phase.

The theory developed here for solute transport in quasi-saturated soil liner is also applicable to capping of the contaminated aqueous sediments and confining of the dredged polluted sediment, in which cases mechanical consolidation can not be ignored and the fully-saturated condition can not be always be satisfied. However, the chemical reaction and other transport mechanisms, e.g., bioturbation in sediments, need to be included.

A fully coupled thermal-hydraulic-mechanical-chemical (THMC) model was proposed in Chapter 5 to describe the migration of volatile organic contaminants (VOCs) in unsaturated landfill liners. Similar to Chapter 4, Lagrangian coordinate system was employed. However, the deformation was calculated based on the primary variable of total vertical stress rather than void ratio. And the mass conservations of porous fluid including liquid and gas were formulated in terms of capillary pressure, air pressure. Motion of solid was reflected in the fluid fluxes. Effect of surface tension due to presence of VOCs and temperature on cappilary pressure were both included. Since capillary pressure influences values of the degree of saturation and void ratio, which in turn control hydraulic conductivity for pore fluid, the effects of temperature on water retention curve and hydraulic conductivity were considered indirectly. The gaseous mixture composed of water vapor, dry air and VOC vapor. The interaction between each component were considered when calculating the diffusion coefficients of water vapor and VOCs gas. For the cases considered, it is satisfactorily accurate for technical calculation to make the assumption that the mixture of gases obey the ideal gas law and Dalton's law, thereby relationships were set up between the individual partial pressure, density and mass concentration of VOCs gas. Each of the soil phases was assumed to retain heat. Besides, the contributions of latent heat of vaporization and exothermic process

of wetting of the porous medium were also considered. Heat transfer mechanisms included conduction, convection, vaporization of heat, gradient of water potential and differential heat of wetting flux. VOCs were assumed to reside in liquid, gaseous and solid phase of soil, and its movement could be caused by diffusion and advection in both liquid and vapor phases. VOCs was taken conservative, namely, the degradation of VOCs was ignored. The adsorbed concentration of VOCs on soil solid consisted of two parts from water phase and air phase, respectively. Under the condition of local chemical equilibrium between each phase, concentration of VOCs in one phase can be evaluated from that in another phase by a linear partitioning coefficient.

The model was bench-marked against a non-isothermal moisture transport in soil column and an analytical solution of multi-phase VOCs transport in an unsaturated soil. Then the breakthrough of VOCs in a unsaturated CCL was examined. The illustrative CCL was identical to them used in the foregoing chapters, except that a boundary condition of time-dependent temperature gradient was added. The simulation results indicated that:

- The small deformation model would underestimate transit of contaminant due to the unchanging thickness of soil column.
- The solid velocity should be incorporated in the VOCs fluxes because the relatively important absortion capacity of solid.
- A two-way coupling approach is essential to get an accuracy determination of water vapor diffusion coefficient with presence of VOCs vapor. On the other hand, either considering VOCs or not when calculating density of dry air does not make discernible difference on the VOCs transport progress.
- Considering adsorption of VOCs from both gas and fluid phase in the composition of total concentration can considerably slow down the migration progress.
- Since the related VOCs dispersion fluxes are several orders of magnitude less than the diffusion flux in gas phase, the mechanical dispersion of fluid phase can be neglected.

- Gas phase diffusion plays a predominant role in the transport of VOCs in an unsaturated soil liner. Consequently, the volume decrease due to mechanical consolidation helps to prevent VOCs migration while higher environmental temperature will speed up movement of VOCs.

- Furthermore, deviation of saturation from fully saturated state can significantly speed up the VOCs motion. Therefore, a non-isothermal multi-phase moisture and VOCs transport modeling should be employed to obtain a reliable prediction of VOCs migration in an unsaturated soil liner exposed to condition of heating and compression.

The model provides a simulation tool to evaluate multi-phase transport of VOCs and assess the equivalence of different composite liners. It can be extended to predict the gasoline leaking underneath a underground storage tank where the consolidation occurs in response to filling of gasoline. Since the gasoline is complex mixture of organic compounds, their chemical characteristics desire to be measured specifically.

6.2 Recommendations

This thesis is concerned with mainly the appropriate mathematical models which can be used to make quantitative predictions of liner performance. However, optimal design of landfill soil liner also requires an understanding of the fundamental mechanisms and the material properties in the certain chemical and hydraulic environment. Herein, the recommendations are presented for these two aspects.

More comprehensive model for landfill liner

- Recently, the technology of air sparging has become a promising method in remediation of groundwater contaminated by VOCs (Zhang and Burns, 2000). The sparging process mobilizes contaminants to the vapor phase through mass transfer into air bubbles, which are pressurized into groundwater through an injection well (Tsai et al., 2007) or generated within the soil using surfactants (Zhang and Burns, 2000). And

hence, the contaminant-containing gas bubbles move to the surface where they can be collected for treatment. Since large portions of the aquifer are not exposed to the stripping gas, its effectiveness is limited. In view of the fact that the smaller bubbles have a large surface area to volume ratio and consequently promotes mass transfer and less prone to channeling, Zhang and Burns (2000) investigated how to use surfactants to enhance air sparging process through the generation of small diameter air bubbles. Therefore, understanding the air flow by diffusion will be constructive to not only landfill barrier design but also the soil remediation.

- Zhou and Rowe (2005) explained the clay liner desiccation in unsaturated soil under non-isothermal condition. They suggested that heat generated in a landfill waste body could lead to significant loss of water content in clay liners and then cracking may occur due to desiccation. In that case, a double porosity formulation should be used. Also, there is another situation where it is necessary for a double porosity formulation to account for the presence of two distinct structural levels in the material. It happen when the mixture of bentonite powder and bentonite pellets are used to reduce the compaction effort required to achieve the value of average dry density necessary of CCL to attain the required low hydraulic conductivity and stiffness (Gens et al., 2011). The heterogeneous fabric of the material requires special approaches in order to describe adequately its behaviour during hydration.

- The classical advection-dispersion equation, is valid only when the transport of a solute has reached the Fickian regime in which the rate of solute spread grows linearly with time and the dispersive flux becomes linearly proportional to the concentration gradient (Padilla et al., 1999). The Fickian regime need be reached when the solute has been able to sample the whole field of velocities and the solute velocity is independent of its initial velocity. In unsaturated soil, a solute plume must travel over a longer distance to interact with many small-scale heterogeneities of the porous medium before Fickian regime is achived. Padilla et al. (1999) performed a series of experiments to investigate the effect of water content on NaCl transport in unsaturated porous media

under steady state flow conditions for water contents ranging between full saturation and 15% by volume. The results suggested that transport processes could not fully developed to the Fickian regime at lower water contents. In this case, the classical advection-dispersion equation which does not adequately describe the movement of solutes under the pre-Fickian regime is not applicable. Therefore, warrant should be taken when the degree of saturation is very low in the soil liner.

Field and laboratory tests

In the illustrative examples of VOCs migration in landfill CCL presented in this thesis, hypothetical constitutive relationships for consolidation and transport coefficients were adopted due to the lack of data. Contaminant transport analysis for a partially saturated soil is influenced by the dependence of the diffusion, dispersion, and partitioning coefficients on the degree of saturation (Fityus et al., 1999) and temperature.

Fityus et al. (1999) proposed a bilinear model to relate the effective diffusion coefficient and volumetric water content. Some empirically fitted constants without definite physical interpretation are involved, which give rise to an doubt for its extrapolation to other soil type. Though the significant dependence of the partitioning coefficient on the volumetric moisture content is well recognized for at least some types of soil, the implications of this for geotechnical design of landfill liners are unclear (Fityus et al., 1999). Compaction may result in occluded pores inaccessible to solute and consequently reduce the available sorption sites. Using a specially designed cell, Oscarson et al. (1994) directly measured the extent of Cs^+ sorption on bentonite compacted to a series of densities ranging from 0.50 to 1.50 Mg/m^3, and compared the results with those obtained from batch tests with loose bentonite. The distribution coefficients, K_d adopted to represent level of sorption for Cs^+ with compacted clay were found to be about one-half to one-third the value of those with loose clay. Oscarson et al. (1994) attributed the lower sorption on compacted clay to small and occluded pores that Cs^+ cannot enter. Furthermore, the assumption that soil bubbles have an insignificant effect on the overall behavior of the soil mass will be questionable. Therefore, a extensive experimental investigations into the properties of CCL materials are need.

Bibliography

Acar, Y. B. and Haider, L. (1990). Transport of low-concentration contaminants in saturated earthen barriers. *Journal of Geotechnical Engineering, ASCE*, 116(7):1031–1052.

Akers, S. A. (2001). *Two-Dimensional Finite Element Analysis of Porous Geomaterials at Multikilobar Stress Levels*. PhD thesis, Civil Engineering, Virginia Polytechnic Institute and State University.

Alonso, E. and Lloret, A. (1982). Behavior of partially saturated soil in undrained loading and step by step embankment construction. In *IUTAM Conference on Deformation and Failure of Granular Materials*.

Alonso, E. E., Battle, F., Gens, A., and Lloret, A. (1988). Consolidation analysis of partially saturated soils-application to earth dam construction. In *Proc., 6th International Conference of Numerical Methods Geomechanics*, pages 1303–1308, Innsbruck.

Alshawabkeh, A., Rahbar, N., Sheahan, T. C., and Tang, G. (2004). Volume change effects in solute transport in clay under consolidation. In *Geo Jordan 2004 : Advances in Geotechnical Engineering with Emphasis on Dams, Highway Materials, and Soil Improvement*, volume 1, pages 105–115, Irbid, Jordan. ASCE.

Alshawabkeh, A. N., Rahbar, N., and Sheahan, T. (2005). A model for contaminant mass flux in capped sediment under consolidation. *Journal of Contaminant Hydrology*, 78(3):147–165.

Anderson, M. (1984). Movement of contaminants in groundwater: Groundwater transport-advection and dispersion. In *Groundwater Contamination, Studies in Geophysics*, pages 37–45, Washington, DC. National Academy Press.

Arega, F. and Hayter, E. (2008). Coupled consolidation and contaminant transport model for simulating migration of contaminants through the sediment and a cap. *Applied Mathematical Modelling*, 32(11):2413–2428.

Azad, F. M., El-Zein, A., Rowe, R. K., and Airey, D. W. (2012). Modelling of thermally induced desiccation of geosynthetic clay liners in double composite liner system. *Geotextiles and Geomembranes*, 34:28–38.

Barbour, S. L., Lim, P. C., and Fredlund, D. G. (1996). A new technique for diffusion testing of unsaturated soil. *American Society for Testing and Materials*, 19(3):247–258.

Barden, L. (1965). Consolidation of compacted and unsaturated clays. *Géotechnique*, 15(3):267–286.

Barden, L. (1974). Consolidation of clays compacted 'dry' and 'wet' of optimum water content. *Géotechnique*, 24(4):605–625.

Barraclough, P. and Tinker, P. (1981). The determination of ionic diffusion coefficients in field soils. I: Diffusion coefficients in sieved soils in relation to water content and dry density. *Journal of Soil Science*, 32:225–236.

Barry, D. A. (1990). Supercomputers and their use in modeling subsurface solute transport. *Reviews of Geophysics*, 28:277–295.

Barry, D. A. (1992). *Modelling Chemical Transport in Soil: Natural and Applied Contaminants*, chapter Modelling contaminant transport in the subsurface: Theory and computer programs, pages 105–144. Lewis Publishers, Boca Raton, Florida, USA.

Barry, D. A. and Sposito, G. (1988). Application of the convection-dispersion model to solute transport in finite soil columns. *Soil Science Society of America Journal*, 52:3–9.

Barry, D. A. and Sposito, G. (1989). Analytical solution of a convection-dispersion model with time-dependent transport coefficients. *Water Resources Research*, 25:2407–2416.

Bear, J. (1972). *Dynamics of Fluids in Porous Mmedia*. Elsevier Scientific Publishing Company, New York.

Bear, J. (1979). *Hydraulics of groundwater*. McGraw-Hill.

Bear, J., Bensabat, J., and Nir, A. (1991). Heat and mass transfer in unsaturated porous media at a hot boundary: I. one-dimensional analytical model. *Transport in Porous Media*, 6:281–298.

Bear, J. and Cheng, A. H.-D. (2010). *Modeling groundwater flow and contaminant transport*. Springer, Heidelberg.

Bear, J. and Corapcioglu, M. Y. (1981a). Centrifugal filtration in deformable porous media. Technical report, Department of Civil Engineering, University of Michigan, Ann Arbor.

Bear, J. and Corapcioglu, M. Y. (1981b). Mathematical model for regional land subsidence due to pumping, 2. integrated aquifer subsidence equations for vertical and horizontal displacements. *Water Resource Research*, 17:947–958.

Bear, J. and Gilman, A. (1995). Migration of salts in the unsaturated zone caused by heating. *Transport in Porous Media*, 19:139–156.

Beldowski, J., Miotk, M., and Pempkowiak, J. (2009). Mercury fluxes through the sediment water interface and bioavailability of mercury in southern balt sea sediment. *Oceanologia*, 51(2):263–285.

Benson, C. H., Daniel, D. E., and Boutwell, G. P. (1999). Field performance of compacted clay liners. *Journal of Geotechnique and Geoenvironmental Engineering, ASCE*, 125(5):390–403.

Bert, V., Seuntjens, P., Dejonghe, W., Lacherez, S., Thuy, H., and Vandecasteele, B. (2009). Phytoremediation as a management option for contaminated sediments in tidal marshes, flood control areas and dredged sediment landfill sites. *Environmental Science and Pollution Research*, 16(7):745–764.

Biot, M. A. (1941). General theory of three-dimensional consolidation. *Journal of Applied Physics*, 12:155–164.

Bishop, A. and Eldin, A. K. G. (1950). Undrained triaxial tests on saturated sands and their significance in the general theory of shear strength. *Géotechnique*, 2(1):13–32.

Bonaparte, R. and Gross, B. (1990). Field behavior of doubleliner systems. In *Waste containment systems: construction, regulation and performance*, volume 26, pages 52–83. ASCE, Geotechnical Special Publication.

Booker, J. R., Quigley, R. M., and Rowe, R. K. (1997). *Clayey Barrier Systems for Waste Disposal Facilities*. Spon Press, London.

Boyd, J. L. and Sivakumar, V. (2011). Experimental observations of the stress regime in unsaturated compacted clay when laterally confined. *Géotechnique*, 61(4):345363.

Cann, D., Stiver, W., and Zytner, R. (2004). Correlating gas phase dispersion and moisture content in undisturbed and disturbed unsaturated soils. In *RemTech 2004 Proceedings*. Environmental Services Association of Alberta (ESAA).

Cartwright, K., Griffin, R. A., and Gilkeson, R. H. (1977). Migration of landfill leachate through glacial tills. *Ground Water*, 15(4):294–305.

Cassel, D. and Nielsen, D. (1969). Soil-water movement in response to imposed temperature gradients. *Soil Science Society of America Journal*, 33:493–500.

Challa, J., Skoff, D., and Quirus, F. J. (1997). Landfill gas as source of vocs in ground water. *Practice Periodical of Hazardous, Toxic, and Radioactive Waste Management*, 1(2):61–75.

Chang, C. and Duncan, J. (1977). Analysis of consolidation of earth and rockfill dams; main text and appendices a and b. Technical report, Contract Report S-77-4, U.S. Army Engineer Waterways Experiment Station, Vicksburg, MS.

Cleall, P. J., Seetharam, S. C., and Thomas, H. R. (2007). Inclusion of some aspects of chemical behavior of unsaturated soil in thermo/hydro/chemical/mechanical models. I: Model development. *Journal of Engineering Mechanics, ASCE*, 133(3):338–347.

Collins, H. J. (1993). Impact of the temperature inside the landfill on the behaviour of barrier systems. In *Proceedings of Fourth International Landfill Symposium*, pages 417–432, Cagliari, Italy.

COMSOL (2010). *COMSOL Multiphysics, 3rd Edition*.

Conca, J. and Wright, J. (1990). Diffusion coefficients in gravel under unsaturated conditions. *Water Resources Research*, 20:1055–1066.

Conte, E. and Troncone, A. (2006). One-dimensional consolidation under general time-dependent loading. *Canadian Geotechnical Journal*, 43:11071116.

Corapcioglu, M. Y. and Bear, J. (1983). A mathematical model for regional land subsidence due to pumping, 3. lntegated equations for a phreatic aquifer. *Water Resources Research*, 19:895–908.

Corey, A. (1957). Measurement of water and air permeability in unsaturated soil. *Proceedings of the Soil Science Society of America*, 21.

Dakshanamurthy, V. and Fredlund, D. (1980). Moisture and air flow in an unsaturated soil. In *Proceedings, 4th International Conference on Expansive Soils*, volume 1, pages 514–532, Denver, CO. ASCE.

Dakshanamurthy, V. and Fredlund, D. (1981). A mathematical model for predicting moisture flow in an unsaturated soil under hydraulic and temperature gradients. *Water Resources Research*, 17(3):714–722.

Dakshanamurthy, V., Fredlund, D. G., and Rahardjo, H. (1984). Coupled three-dimensional consolidation theory of unsaturated porous media. Adelaide, Australia. The Fifth International Conference on Expansive Soils.

Danckwerts, P. V. (1953). Continuous flow systems : Distribution of residence times. *Chemical Engineering Science*, 2:1–13.

Davis, E. H. and Raymond, G. P. (1965). A non-linear theory of consolidation. *Géotechnique*, 15(2):161–173.

de Vries, D. A. (1958). Simultaneous transfer of heat and moisture in porous media. *Eos Trans. AGU*, 39:909–916.

Döll, P. (1996). Desiccation of mineral liners below landfills with heat generation. *Journal of Geotechnical and Geoenvironmental Engineering. ASCE*, 123:1001–1009.

Edil, T. B. (2003). A review of aqueous-phase voc transport in modern landfill liners. *Waste Management*, 23:561–571.

Ewen, J. and Thomas, H. R. (1989). Heating unsaturated medium sand. *Géotechnique*, 39:455–470.

Fityus, S. G., Smith, D. W., and Booker, J. R. (1999). Contaminant transport through an unsaturated soil liner beneath a landfill. *Canadian Geotechnical Journal*, 36(2):330–354.

Foose, G. J. (2002). Transit-time design for diffusion through composite liners. *Journal of Geotechnical and Geoenvironmental Engineering. ASCE*, 128(1):590–601.

Foose, G. J., Benson, C. H., and Edil, T. B. (2002). Comparison of solute transport in three composite liners. *Journal of Geotechnical and Geoenvironmental Engineering. ASCE*, 128(5):391403.

Fourie, A. B., Hofmann, B. A., Mikula, R. J., Lord, E. R. F., and Robertson, P. K. (2001). Partially saturated tailings sand below the phreatic surface. *Géotechnique*, 51(7):577–585.

Fox, P. (2007a). Coupled large strain consolidation and solute transport. I: Model development. *Journal of Geotechnical and Geoenvironmental Engineering*, 133(1):3–15.

Fox, P. (2007b). Coupled large strain consolidation and solute transport. II: Model verification and simulation results. *Journal of Geotechnical and Geoenvironmental Engineering. ASCE*, 133(1):16–29.

Fox, P. and Berles, J. (1997). A piecewise-linear model for large strain consolidation. *International Journal for Numerical and Analytical Methods in Geomechanics*, 21:453–475.

Fox, P. and Lee, J. (2008). Model for consolidation-induced solute transport with nonlinear and nonequilibrium sorption. *International Journal of Geomechanics. ASCE*, 8(3):188–198.

Fredlund, D. (1976). Density and compressibility characteristics of air-water mixtures. *Canadian Geotechnical Journal*, 13(4):386–396.

Fredlund, D. (1982). Consolidation of unsaturated porous media. In *Proceedings, Symposium on the Mechanics of Fluid in Porous Media-New Approaches in Research*, Newark, DL. NATO Advance Study Institute.

Fredlund, D. and Hasan, J. (1979). One-dimensional consolidation theory: Unsaturated soils. *Canadian Geotechnical Journal*, 16(3):521–531.

Fredlund, D. and Rahardjo, H. (1993). *Soil mechanics for unsaturated soils*. Wiley.

Fukue, M., Nakamura, T., Kato, Y., and Yamasaki, S. (1999). Degree of pollution for marine sediments. *Engineering Geology*, 53(2):131 – 137.

Fuller, E., Schettler, P., and Giddings, J. (1966). A new method for prediction of binary gas-phase diffusion coefficients. *Industrial and Engineering Chemistry*, 58:18–27.

Gardner, W. R. (1960). Soil suction and water movement. In *Pore-pressure and suction in soils*, pages 137–140, London. Butterworths.

Gens, A., Vallejan, B., Sanchez, M., Imbert, C., Villar, M. V., and Geet, M. V. (2011). Hydromechanical behaviour of a heterogeneous compacted soil: experimental observations and modelling. *Géotechnique*, 61:367–386.

Gibbon, R. D., Dolan, D., Keough, H., O'Leary, K., and O'Hara, R. (1992). A comparison of chemical constituents in leachate from industrial hazardous waste & municipal solid waste landfills. In *Proceedings of the 15th Annual Madison Waste Conference*, pages 251–276, Madison, U.S.A. University of Wisconsin-Madison.

Gibson, R. E., England, G. L., and Hussey, M. J. L. (1967). The theory of onedimensional consolidation of saturated clays, i. finite non-linear consolidation of thin homogeneous layers. *Géotechnique*, 17(3):261–273.

Gilbert, O. (1959). The influence of negative pore water pressures on the strength of compacted clays. Master's thesis, Massachusetts Institute of Tecnology.

Giroud, J. and Bonaparte, R. (1989). Leakage through liners constructed with geomembranes. part I. geomembrane liners. part II. composite liners. *Geotextiles and Geomembranes*, 8:27–68, 71–112.

Guerrero, J. and Skaggs, T. (2010). Analytical solution for one-dimensional advection-dispersion transport equation with distance-dependent coefficients. *Journal of Hydrology*, 390(1-2):57–65.

Hamamoto, S., Perera, M. S. A., Resurreccion, A., Kawamoto, K., Hasegawa, S., Komatsu, T., and Mldrup, P. (2009). The solute diffusion coefficient in variably compacted, unsaturated volcanic ash soils. *Soil Science Society of America*, 8(4):942–952.

Haxo, H. E. and Lahey, T. P. (1988). Transport dissolved organics from dilute aqueous solutions through flexible membrane liners. *Hazardous Waste and Hazardous Materials*, 5(4):275–294.

Hilf, J. W. (1956). An investigation of pore water pressures in compacted cohesive soils. Technical report, U. S. Department of the Interior, Bureau of Reclamation, Denver, Colorado.

Ho, C. K. (2006). *Gas Transport in Porous Media*, chapter 4, pages 47–54. Springer.

Hodgson, A., Garbesi, K., Sextro, R., and Daisey, J. (1992). Soil-gas contamination and entry of volatile organic compounds into a house near a landfill. *Air and Waste Management*, 42:277–283.

Hsu, J. R. C., Jeng, D.-S., and Lee, C. P. (1995). Oscillatory soil response and liquefaction in an unsaturated layered seabed. *International Journal for Numerical and Analytical Methods in Geomechanics*, 19(12):825–849.

Hunt, A. G. and Ewing, R. P. (2003). On the vanishing of solute diffusion in porous media at a threshold moisture content. *Soil Science Society of America Journal*, 67:1701–1702.

Ishihara, K. (1993). *At-rest and compaction-induced lateral earth pressures of moist soils*. PhD thesis, Civil engineering, Virginia Polytechnic Institute and State University.

Jeng, D.-S. and Lin, Y. S. (1997). Non-linear wave-induced response of porous seabed: A finite element analysis. *International Journal for Numerical and Analytical Methods in Geomechanics*, 21(1):15–42.

Jury, W. A., Russo, D., Streile, G., and El-Abd, H. (1990). Evaluation of volatilization by organic chemicals residing below the soil surface. *Water Resource Research*, 26:13–20.

Kaczmarek, M. and Hueckel, T. (1998). Chemo-mechanical consolidation of clays: analytical solutions for a linearized onedimensional problem. *Transport in Porous Media*, 32:49–74.

Kay, B. D. and Groenevelt, P. H. (1974). On the interaction of water and heat in frozen and unfrozen solids: I. basic theory-the vapor phase. *Soil Science Society of America*, 38:395–400.

Kim, J.-M. (2000). A fully coupled finite element analysis of water-table fluctuation and land deformation in partially saturated soils due to surface loading. *International Journal for Numerical Methods in Engineering*, 49:1101–1119.

Kim, J. M. and Parizek, R. R. (1999). Three-dimensional finite element modelling for consolidation due to groundwater withdrawal in a desaturating anisotropic aquifer system. *International Journal for Numerical and Analytical Methods in Geomechanics*, 23:549–571.

Kim, J. Y. (1997). Migration of volatile organic compounds from the landfill liner systems. *Environmental Engineering Research*, 2(4):233–243.

Kim, J. Y., Park, J. K., Emmons, B., and Armstrong, D. K. (1995). Survey of volatile organic compounds at a municipal solid waste cocomposting facility. *Water Environment Research*, 67(7):1044–1051.

Klett, N., Edil, T. B., Benson, C. H., and Connelly, J. (2005). Evaluation of volatile organic compounds in wisconsin landfill leachate and lysimeter samples. Technical report, Department of Civil and Environmental Engineering, University of Wisconsin-Madison, Madison, USA.

Krug, M. N. and Ham, R. K. (1995). Analysis of longterm leachate characteristics in wisconsin landfills. In *Proceedings of the 18th International Madison Waste Conference*, pages 168–184, Madison, U.S.A. University of Wisconsin-Madison.

Lambe, T. W. and Whitman, R. V. (1969). *Soil mechanics*. J. Wiley., New York.

Lewis, T. W. (2009). *Theoretical effects of consoldation on solute transport in soil barriers*. PhD thesis, The University of Newcastle, Australia.

Lewis, T. W., Pivonka, P., and Smith, D. W. (2009). Theoretical investigation of the effects of consolidation on contaminant transport through clay barriers. *International Journal for Numerical And Analytical Methods In Geomechanics*, 33:95–116.

Li, L., Barry, D. A., and Jeng, D.-S. (2001). Tidal fluctuations in a leaky confined aquifer: Dynamic effects of an overlying phreatic aquifer. *Water Resources Research*, 37(4):1095–1098.

Li, S. and Liu, Y. (2006). Application of fractal models to water and solute transport in unsaturated soils. In *Advances in Unsaturated Soil, Seepage, and Environmental Geotechnics (GSP 148), Proceedings of Sessions of GeoShanghai 2006*.

Li, Y.-C. and Cleall, P. J. (2011). Analytical solutions for advectivedispersive solute transport in double-layered finite porous media. *International Journal for Numerical and Analytical Methods in Geomechanics*, 35(4):438–460.

Lin, J.-S. and Hildemann, L. M. (1995). A nonsteady-state analytical model to predict gaseous emissions of volatile organic compounds from landfills. *Journal of Hazardous Materials*, 40:271–295.

Lindstrom, F. T. and Piver, W. T. (1985). Vertical transport and fate of low solubility chemicals in unsaturated soils. *Journal of Hydrology*, 82:93–141.

Lloret, A. and Alonso, E. E. (1980). Consolidation of unsaturated soils including swelling and collapse behavior. *Géotechnique*, 30(4):449–477.

Lloret, A. and Alonso, E. E. (1985). State surfaces for partially saturated soils. In *Proc. 11th I.C.S.M.F.E.*, volume 2, pages 557–562, San Francisco.

Massoudieh, A., Bombardelli, F. A., and Ginn, T. R. (2010). A biogeochemical model of contaminant fate and transport in river waters and sediments. *Journal of Contaminant Hydrology*, 112(1-4):103 – 117.

Mathur, S. and Jayawardena, L. P. (2008). Thickness of compacted natural clay barriers in msw landfills. *Practice Periodical of Hazardous, Toxic, and Radioactive Waste Management*, 12(1):53–57.

Matyas, E. L. and Radhakrishna, H. S. (1968). Volume change characteristics of partially saturated soils. *Géotechnique*, 18(4):432–448.

Means, R. and JV., P. (1964). *Physical Properties of Soils*. Constable and Company Ltd., London.

Milly, P. (1984). A simulation analysis of thermal effects on evaporation from soil. *Water Resource Research*, 20:1087–1098.

Milly, P. C. D. (1982a). Moisture and heat transport in hysteretic inhomogeneous porous media: A matric head based formulation and a numerical model. *Water Resources Research*, 18:485–498.

Milly, P. C. D. (1982b). Moisture and heat transport in hysteretic, inhomogeneous porous media: A matric heat-based formulation and a numerical model. *Water Resource Research*, 18:489–498.

Mitchelll, J. K. (1993). *Fundamentals of Soil Behaviour*. Wiley, New York.

Morris, P. H. (2005). Analytical solutions of linear finite- and small-strain one-dimensional consolidation. *International Journal for Numerical and Analytical Methods in Geomechanics*, 29:127–140.

Mueller, W., Jakob, R., Tatzky-Gerth, R., and August, H. (1998). Solubilities, diffusion, and partition coefficients of organic pollutants in hdpe geomembranes: Experimental results and calculations. In *Proceedings from the 6th International Conference on Geosynthetics*, pages 239–248, Berlin, Germany. Federal Institute for Materials Research and Testing, BAM,.

Nassar, I. and Horton, R. (1999). Transport and fate of volatile organic chemicals in unsaturated, nonisothermal, salty porous media: 1. theoretical development. *Journal of Hazardous Materials*, 69(2):151–167.

Nassar, I., Ukrainczyk, L., and Horton, R. (1999). Transport and fate of volatile organic chemicals in unsaturated, nonisothermal, salty porous media: 2. experimental and numerical studies for benzene. *Journal of Hazardous Materials*, 69(2):169–185.

Nassar, I. N. and Horton, R. (1992). Simultaneous transfer of heat, water, and solute in porous media:I. theoretical development. *Soil Science Society of America Journal*, 56:1350–1356.

Nassar, I. N. and Horton, R. (1997). Heat, water, and solution transfer in unsaturated porous media: I -theory development and transport coefficient evaluation. *Transport in Porous Media*, 27:17–38.

Nguyen, T.-B., Lim, J., Choi, H., and Stark, T. D. (2011). Numerical modeling of diffusion for volatile organic compounds through composite landfill liner systems. *KSCE Journal of Civil Engineering*, 15(6):1033–1039.

Olivella, S., Carrera, J., Gens, A., and Alonso, E. E. (1994). Nonisothermal multiphase flow of brine and gas through saline media. *Transport in Porous Media*, 15(3):271–293.

Olson, R. E. (1977). Consolidation under time-dependent loading. *Journal of the Geotechnical Engineering Division, ASCE*, 103(1):55–60.

Oscarson, D. W., Hume, H. B., and King, F. (1994). Sorption of cesium on compacted bentonite. *Clays and Clay Minerals*, 42(6):731–736.

Othman, M. A., Bonaparte, R., and Gross, B. A. (1997). Preliminary results of composite liner field performance study. *Geotextiles and Geomembranes*, 15(4-6):289–312.

Padilla, I. Y., Yeh, T.-C. J., and Conklin, M. H. (1999). The effect of water content on solute transport in unsaturated porous media. *Water Resources Research*, 35(11):3303–3313.

Papanicolaou, A. and Diplas, P. (1999). Numerical solution of a non-linear model for self-weight solids settlement. *Applied Mathematical Modelling*, 23:345–362.

Park, J. K. and Nibras, M. (1993). Mass flux of organic chemicals through polyethylene geomembranes. *Water Environment Research*, 65(3):227–237.

Peters, G. P. and Smith, D. W. (2001). Numerical study of boundary conditions for solute transport through aporous medium. *International Journal for Numerical and Analytical Methods in Geomechanics*, 25(7):629–650.

Peters, G. P. and Smith, D. W. (2002). Solute transport through a deforming porous medium. *International Journal for Numerical and Analytical Methods in Geomechanics*, 26(7):683–717.

Petersen, L. W., Moldrup, P., EI-Farhan, Y., Jacobsen, O. H., Yamaguchi, T., and Rolston, D. E. (1995). The effect of moisture and soil texture on the adsorption of organic vapors. *Journal of Enviromental Quality*, 24:752–759.

Philip, J. and de Vries, D. (1957). Moisture movement in porous materials under temperature gradients. *Transactions American Geophysical Union*, 38:222–232.

Pierson, P. and Barroso, M. (2002). A pouch test for characterizing gas permeability of geomembranes. *Geosynthetics International*, 9(4):345–372.

Porter, L., Kemper, W., Jackson, R., and Stewart, B. (1960). Chloride diff usion in soils as infl uenced by moisture content. In *Soil Sci. Soc. Am. Proc.*, 24, pages 460–463.

Potter, L. J., Savvidou, C., and Gibson, R. E. (1994). Consolidation and pollutant transport associated with slurried mineral waste disposal. In *1st International Conference on Environmental Geotechnics*, pages 525–530, Edmonton, Canada.

Poulsen, T. G., Massmann, J. w., and Moldrup, P. (1996). Effects of vapor extraction on contaminant flux to atmosphere and ground water. *Journal of Enviromental Engineering*, 122(8):700–706.

Poulsen, T. G., Moldrup, P., Yamaguchi, T., Massmann, J. W., and Hansen, J. A. (1998). Voc vapor sorption in soil: soil type dependent model and implications for vapor extraction. *Journal of Environmental Engineering*, 124(2):146–155.

Prunty, L. (2002). Spatial distribution of heat of wetting in porous media. In *2002 ASAE Annual International Meeting / CIGR XVth World Congress*, Chicago, Illinois, USA. Sponsored by ASAE and CIGR.

Reid, R., Prausintz, J., and Poling, B. (1987a). *The Properties of Gases and Liquids*. McGraw-Hill, New York.

Reid, R. C., Prausnitz, J. M., and Poling, B. E. (1987b). *The properties of gases and liquids*, chapter 11, pages 587–588. McGraw-Hill.

Rowe, R. K. (1989). Movement of pollutants through clayey soil. In *Proceeding of 37th Annual Geotechnical Conference*, pages 1–34, St. Paul, U.S.A.

Rowe, R. K. (1998). Geosynthetics and the minimization of contaminant migration through barrier systems beneath solid waste. In *6th International Conference on Geosynthetics*, pages 27–102, Atlanta, GA.

Rowe, R. K. (2005). Long-term performance of contaminant barrier systems. *Géotechnique*, 55(9):631–678.

Rowe, R. K. and Badv, K. (1996a). Advective-diffusive contaminant migration in unsaturated sand and gravel. *Journal of Geotechnical Engineering, ASCE*, 122(12):965–975.

Rowe, R. K. and Badv, K. (1996b). Chloride migration through clayey silt underlain by fine sand or silt. *Journal of Geotechnical Engineering, ASCE*, 122(1):60–68.

Rowe, R. K. and Booker, J. R. (1985). 1-d pollutant migration in soils of finite depth. *Journal of Geotechnical Engineering*, 111(4):479–499.

Rowe, R. K. and Booker, J. R. (1986). A finite layer technique for calculating three-dimensional pollutant migration in soil. *Géotechnique*, 36(2):205–214.

Scanlon, B. and Milly, P. (1994). Water and heat fluxes in desert soils, 2. numerical simulations. *Water Resources Research*, 30:721–733.

Schuurman, I. (1966). The compressibility of an air/water mixture and a theoretical relation between the air and water pressures. *Géotechnique*, 16(4):269–281.

Senten, J. R. and Charlier, R. H. (1991). Heavy metals sediments pollution in estuarine and coastal waters: corrective measures for existing problems. *International Journal of Environmental Studies*, 37(1&2):79–96.

Shan, C. and Stephens, D. B. (1995). An analytical solution for vertical transport of volatile chemicals in the vadose zone. *Journal of Contaminant Hydrology*, 18(4):259–277.

Sherard, J. L., Woodward, R. J., Gizienski, S. F., and Clevenger, W. A. (1963). *Earth and earth-rock dams*, pages 245–246. John Wiley and Sons, New York.

Smith, D. W. (2000). One-dimensional contaminant transport through a deforming porous medium : Theory and a solution for a quasi-steady-state problem. *International journal for numerical and analytical methods in geomechanics*, 24(8):693–722.

Smith, J. E. and Gillham, R. W. (1994). The effect of concentration-dependent surface tension on the flow of water and transport of dissolved organic compounds: a pressure head-based formulation and numerical model. *Water Resource Research*, 30:343–354.

Soltani-Ahmadi, H. (2000). A review of the literature regarding non-methane and volatile organic compounds in municipal solid waste landfill gas. Technical report, Department of civil enviromental engineering, University of Delaware.

St-Arnaud, G. (1995). The high pore pressures within embankment dams: an unsaturated soil approach. *Canadian Geotechnical Journal*, 32:892–898.

Stark, T. D. and Choi, H. (2005). Methane gas migration through geomembranes. *Geosynthetics International*, 12(2):120–126.

Staudinger, J. and Roberts, P. V. (2001). A critical compilation of henry's law constant temperature dependence relations for organic compounds in dilute aqueous solutions. *Chemosphere*, 44:561–576.

Terzaghi, K. (1925). *Erdbaumechanik auf Bodenphysikalischer Grundlage*. Leipzig u. Wien, F. Deuticke, Vienna, Deuticke.

Terzaghi, K. (1943). *Theoretical soil mechanics*. Wiley, New York.

Thomas, H., He, Y., Sansom, M., and Li, C. (1996). On the development of a model of the thermo-mechanical-hydraulic behaviour of unsaturated soils. *Engineering Geology*, 41(1-4):197–218.

Thomas, H. R. and Ferguson, W. J. (1999). A fully coupled heat and mass transfer model incorporating contaminant gas transfer in an unsaturated porous medium. *Computers and Geotechnics*, 24:65–87.

Thomas, H. R. and He, Y. (1997). A coupled heat-moisture transfer theory for deformable unsaturated soil and its algorithmic implementation. *International Journal for Numerical Methods in Engineering*, 40:3421–3441.

Thomas, H. R. and King, S. D. (1994). A non-linear, two-dimensional, potential based analysis of coupled heat and mass transfer in a porous medium. *International Journal for Numerical Methods in Engineering*, 37:3707–3722.

Thomas, H. R. and Sansom, M. R. (1995). Fully coupled analysis of heat, moisture and air transfer in unsaturated soil. *Journal of Engineering Mechanics, ASCE*, 121:392–405.

Tsai, T.-L., Chang, K.-C., and Huang, L.-H. (2006). Body force effect on consolidation of porous elastic media due to pumping. *Journal of Chinese Institute of Engineers*, 29(1):75–82.

Tsai, Y. J., Kuo, Y. C., and Chen, T. C. (2007). Groundwater remediation using a novel micro-bubble sparging method. *Journal of Environmental Engineering and Management*, 17(2):151–155.

Tuckermann, R. (2007). Surface tension of aqueous solutions of water-soluble organic and inorganic compounds. *Atmospheric Environment*, 41(29):6265–6275.

Tuckermann, R. and Cammenga, H. K. (2004). The surface tension of aqueous solutions of some atmospheric water-soluble organic compounds. *Atmospheric Environment*, 38(36):6135–6138.

USEPA (1997). The incidence and severity of contamination in surface waters of the united states, national sediment quality survey, epa 823-r-97-006,. Technical report, United States Environmental Protection Agency, Office of Science and Technology, Washington, DC.

USEPA (2004). The incidence and severity of sediment contamination in surface waters of the united states, national sediment quality survey: Second edition, epa 823/r-04-007. Technical report, United States Environmental Protection Agency, Office of Science and Technology, Washington, DC.

USEPA (2007). Municipal solid waste generation, recycling, and disposal in the united states: Facts and figures for 2006. Technical report, EPA 530-F-07-030, Washington, D.C.

van Genuchten, M. (1981). Analytic solutions for chemical transport with simultaneous adsorption, zero-order production and first order decay. *Journal of Hydrology*, 49:213–233.

van Genuchten, M. (1991). Recent progress in modelling water flow and chemical transport in the unsaturated zone. In *Proceedings of the 20th General Assembly of the International Union of Geodesy and Geophysics*, pages 169–183, Vienna, Austria. Institute of Hydrology, Wallingford, U.K.

Vaughan, P. R. (2003). Observations on the behaviour of clay fill containing occluded air bubbles. *Géotechnique*, 53(2):265–272.

Vaziri, H. H. and Christian, H. A. (1994). Application of terzaghi's consolidation theory to nearly saturated soils. *Canadian Geotechnical Journal*, 31(2):311–317.

Verruijt, A. (1969). *Flow Through Porous Media*, chapter Elastic storage of aquifers, pages 331–376. Academic Press, London, UK.

Weast, R. (1980). *CRC Handbook of Chemistry and Physics*. CRC Press, Inc., Boca Raton, Florida.

Welty, J., Wicks, C., and Wilson, R. E. (1984). *Foundamentals of Momentum, Heat, and Mass Transfer*, chapter 24. Wiley.

Workman, J. P. (1993). *Geosynthetic liner systems: Innovations, concerns, and designs*, chapter Interpretation of leakage rates in double-liner systems, pages 95–112. Industrial Fabrics Association International.

Yeh, H. D., Lu, R. H., and Yeh, G. T. (1999). Finite element modelling for land displacements due to pumping. *International Journal for Numerical and Analytical Methods in Geomechanics*, 20:79 –99.

Yong, R., Mohamed, A., and Warkentin, B. (1992). *Principles of contaminant transport in soils*. Elsevier Science, New York.

Yule, D. F. and Gardner, W. R. (1978). Longitudinal and transverse dispersion coefficients in unsaturated plainfield sand. *Water Resource Research*, 14(4):582588.

Zhang, H. J., Jeng, D.-S., Seymour, B. R., Barry, D. A., and Li, L. (2012). Solute transport in partially-saturated deformable porous media: Application to a landfill clay liner. *Advances in Water Resources*, 40:1–10.

Zhang, L. and Szeri, A. (2005). Transport of neutral solute in articular cartilage: effects of loading and particle size. *Proceedings of the royal society a-mathematical physical and engineering sciences*, 461(2059):2021–2042.

Zhang, M. and Burns, S. E. (2000). Surfactant effects on the transport of air bubbles in porous media. In *GeoDenver 2000 Environmental Geotechnics, ASCE*, Denver, Colorado, United States.

Zhou, Y. and Rajapakse, R. K. N. D. (1998). Coupled heat-moisture-are transport in deformable unsaturated media. *Journal of Engineering Mechanics*, 24(10):1090–1099.

Zhou, Y. and Rowe, R. K. (2003). Development of a technique for modelling clay liner desiccation. *International Journal for Numerical and Analytical Methods in Geomechanics*, 27:473–493.

Zhou, Y. and Rowe, R. K. (2005). Modeling of clay liner desiccation. *International Journal of Geomechanics, ASCE*, 5(1):1–9.